

Dissertation

submitted to the

Combined Faculty of Natural Sciences and Mathematics

of the Ruperto Carola University Heidelberg, Germany

for the degree of

Doctor of Natural Sciences

presented by:

Felix Schmitt-Hoffner, M.Sc.

born in: Heidelberg, Germany

Oral examination: 14.03.2022

Molecular and clinical characterization of *FOXR2*-activated pediatric cancer

Referees:

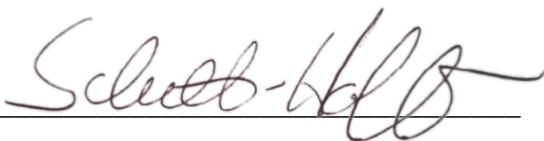
Prof. Dr. Andreas Trumpp

Prof. Dr. Stefan M. Pfister

Declaration

The work and results of the following dissertation were performed and obtained from March 2019 until December 2021 under the supervision of Dr. Marcel Kool and Prof. Dr. Stefan M. Pfister in the Division of Pediatric Neurooncology at the German Cancer Research Center (DKFZ), Heidelberg, Germany and the Hopp Children's Cancer Center (KiTZ), Heidelberg, Germany. The results and discussion of the first chapter are based on the publication "FOXR2 Stabilizes MYCN Protein and Identifies Non-MYCN-Amplified Neuroblastoma Patients With Unfavorable Outcome" in JCO (Schmitt-Hoffner et al., 2021), which was written and coordinated by me. Experiments and analyses were conducted by me, building on previous work by Sjoerd van Rijn who performed the *in vitro* experiments on 293T cells shown in Figure 17. The results and discussion of the second chapter are based on collaborative publications together with Katja von Hoff et al. and Andrey Korshunov et al. (Korshunov et al., 2021; von Hoff et al., 2021). Katja von Hoff et al. collected the cases and data for the CNS-PNET cohort and performed the clinical analyses. I performed the molecular re-evaluation of the CNS-PNET cohort, analyzed molecular and patient characteristics and provided figures. Andrey Korshunov et al. analyzed the CNS-PNET cohort and the RNA-seq dataset. In parallel, I analyzed the Affymetrix dataset and provided figures. Our collaborative findings were validated by stainings performed by Andrey Korshunov et al.

I hereby declare that I have written and submitted this dissertation myself and have not used any other sources than those indicated. Furthermore, I declare that I have not applied to be examined at any other institution, nor have I used the dissertation in this or any other form at any other institution as an examination paper, nor submitted it to any other faculty as a dissertation.

A handwritten signature in black ink, appearing to read 'Schmitt-Hoffner', is written over a horizontal line.

Felix Schmitt-Hoffner

Zusammenfassung

Krebs gilt als häufigste Todesursache bei Krankheiten im Kinder- und Jugendalter in der Europäischen Union und in den Vereinigten Staaten. Daher sind dringend eine präzise Diagnostik und neue therapeutische Ansätze erforderlich, um den klinischen Verlauf pädiatrischer Krebspatienten zu verbessern. Heutzutage bieten moderne Sequenzierungstechnologien die Möglichkeit molekulare Mechanismen und Eigenschaften von Tumoren zu erforschen, was zu einem rasanten Wissenszuwachs im Feld der pädiatrischen Onkologie geführt hat. Schlüsselfaktoren sind hierbei die Identifizierung und Charakterisierung von krebsverursachenden Onkogenen, die es ermöglichen, eine differenzierte molekulare und klinische Perspektive auf verschiedene Tumoreinheiten sowie auf dem Wirkmechanismus basierende therapeutische Ansätze zu entwickeln. Im Rahmen dieser Doktorarbeit wurde die molekulare und klinische Bedeutung des Onkogens *FOXR2* in pädiatrischen Krebserkrankungen untersucht.

Im ersten Kapitel wird die klinische und mechanistische Funktion von *FOXR2* in peripheren Neuroblastomen beleuchtet. Diese weisen ein breites Spektrum an klinischen Verläufen auf, die von spontaner Regression bis hin zu aggressiver Ausbreitung des Tumors mit Todesfolge reichen. Ein präzises Verständnis der Mechanismen, die zur Tumorentstehung und Ausbreitung führen, ist daher zur Risikostratifizierung und zielgerichteten Behandlung von Neuroblastompatienten erforderlich. In dieser Studie wurden Genexpressions- und klinische Daten von 1030 Neuroblastompatienten untersucht. Des Weiteren wurden die Auswirkungen eines shRNA induzierten Knockdowns von *FOXR2 in vitro* sowie die mechanistische Rolle von *FOXR2* in Zelllinien und Patientenproben erforscht. Insgesamt wurde in 9% der Neuroblastompatienten eine erhöhte *FOXR2* Expression detektiert. Diese Patienten zeigten in den drei untersuchten Datensätzen einen schlechten klinischen Verlauf mit einer 10-Jahres Gesamtüberlebensrate von 53% bis 59%. Darüber hinaus wurde gezeigt, dass die Expression von *FOXR2* Patienten mit schlechten Überlebensraten identifiziert, unabhängig von bereits etablierten prognostischen Markern wie *MYCN* Amplifikation, INSS4, einem Diagnosealter von über 18 Monaten oder Hochrisiko-Stadium. *In vitro* führte der Knockdown von *FOXR2* zu einer verringerten Zellproliferation, Zelltod, Verlangsamung des Zellzyklus und zu einer geringeren *MYCN* Proteinexpression, was die essentielle Rolle von *FOXR2* für die Ausbreitung des Tumors unterstreicht. Des Weiteren wurde festgestellt, dass *FOXR2* exprimierende und *MYCN* amplifizierte Neuroblastome eine ähnliche transkriptionelle Signatur aufweisen, was auf einen gemeinsamen tumortreibenden Mechanismus hinweist. Tatsächlich wurde *in vitro* gezeigt, dass *FOXR2* Protein an *MYC* und *MYCN* Protein bindet und es dadurch stabilisiert. Auch in

Patientenproben wurden stark erhöhte MYCN Proteinmengen in *FOXR2* exprimierenden Neuroblastomen nachgewiesen. Diese Ergebnisse zeigen, dass der stabilisierende Einfluss von *FOXR2* auf *MYCN* eine Alternative zu *MYCN* Amplifikationen in Neuroblastomen darstellt. Die Expression von *FOXR2* definiert somit einen neuen und unabhängigen prognostischen Faktor, der schlechte Gesamtüberlebensraten bei Patienten mit Neuroblastom anzeigt und verbessert die Risikostratifizierung dieser klinisch heterogenen Krebsart.

Im zweiten Kapitel wurden molekulare und klinische Charakteristika von Neuroblastomen des zentralen Nervensystems mit *FOXR2* Aktivierung (CNS NB-*FOXR2*) in Kollaborationen mit Katja von Hoff et al. und Andrey Korshunov et al. beschrieben und analysiert. CNS NB-*FOXR2* wurden erstmals im Rahmen einer molekularen Charakterisierung von institutionell diagnostizierten primitiven neuroektodermalen Tumoren des zentralen Nervensystems (CNS-PNET) von Sturm et al. beschrieben. Bei diesen handelt es sich um hoch aggressive und wenig differenzierte embryonale Tumore mit zunächst vermutetem schlechten klinischen Verlauf. Erste Analysen in kleineren Kohorten von re-evaluierten CNS-PNETs haben jedoch gezeigt, dass der schlechte klinische Verlauf in vielen Fällen auf fälschlich als CNS-PNET klassifizierte hochgradige Gliome (HGG) zurückzuführen ist. Um die klinischen Charakteristika von CNS NB-*FOXR2* tiefer zu erforschen, wurden Gewebeproben und klinische Daten von 307 histologisch diagnostizierten CNS-PNET gesammelt und auf molekularer Ebene re-evaluiert. In 36 von 307 Fällen wurden CNS NB-*FOXR2* mittels DNA Methylierungsanalyse klassifiziert. Diese Patienten wiesen eine günstige 5-Jahres Gesamtüberlebensrate von 85% auf. Im Gegensatz zu CNS NB-*FOXR2* zeigten die Gesamtkohorte der CNS-PNET eine 5-Jahres Gesamtüberlebensrate von nur 51 % auf, welche hauptsächlich auf die schlechte Gesamtüberlebensrate von (molekular bestätigten) ETMR und HGG (24%, bzw. 25%) zurückgeführt werden kann. Diese Ergebnisse ermöglichen somit eine differenzierte klinische Betrachtung und unterstreichen die Notwendigkeit für eine angepasste Behandlungsstrategie für CNS NB-*FOXR2*, die in der im Jahr 2021 veröffentlichten 5. Auflage der „WHO classification of tumors of the central nervous system“ gelistet sind. Im Rahmen einer weiteren Studie wurden diagnostische Marker für CNS NB-*FOXR2* analysiert, um diese von morphologisch ähnlichen Entitäten zu unterscheiden. Zu diesem Zweck wurden 84 CNS-PNET auf molekularer Ebene mittels DNA Methylierungsanalyse re-evaluiert. Insgesamt konnten 20 CNS NB-*FOXR2* in dieser Kohorte ausgemacht werden. Basierend auf Genexpressionsanalysen wurden *SOX10* und *ANKRD55* als spezifisch in CNS NB-*FOXR2* exprimierte Gene identifiziert. Mittels immunohistochemischer Färbungen wurde die Expression dieser Gene auf Proteinebene validiert. Dafür wurden 20 CNS NB-*FOXR2* sowie eine Vielzahl anderer pädiatrischer CNS Tumore, welche die Morphologie von CNS-PNET

aufweisen können (einschließlich Ependymoma, ETMR, AT/RT und mehrere HGG), immunohistochemisch evaluiert. Diese Vorgehensweise ergab, dass die kombinierte Expression der Proteine SOX10 und ANKRD55 CNS NB-*FOXR2* sehr präzise von morphologisch ähnlichen Entitäten unterscheiden kann.

Zusammenfassend wurde im Rahmen dieser Doktorarbeit *FOXR2* als unabhängiger prognostischer Faktor in peripheren Neuroblastomen entdeckt, welcher mit einem ungünstigen klinischen Verlauf assoziiert ist. Darüber hinaus wurde erstmals die mechanistische Interaktion von *FOXR2* und *MYCN* beschrieben, welche die Stabilisierung des Hochrisiko-assoziierten Onkogens *MYCN* zur Folge hat. Des Weiteren wurden klinische Charakteristika der kürzlich erstmalig beschriebenen Tumorentität CNS NB-*FOXR2* erfasst und diagnostische Marker identifiziert, die CNS NB-*FOXR2* von morphologisch ähnlichen Entitäten unterscheiden können.

Summary

Cancer is the leading disease-related cause of death in children in the European Union and the United States. Therefore, better diagnostics and novel therapeutic approaches are urgently needed to improve the outcome of pediatric cancer patients. Advances in modern sequencing technologies provided the basis for a substantial increase of knowledge, leading to the molecular understanding of pediatric malignancies that we have today. The identification and characterization of cancer-driving oncogenes is key to enable a differentiated molecular and clinical view on tumor entities and to find specific therapeutic approaches that are based on the mode of action. In this study, I investigated the molecular and clinical role of the oncogene *FOXR2* in pediatric cancer.

The first chapter sheds light on the clinical and mechanistic role of *FOXR2* in peripheral neuroblastoma. Since neuroblastoma shows a broad spectrum of clinical outcomes, ranging from spontaneous tumor regression to disease related death, the understanding of mechanisms that induce and drive the tumor is crucial for risk stratification and targeted treatment of patients. I therefore investigated gene expression and clinical data of 1.030 neuroblastoma patients of three independent cohorts and studied the implications of silencing *FOXR2* expression *in vitro*. Furthermore, the mechanistic role of *FOXR2* was analyzed in cell lines and patient samples. In the total neuroblastoma cohort, *FOXR2* expression was present in 9% of neuroblastoma patients and turned out to be a prognostic factor indicating unfavorable survival of patients with 10-year overall survival rates of 53% to 59%. Importantly, *FOXR2* expression indicated poor survival independently from well-established prognostic markers including *MYCN* amplification, INSS4, age at diagnosis above 18 months or high-risk stage. *In vitro*, the knockdown of *FOXR2* resulted in reduced cell proliferation, cell death, cell cycle arrest and reduced *MYCN* protein levels, indicating the essential role of *FOXR2* for tumor progression. Furthermore, *FOXR2* expressing neuroblastoma showed a high transcriptional similarity to *MYCN*-amplified cases, suggesting a common mechanism driving the tumors. In line with this, it was observed that *FOXR2* protein binds and stabilizes *MYC* and *MYCN* protein and in patient samples *MYCN* levels in *FOXR2* mRNA expressing tumors are highly increased. Overall, these results indicate that the stabilization mechanism of *FOXR2* and *MYCN* represent an alternative to *MYCN* amplifications in neuroblastoma leading to a similar transcriptional signature indicative of an aggressive tumor. In line with this, *FOXR2* identifies a novel and independent prognostic factor in neuroblastoma indicating unfavorable clinical outcome and improving risk stratification of this clinically highly heterogeneous tumor type.

In the second chapter, molecular and clinical characteristics of CNS neuroblastoma with *FOXR2* activation (CNS NB-*FOXR2*) were described and analyzed based on collaborations with Katja von Hoff et al. and Andrey Korshunov et al. CNS NB-*FOXR2* tumors were only recently described by Sturm and colleagues and emerged from institutionally diagnosed CNS primitive neuroectodermal tumors (PNET). CNS-PNET are highly aggressive and poorly differentiated embryonal tumors with a poor outcome. However, first analyses in small cohorts of molecularly re-evaluated CNS-PNET suggest that the poor outcome for this group of tumors is mostly driven by misclassified high-grade gliomas (HGG). To further investigate the clinical characteristics of CNS NB-*FOXR2*, tissue samples and clinical data of 307 histologically diagnosed CNS-PNET were collected and molecularly re-evaluated. Out of 307 cases, 36 cases were classified as CNS NB-*FOXR2* by means of DNA methylation profiling. These patients clearly showed a favorable survival with a 5-year overall survival rate of 85%. In contrast to CNS NB-*FOXR2*, the 5-year overall survival of the entire CNS-PNET cohort is 51%, which can be attributed to the poor overall survival of ETMR and HGG (24% and 25%, respectively) that were also molecularly identified in the CNS-PNET cohort. These results provide a differentiated clinical view and point out the need for an adjusted treatment strategy for CNS NB-*FOXR2*, now listed as a new distinct entity of embryonal tumors in the 2021 update of the “WHO classification of tumors of the central nervous system”. In the context of an additional collaborative effort, we aimed to identify immunohistochemical markers for CNS NB-*FOXR2* to clearly discriminate them from morphological mimics. Therefore, 84 CNS-PNET cases were molecularly re-evaluated using DNA methylation profiling, resulting in the identification of 20 CNS NB-*FOXR2* in this cohort. Based on differential gene expression analyses the expression of *SOX10* and *ANKRD55* was identified to discriminate CNS NB-*FOXR2* from histologically diagnosed CNS-PNET. By means of immunohistochemistry, these results were validated on protein level, staining 20 CNS NB-*FOXR2* and a variety of other pediatric CNS tumors that can present CNS-PNET like morphologies, including amongst others ependymoma, ETMR, AT/RT and several high-grade gliomas. Indeed, the combined expression of *SOX10* and *ANKRD55* protein was found to clearly identify CNS NB-*FOXR2* from morphological mimics.

Taken together, this study has shown that *FOXR2* represents an independent prognostic factor in peripheral neuroblastoma, identifying patients with unfavorable survival. Additionally, the mechanistic interaction of *FOXR2* and *MYCN* leading to a stabilization of the high-risk associated oncogene *MYCN* was described for the first time. Moreover, in the context of this study clinical characteristics of the novel brain tumor entity CNS NB-*FOXR2* were revealed

and diagnostic markers to distinguish CNS NB-*FOXR2* from morphological mimics were identified.

List of abbreviations

ALL	Acute Lymphocytic Leukemia
ALT	Alternative Lengthening of Telomeres
ANKRD55	Ankyrin Repeat Domain 55
ANOVA	Analysis of Variance
AT/RT	Atypical Teratoid/Rhabdoid Tumor
AURKA	Aurora A kinase
AURKB	Aurora B kinase
BCA	Bicinchoninic Acid Assay
BCOR	BCL6 Corepressor
BSL	Biosafety Level
ChIP	Chromatin Immunoprecipitation
CHX	Cyclohexamide
CI	Confidence Interval
CNS	Central Nervous System
CNS EFT- <i>CIC</i>	CNS Ewing sarcoma family tumor with <i>CIC</i> alteration
CNS HGNET- <i>BCOR</i>	CNS High Grade Neuroepithelial Tumor <i>BCOR</i> alteration
CNS HGNET- <i>MN1</i>	CNS High Grade Neuroepithelial Tumor <i>MN1</i> alteration
CNS NB- <i>FOXR2</i>	CNS neuroblastoma with <i>FOXR2</i> activation
CNS-PNET	Primitive Neuroectodermal Tumors of the Central Nervous System
DKFZ	German Cancer Research Center
DMG	Diffuse Midline Glioma
DNA	Deoxyribonucleic acid
EFS	Event-free Survival
EPN	Ependymoma
ETMR	Embryonal Tumors with Multilayered Rosettes

FBW7	F-box and WD repeat domain-containing 7
FCS	Fetal Calf Serum
FDR	False Discovery Rate
FFPE	Formalin-fixed Paraffin-embedded
FOX	Forkhead Box
FOXR1	Forkhead Box R1
FOXR2	Forkhead Box R2
GBM	Glioblastoma
GEO	Gene Expression Omnibus
GFP	Green Fluorescent Protein
GSEA	Gene Set Enrichment Analyses
HGG	High Grade Glioma
HRP	Horseradish Peroxidase
IDH	Isocitrate Dehydrogenase
IHC	Immunohistochemistry
INRG	International Neuroblastoma Risk Group
INSS	International Neuroblastoma Staging System
IPA	Ingenuity Pathway Analysis
M+	Metastatic disease
MOR+/MORx	Localized disease with incomplete or unknown resection
MOR0	Localized disease with complete resection
MN1	Meningioma 1
mRNA	Messenger Ribonucleic Acid
NIH	National Health Institute
NRC	Neuroblastoma Research Consortium
NSC	Neural Stem Cell
NSCLC	Non-small Cell Lung Cancer
OS	Overall Survival

PBS	Phosphate Buffered Saline
PCA	Principle Component Analysis
PFS	Progression-free Survival
PI	Propidium Iodide
PVDF	Polyvinylidene Difluoride
RFP	Red Fluorescent Protein
RIPA	Radioimmunoprecipitation Assay
RPKM	Reads per kilobase of transcript per Million mapped reads
RT-PCR	Reverse Transcription Polymerase Chain Reaction
S62	Serine 62
SCA	Segmental Chromosome Aberrations
shRNA	small hairpin RNA
SOX10	SRY-Box Transcription Factor 10
T58	Threonine 58
TARGET	Therapeutically Applicable Research to Generate Effective Treatments
TBS-T	Tris-buffered saline with Tween
TERT	Telomerase Reverse Transcriptase
TMM	Telomerase Maintenance Mechanisms
t-SNE	t-distributed Stochastic Neighbor Embedding
US	United States
USP9X	Ubiquitin Specific Peptidase 9 X-Linked
WHO	World Health Organization

Contents

1	Introduction	1
1.1	Pediatric cancer	1
1.1.1	Overview	1
1.1.2	Incidence and survival rates in pediatric cancer	2
1.1.3	Hallmarks of cancer.....	5
1.1.4	FOXR2 in pediatric cancer	5
2	Materials and Methods	8
2.1	Materials and methods based on “FOXR2 Stabilizes MYCN Protein and Identifies Non–MYCN-Amplified Neuroblastoma Patients With Unfavorable Outcome”	9
2.1.1	Neuroblastoma cohorts	9
2.1.2	Cell culture	9
2.1.3	Production of lentiviral vectors and generation of stable cell lines	10
2.1.4	Quantitative RT-PCR.....	10
2.1.5	Cell viability	11
2.1.6	Cell cycle and cell death.....	11
2.1.7	Western blot analysis	11
2.1.8	CHX assay	12
2.1.9	Co-immunoprecipitation	12
2.1.10	Gene expression analysis	12
2.1.11	Statistical analyses.....	13

2.2	Material and methods based on “Therapeutic implications of improved molecular diagnostics for rare CNS-embryonal tumor entities – results of an international, retrospective study”	15
2.2.1	Study design and participants	15
2.2.2	Histological and molecular re-evaluation	15
2.2.3	Cohort description and clinical data	15
2.3	Material and methods based on “Molecular analysis of pediatric CNS-PNET revealed nosologic heterogeneity and potent diagnostic markers for CNS neuroblastoma with <i>FOXR2</i> -activation”	16
2.3.1	Patient cohort	16
2.3.2	DNA methylation array processing	16
2.3.3	RNA-sequencing and gene expression analyses	17
2.3.4	Immunohistochemistry	17
3	First chapter: The role of <i>FOXR2</i> in peripheral neuroblastoma	19
3.1	Introduction	19
3.1.1	An overview on neuroblastoma	19
3.1.2	Risk stratification in neuroblastoma	19
3.1.3	Aim of this study	21
3.2	Results	22
3.2.1	Expression of <i>FOXR2</i> in peripheral neuroblastoma	22
3.2.2	<i>FOXR2</i> -expressing cases do not show ALT phenotype but increased TERT expression	25
3.2.3	<i>FOXR2</i> expression identifies neuroblastoma patients with unfavorable outcome independent from established prognostic factors	26
3.2.4	Mechanism of <i>FOXR2</i> activation in neuroblastoma	33

3.2.5	FOXR2 knockdown in neuroblastoma cell lines results in decreased proliferation.....	33
3.2.6	Transcriptome analyses of <i>FOXR2</i> -expressing neuroblastoma reveals similarities to the <i>MYCN</i> group	38
3.2.7	<i>MYCN</i> and <i>MYC</i> is stabilized by <i>FOXR2</i> on a protein level	41
3.3	Discussion.....	44
4	Second chapter: Molecular and clinical characterization of CNS NB- <i>FOXR2</i>	49
4.1	Introduction	49
4.1.1	Molecular re-evaluation of CNS-PNET	49
4.1.2	CNS NB- <i>FOXR2</i>	51
4.1.3	Aim of this study.....	52
4.2	Results.....	53
4.2.1	Methylation-based characterization of the CNS-PNET cohort	54
4.2.2	Molecular and patient characteristics of CNS NB- <i>FOXR2</i>	56
4.2.3	Survival analyses of CNS NB- <i>FOXR2</i> in comparison to other entities originally classified as CNS-PNET.....	57
4.2.4	Diagnostic markers for CNS NB- <i>FOXR2</i>	59
4.3	Discussion.....	67
5	Concluding discussion and outlook	71
6	References.....	73
7	Supplementary data	89
8	Acknowledgements	95

List of Figures

Figure 1: Childhood cancer is based on a dysfunctional development of maturing cells.	2
Figure 2: Cancer in childhood and adolescence.	3
Figure 3: Death rates in types of childhood cancer.	4
Figure 4: Expression of <i>FOXR2</i> mRNA in pediatric brain cancer and in peripheral neuroblastoma.	7
Figure 5: INRG pretreatment classification scheme.	21
Figure 6: <i>FOXR2</i> expression in a subset of neuroblastoma.	24
Figure 7: <i>TERT</i>-expression is increased in the <i>FOXR2</i> group.	26
Figure 8: Survival analyses of the <i>FOXR2</i>, <i>FOXR1</i>, <i>MYC</i>, <i>MYCN</i> and OTHER group.	28
Figure 9: Survival analysis in the high-risk subsets of the RNA-seq, NRC and the TARGET dataset.	29
Figure 10: Survival analyses of the ALT annotated subset of the RNA-seq dataset.	30
Figure 11: <i>FOXR2</i> is a significant independent risk factor.	32
Figure 12: Knockdown of <i>FOXR2</i> results in decreased proliferation.	35
Figure 13: Pathway analyses suggest oncogenic roles of <i>FOXR2</i>.	36
Figure 14: <i>FOXR2</i> knockdown is associated with cellular death and cell cycle arrest.	37
Figure 15: The <i>FOXR2</i> and the <i>MYCN</i> group are transcriptionally related.	39
Figure 16: <i>FOXR2</i> cases show a positive <i>MYCN</i> activity score.	40
Figure 17: <i>FOXR2</i> binds and stabilizes <i>MYCN</i> on a protein level.	42
Figure 18: <i>FOXR2</i>-expressing neuroblastoma show high <i>MYCN</i> protein levels.	43

Figure 19: Stabilization of MYCN by FOXR2 might function as an alternative mechanism to MYCN-amplifications.	48
Figure 20: DNA methylation profiling based classification of institutionally diagnosed CNS-PNET.	51
Figure 21: Classification of the CNS-PNET cohort based on methylation data.	55
Figure 22: Molecular and patient characteristics of CNS NB-FOXR2.	56
Figure 23: Survival analyses of molecular groups with a focus on CNS NB-FOXR2.	58
Figure 24: Histopathological analyses of CNS-PNET.	59
Figure 25: Methylation data based classification of CNS-PNET cohort.	60
Figure 26: Transcriptomic analyses of EPN-RELA, GBM-MYCN, GBM-G34 and CNS NB-FOXR2.	61
Figure 27: Identification of marker genes for CNS NB-FOXR2 based on expression data.	62
Figure 28: SOX10 as a immunohistochemical marker for CNS NB-FOXR2.	63
Figure 29: ANKRD55 is a marker to distinguish CNS NB-FOXR2 from GBM-MID.	65

List of Tables

Table 1: Primers used for quantitative RT-PCR. Table from (Schmitt-Hoffner et al., 2021)...10

Table 2: Proportional distribution of risk factors and expression groups in the RNA-seq, NRC and TARGET dataset. Table from (Schmitt-Hoffner et al., 2021).14

Table 3: Hazard ratios and 95% confidence intervals of the multivariable analyses on overall and event-/progression-free survival in the RNA-seq and the NRC dataset. Table from (Schmitt-Hoffner et al., 2021).....33

Table 4: Percentage of entities with a potential CNS-PNET like histology that show no, low, intermediate or high signal intensity for SOX10 IHC. Table from collaborative publication, generated by Korshunov et al. (Korshunov et al., 2021).64

Table 5: Percentage of entities with a potential CNS-PNET like histology that show no, low, intermediate or high signal intensity for ANKRD55 IHC. Table from collaborative publication, generated by Korshunov et al. (Korshunov et al., 2021).66

Supplementary Data

Suppl. table 1: *FOXR2* signature based on the top100 differentially expressed genes of the *FOXR2* and OTHER group in the RNA-seq dataset. Table from (Schmitt-Hoffner et al., 2021).89

1 Introduction

1.1 Pediatric cancer

1.1.1 Overview

Cancer is not a single disease but a large group of diseases that can occur in almost any tissue and at variable age (NIH, accessed 04.11.2021b). It originates from an uncontrolled proliferation of cells and their ability to invade surrounding and/or distant organs or tissue (WHO, accessed 04.11.2021). Cancer is a leading cause of death in children as well as in adults, however in absolute numbers the incidence differs substantially due to the rarity of childhood malignancies (Kattner et al., 2019). Children aged 0 to 19 years show an annual incidence of 186.6 per 1 million in the United States (US), whereas the overall cancer incidence in the US including adults is around 4424 per 1 million per year (NIH, accessed 04.11.2021a; Ward et al., 2014). Furthermore, childhood and adult cancer often differ in their origins. Adult malignancies mostly derive from adult epithelial tissues forming carcinomas, which account for over 90% of tumors. In children only around 3.5% of cancers are carcinomas and malignancies of the hematological system such as leukemia and lymphoma (40.9%), as well as tumors of the developing central nervous system are most prevalent (20.2%) (Cooper, 2000; Gröbner, 2017; Ma et al., 2018). Advances in molecular understanding of cancer based on modern next-generation sequencing technologies further revealed that in contrast to adults the mutational burden in pediatric cancer is clearly lower (Gröbner et al., 2018; Ma et al., 2018). Instead of an accumulation of mutational hits in adult malignancies, specific mutations in genes important for a normal development or fusion genes, often defining a single driver for a tumor entity, are commonly found in childhood cancer (Figure 1) (Behjati et al., 2021; Dupain et al., 2017). Furthermore, epigenetic alterations also play a key role in many pediatric malignancies. Over the last decade an increasing number of disease-causing epigenetic events, often induced by gene alterations in epigenetic regulators or chromatin complexes, were identified (Bender et al., 2013; Gröbner et al., 2018; Panditharatna and Filbin, 2020; Schwartzentruber et al., 2012; Sturm et al., 2012; Wu et al., 2012). The distinct DNA methylation patterns that are found in pediatric cancer entities were utilized for a more precise classification of brain tumors. This has also led to the discovery of a multitude of novel entities and subgroups, which are also recognized in the 2021 WHO Classification of Tumors of the Central Nervous System (Capper et al., 2018a; Capper et al., 2018b; Koelsche et al., 2021; Louis et al., 2021; Papanicolau-Sengos and Aldape, 2021; Stefan M. Pfister et al., 2021, in press; Sturm et al., 2016).

Overall, the molecular data and *in vivo* studies on the development of pediatric cancer suggest that on a cellular level cancer in children is linked to dysregulated development, caused by cells that are kept in a stem cell-like or progenitor-like state, thereby preventing differentiation and favoring self-renewal of these cells (Figure 1) (Behjati et al., 2021; Cozzio et al., 2003; Filbin and Monje, 2019; Funato et al., 2014; Li et al., 2005; Ng et al., 2015; Pathania et al., 2017; Vitte et al., 2017).

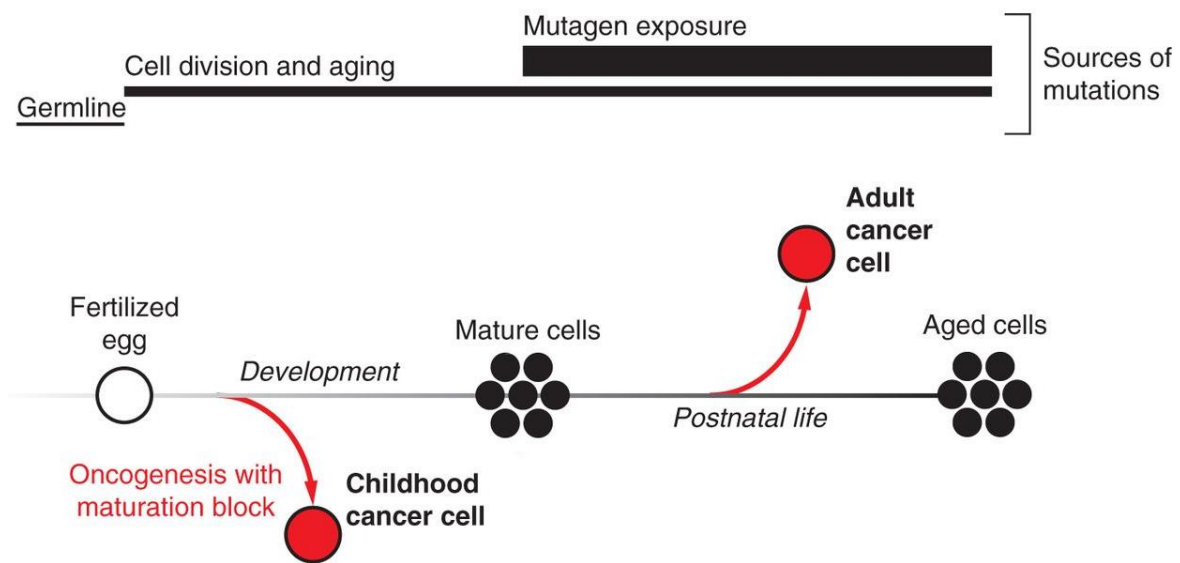


Figure 1: **Childhood cancer is based on a dysfunctional development of maturing cells.**

Childhood malignancies show a substantially lower mutational burden than adult cancers. Instead of mutational accumulations guiding a mature cell into an adult cancer cell, in childhood cancer specific mutations preventing the maturation of cells during development lead to oncogenesis. Figure modified from (Behjati et al., 2021).

1.1.2 Incidence and survival rates in pediatric cancer

In the US, the chance of developing cancer under the age of 15 is around 0.24% and under the age of 20, around 0.35% of the population develop a malignancy (Ward et al., 2014). Which type of cancer develops most frequently in these children and adolescents, however, varies by age. Based on an estimate of newly diagnosed childhood and adolescent cancers in the US for the year 2014 in the age group 0-14, the most common cancer types are acute lymphocytic leukemia (ALL) and CNS tumors, which account for around 26% and 21% of cases, respectively. These data are in line with the observations of the most recent cancer statistics

report of the American Cancer Society (Siegel et al., 2021; Ward et al., 2014). Neuroblastoma is found in 7% of cases in this age group, representing the most common extra-cranial solid tumor in childhood (Figure 2) (Hwang et al., 2019; Newman et al., 2019; Ward et al., 2014). Other frequently occurring malignancies in children below the age of 15 are Non-Hodgkin lymphoma (6%), Wilms tumor (5%), bone tumors (4%), and Hodgkin lymphoma (4%). In adolescent patients, aged between 15 and 19 years ALL occurs in 8% of patients, divergent from the 26% of patients below 15 years. Moreover, neuroblastoma is only rarely being diagnosed in adolescent patients (Gaspar et al., 2003; Louis and Shohet, 2015; Matthay, 1997; Mossé et al., 2014). Instead Hodgkin lymphoma (15%), thyroid carcinoma (11%), CNS tumors (10%), testicular germ cell tumors (8%), and Non-Hodgkin lymphoma (8%), are the most commonly occurring malignancies (Figure 2) (Ward et al., 2014). These differences in distribution from childhood to adolescent cancers are in many cases based on the developmental state from which the cancer originated (Behjati et al., 2021).

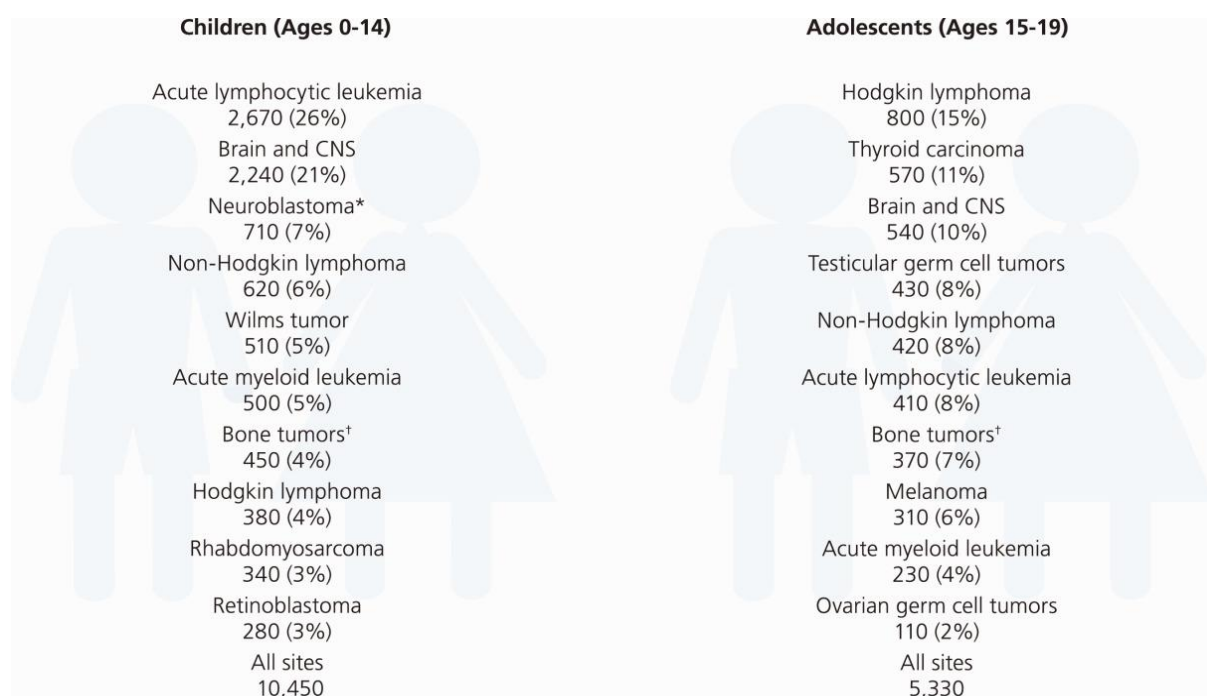


Figure 2: **Cancer in childhood and adolescence.**

Estimated percentage of new cases of childhood and adolescent cancers for the US in the year 2014 by the American Cancer Society. Figure adapted from (Ward et al., 2014).

In the European Union and the United States, cancer is the leading cause of disease-related mortality in children (Filbin and Monje, 2019; Johnson et al., 2014; Kyu et al., 2018; Siegel et al., 2021; Siegel et al., 2018). Only deaths caused by accidents occur more frequently in children than cancer related deaths (Filbin and Monje, 2019; Kyu et al., 2018). Since 1975 childhood cancer death rates are declining by around 2.1% per year (Ward et al., 2014). Generally, the 5-year overall survival in children in the US increased to a rate of 84% due to improvements in treatment approaches and strategies (American_Cancer_Society, accessed 12.11.2021). Still, for many entities improvements in survival rates have reached a plateau for the past 20 years and the survival of patients can vary substantially in different cancer types (Madanat-Harjuoja et al., 2014; Pollack et al., 2019; Siegel et al., 2021). Despite therapeutic advances some childhood cancers still show low survival rates, including several pediatric brain tumors, which account for most cancer-related pediatric deaths in the US (Figure 3) (Siegel et al., 2019; Siegel et al., 2021; Siegel et al., 2020; Ward et al., 2014).

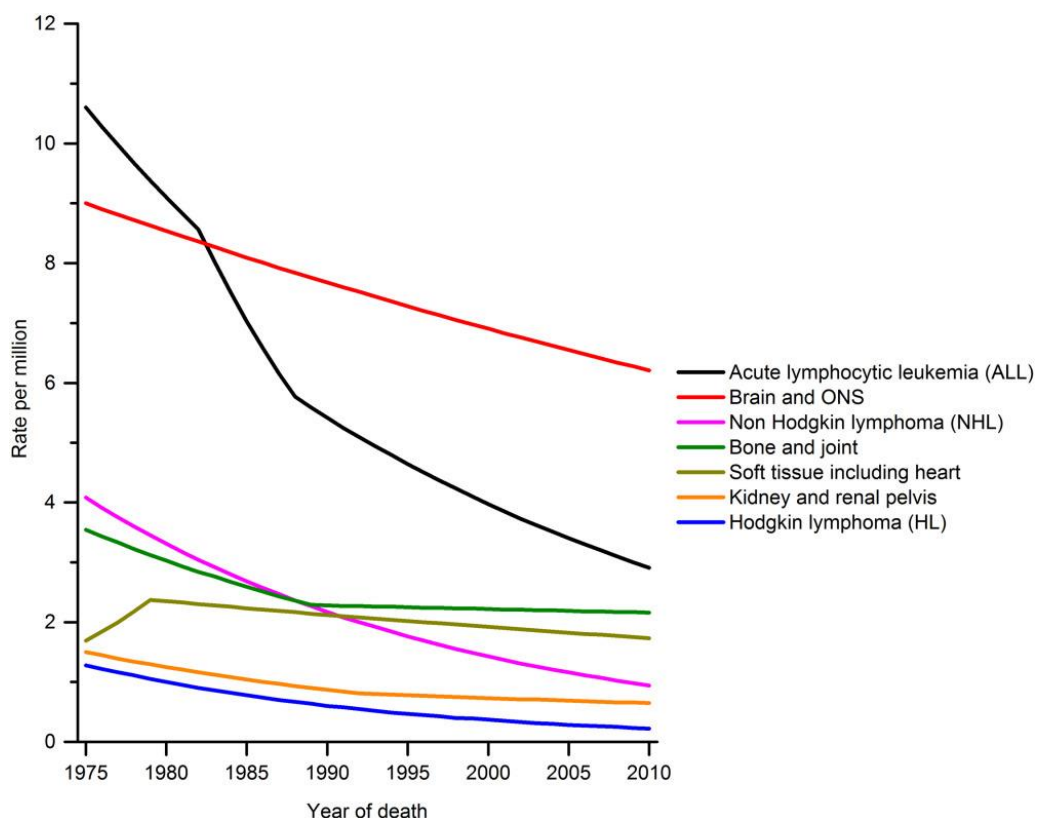


Figure 3: **Death rates in types of childhood cancer.**

Death rates in childhood cancer vary by cancer type and have decreased over the last decades. Figure adapted from (Ward et al., 2014).

1.1.3 Hallmarks of cancer

Tumorigenesis is a multistep process, involving the acquirement of six biological traits, which were described by Hanahan and Weinberg in 2000 (Hanahan and Weinberg, 2000). These proposed hallmarks of cancer include the evasion of growth suppressors, resistance to cell death, activation of invasion and metastasis, induction of angiogenesis as well as the ability to sustain proliferative signaling and to enable replicative immortality (Hanahan and Weinberg, 2000). In 2011, these biological capabilities were further extended by the ability to evade immune destruction and the reprogramming of the energy metabolism, as described in “Hallmarks in Cancer: The Next Generation” (Hanahan and Weinberg, 2011). Furthermore, enabling characteristics, which underlie hallmarks of cancer were defined, namely “genome instability and mutation” inducing genetic variability as well as “tumor-promoting inflammation” (Hanahan and Weinberg, 2011). Key roles in the deregulation of cellular processes and important regulators for hallmarks of cancer are tumor suppressor genes and oncogenes. The term tumor suppressor gene defines regulatory genes that limit cell proliferation, prevent unrestrained cell growth and therefore often show loss-of-function mutations in cancer (Aubrey et al., 2016; Lee and Muller, 2010). Contrarily, oncogenes, such as *Forkhead Box R2*, which I studied in the context of my PhD, comprise gain-of-function mutations inducing cell growth, cell cycle progression and survival of cells (Hübner, 2019; Lee and Muller, 2010).

1.1.4 FOXR2 in pediatric cancer

Forkhead Box R2 (FOXR2) belongs to the family of Forkhead Box transcription factors, which are involved in various biological processes such as cell proliferation and differentiation as well as transcriptional regulation and DNA repair (Katoh et al., 2013; Myatt and Lam, 2007). The protein structure of all FOX family members is defined by the conserved forkhead box domain, which is a DNA binding domain (Myatt and Lam, 2007). The *FOXR2* gene, located on chromosome Xp11.21 and the transcription factor FOXR2 were for the first time described and characterized in the year 2004 by Katoh et al. (Katoh and Katoh, 2004a, c). FOXR2 shows a high homology (57.7%) to FOXR1, a transcription factor also identified and characterized in 2004, and found to be expressed and linked to cell proliferation in a small subset of neuroblastoma (Katoh and Katoh, 2004b; Santo et al., 2012). The function of FOXR2 itself is largely unknown, however, it has been frequently related to tumorigenesis, aberrant cell growth or tumor progression (Koso et al., 2014; Li et al., 2016; Liu et al., 2017; Poh et al., 2019;

Rahrmann et al., 2013; Schmitt-Hoffner et al., 2020). In contrast to healthy tissue where FOXR2 is only expressed in testis (ProteinAtlas, accessed 12.11.2021), it has been found to be expressed in several tumor types, amongst them breast, colorectal, hepatocellular, ovarian and prostate cancer (Li et al., 2018; Lu et al., 2017; Song et al., 2016; Wang et al., 2016; Xu et al., 2017). Expression of *FOXR2* in pediatric tumors is primarily detected in nearly all CNS neuroblastomas with *FOXR2* activation (CNS NB-*FOXR2*), a recently identified entity that was described in 2016 in the context of a molecular re-evaluation of primitive neuroectodermal tumors of the central nervous system (CNS-PNET) (Sturm et al., 2016). Furthermore, subsets or single cases of medulloblastoma, pineoblastoma, glioblastoma and diffuse midline glioma (DMG) also express *FOXR2* (Koso et al., 2014; Liu et al., 2019; Liu et al., 2017). In addition, in the context of this study, *FOXR2* expression was observed in a clinically relevant subset of neuroblastoma (Figure 4) (Schmitt-Hoffner et al., 2021). In subsets of other non-brain pediatric tumors, *FOXR2* expression was not identified, yet. Mechanistically, the FOXR2 protein was found to bind to MYC and MYCN proteins, which are broadly implicated in the oncogenesis of poorly differentiated and often aggressive cancers (Beckmann et al., 2019; Li et al., 2016; Vita and Henriksson, 2006). The interaction between MYC and FOXR2 proteins results in a stabilization of the short-lived MYC protein as has been shown in a human Schwann cell line (Beckmann et al., 2019). In mice it was demonstrated that FOXR2 increases tumor growth and thereby decreases survival (Beckmann et al., 2019). Furthermore, it has been shown that FOXR2 induces the formation of CNS embryonal tumors in *Trp53* deficient mice (Poh et al., 2019). These results affirm the importance of *FOXR2* as a proto-oncogene and make it a promising therapeutic target to treat FOXR2-driven pediatric cancers. The molecular and clinical characterization of FOXR2 activated pediatric tumors may therefore provide a platform to improve our understanding of the mechanisms how FOXR2 drives tumor formation and to enable a differentiated clinical view on these tumors.

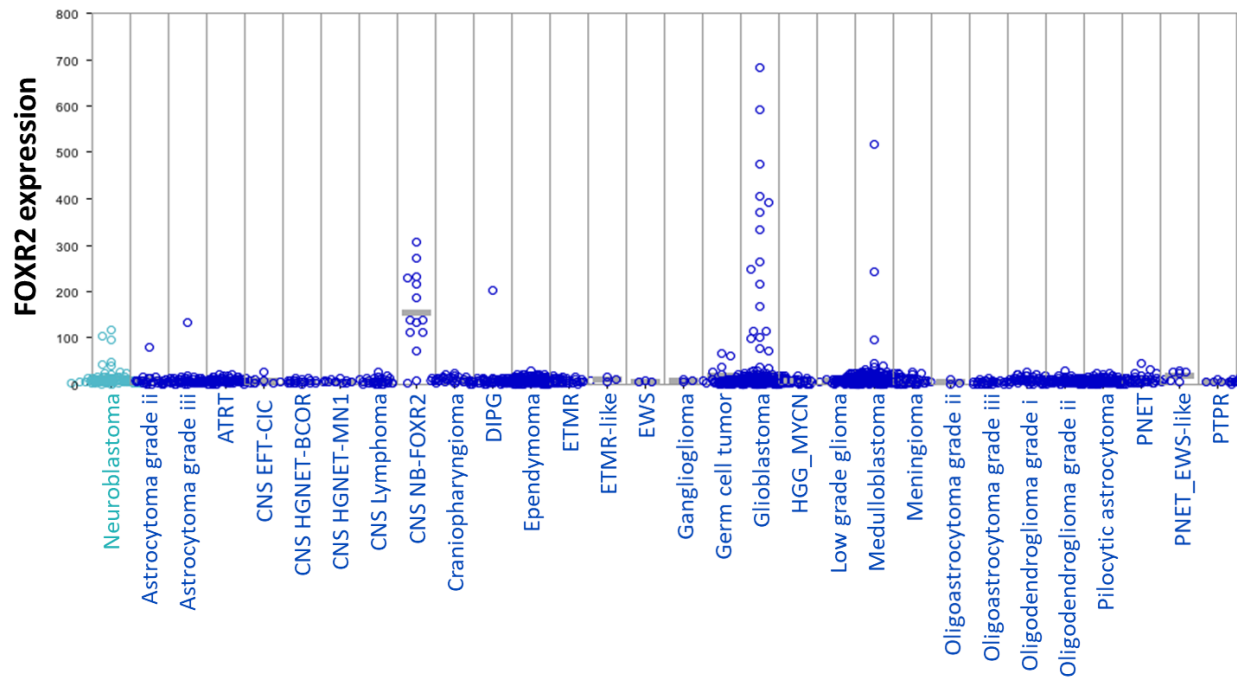


Figure 4: Expression of *FOXR2* mRNA in pediatric brain cancer and in peripheral neuroblastoma.

Subsets of pediatric brain cancer entities and a subset of neuroblastoma patients show mRNA expression of *FOXR2*. In CNS NB-*FOXR2* almost all cases show high expression levels of *FOXR2*. This figure was generated with the genomics analysis and visualization platform R2.

2 Materials and Methods

Materials and Methods are based on and are in parts directly adopted from the following joint publications:

Felix Schmitt-Hoffner*, Sjoerd van Rijn*, Umut H. Toprak, Monika Mauermann, Felix Rosemann, Anke Heit-Mondrzyk, Jens-Martin Hübner, Aylin Camgöz, Sabine Hartlieb, Stefan M. Pfister, Kai-Oliver Henrich, Frank Westermann*, Marcel Kool*; **“FOXR2 Stabilizes MYCN Protein and Identifies Non–MYCN-Amplified Neuroblastoma Patients With Unfavorable Outcome”**, Journal of Clinical Oncology, 2021, DOI: 10.1200/JCO.20.02540

Felix Schmitt-Hoffner and Sjoerd van Rijn are shared first authors. Marcel Kool and Frank Westermann are co-senior authors.

Katja von Hoff, Christine Haberler, **Felix Schmitt-Hoffner**, Elizabeth Schepke, Teresa de Rojas, Sandra Jacobs, Michal Zapotocky, David Sumerauer, Marta Perek-Polnik, Christelle Dufour, Dannis van Vuurden, Irene Slavc, Johannes Gojo, Jessica C. Pickles, Nicolas U. Gerber, Maura Massimino, Maria Joao Gil-da-Costa, Miklos Garami, Ella Kumirova, Astrid Sehested, David Scheie, Ofelia Cruz, Lucas Moreno, Jaeho Cho, Bernward Zeller, Niels Bovenschen, Michael Grotzer, Daniel Alderete, Matija Snuderl, Olga Zheludkova, Andrey Golanov, Konstantin Okonechnikov, Martin Mynarek, B. Ole Juhnke, Stefan Rutkowski, Ulrich Schüller, Barry Pizer, Barbara v. Zezschwitz, Robert Kwiecien, Maximilian Wechsung, Frank Konietzschke, Eugene I. Hwang, Dominik Sturm, Stefan M. Pfister, Andreas von Deimling, Elisabeth J. Rushing, Marina Ryzhova, Peter Hauser, Maria Łastowska, Pieter Wesseling, Felice Giangaspero, Cynthia Hawkins, Dominique Figarella-Branger, Charles Eberhart, Peter Burger, Marco Gessi, Andrey Korshunov, Tom S. Jacques, David Capper, Torsten Pietsch, Marcel Kool; **“Therapeutic implications of improved molecular diagnostics for rare CNS-embryonal tumor entities – results of an international, retrospective study”**;

Neuro-Oncology; 2021; <https://doi.org/10.1093/neuonc/noab136>

Andrey Korshunov, Konstantin Okonechnikov, **Felix Schmitt-Hoffner**, Marina Ryzhova, Felix Sahm, Damian Stichel, Daniel Schrimpf, David E. Reuss, Philipp Sievers, Abigail Kora Suwala, Ella Kumirova, Olga Zheludkova, Andrey Golanov, David T. W. Jones, Stefan M. Pfister,

Marcel Kool, Andreas von Deimling; **“Molecular analysis of pediatric CNS-PNET revealed nosologic heterogeneity and potent diagnostic markers for CNS neuroblastoma with *FOXR2*-activation”**

Acta Neuropathologica Communications; 2021; <https://doi.org/10.1186/s40478-021-01118-5>

2.1 Materials and methods based on “*FOXR2* Stabilizes *MYCN* Protein and Identifies Non-*MYCN*-Amplified Neuroblastoma Patients With Unfavorable Outcome”

2.1.1 Neuroblastoma cohorts

To investigate *FOXR2* in neuroblastoma the R2 dataset “Tumor Neuroblastoma - SEQC - 498 - RPM - seqcnb1” was consulted, containing RNA-seq data on 498 primary neuroblastomas (Su et al., 2014). The dataset includes full clinical annotation as well as annotations on INSS, age, sex and high-risk status (Gene Expression Omnibus (GEO) accession gse62564). Furthermore, a microarray dataset of 283 primary neuroblastomas with full clinical annotation was consulted to confirm the findings: “Tumor Neuroblastoma Primary - NRC - 283 - rma_sketch (bc) - huex10t” by the Neuroblastoma Research Consortium (NRC), which is deposited under GEO ID: gse85047. The TARGET dataset containing primarily high-risk neuroblastoma was consulted via R2 “Tumor Neuroblastoma TARGET - Asgharzadeh - 249 - custom - huex10t” (Pugh et al., 2013). The dbGaP Study Accession ID is: phs000218.v22.p8. All datasets were analyzed in the R2 platform for genomic data analysis and visualization (<http://r2.amc.nl>).

2.1.2 Cell culture

HEK293T cells were cultivated in Dulbecco’s modified Eagle’s medium supplemented with 10% fetal calf serum (FCS). SK-N-AS and SK-N-FI were cultured in RPMI-1640 medium

supplemented with 10% FCS. All cells were incubated at 37°C in a humidified incubator with 5% CO₂.

2.1.3 Production of lentiviral vectors and generation of stable cell lines

shRNAs were used to knock down FOXR2 in SK-N-AS and SK-N-FI. Lentiviral transduction of pLKO-TET-ON was used to establish stable cell lines (Wee et al., 2008; Wiederschain et al., 2009) with the inducible FOXR2 shRNA insert 5'-CTGGAAGAGCACCATTCATTA-3' and the scrambled insert 5'-CCTAAGGTTAAGTCGCCCTCG-3', which was used as a control. Lentivirus was produced in HEK293T cells by co-transfection of psPax2 and pMD2.G using FugeneHD (Promega). The supernatant containing the lentivirus was filtered and transferred to SK-N-AS and SK-N-FI. Successfully transfected cells were selected by 1µg/ml puromycin and induced by 1µg/ml doxycycline (Hübner et al., 2019). In accordance with the National Institutes of Health Guidelines these experiments were performed under Biosafety Level 2 (BSL-2) conditions.

2.1.4 Quantitative RT-PCR

RNA isolation was conducted with the Maxwell® RSC instrument applying the simplyRNA Tissue Kit according to the manufacturer's protocol. Quantitative RT-PCR was performed using the Power SYBR® Green RNA-to-CT™ 1-Step Kit (Applied Biosystems) according to the manufacturer's protocol. The expression fold change was determined according to the 2- $\Delta\Delta$ ct method taking into account the housekeeping gene GAPDH and the difference between scrambled and FOXR2 shRNA. Primers that were applied for quantitative RT-PCR are specified in Table 1.

Table 1: Primers used for quantitative RT-PCR. Table from (Schmitt-Hoffner et al., 2021).

Target	Direction	Sequence (5'-3')
GAPDH	forward	CAACAGCCTCAAGATCATCAG
GAPDH	reverse	ATGGACTGTGGTCATGAGTC
FOXR2	forward	GACCCCAATATCCTGTGCC
FOXR2	reverse	GCTCAAAGTCACTGGGGGAA
MYCN	forward	GATGCACCCACAGAAGAA
MYCN	reverse	CTCCGAGTCAGAGTTTCGGG

2.1.5 Cell viability

CellTiter-Glo® Luminescent Cell Viability Assay (Promega) was used to determine the viability of SK-N-AS according to the manufacturer's protocol. The viability of SK-N-FI was determined using RealTime-Glo™ MT Cell Viability Assay (Promega). The cells were incubated with RealTime-Glo dilution for 1h at 37°C before measuring. Directly after the measurement the medium was replaced. SK-N-AS and SK-N-FI were seeded in 96 well plates at a seeding density of 2000 and 1000 cells per well, respectively. The luminescent signal was measured using the Mithras LB 940 microplate reader.

2.1.6 Cell cycle and cell death

The Annexin V-FITC Apoptosis Detection Kit (Sigma-Aldrich) was applied to assess cell death according to the manufacturer's protocol. Flow cytometry using BD FACSCanto II was used for detection. For quantification of dead and live cells, the Propidium Iodide (PI) positive cells (quadrant 1 and 2) were compared to the PI negative cells (quadrant 3 and 4). Cellular DNA content was stained by PI and detected and quantified by flow cytometry for cell cycle analysis. Cells were harvested, washed and resuspended in PBS at 4°C. Subsequently, the cells were fixed in 70% ethanol and incubated at 4°C for 2h. After two further washing steps the cells were resuspended in PI staining solution (0.1% Triton X-100, 10 µg/ml PI and 100 µg/ml DNase-free RNase) and incubated for 30 min at 37°C protected from light. Read out and analysis were performed applying flow cytometry and FlowJo. The data of each sample is based on a minimum of 10,000 events.

2.1.7 Western blot analysis

Cells were lysed in Radioimmunoprecipitation assay (RIPA) buffer (Sigma-Aldrich) or 8 M Urea containing phosphatase and protease inhibitors (Thermo Scientific). A bicinchoninic acid assay (BCA) (Thermo Fisher Scientific) was performed to determine protein concentrations. Lysates were separated using a 4-12% Bis-Tris gradient gel (Invitrogen) and transferred on a 0.2 µm polyvinylidene difluoride (PVDF) membrane. To block the PVDF membrane, it was incubated for 1h in 5% skim milk (Sigma-Aldrich) in Tris-buffered saline with Tween (TBS-T) solution. Primary antibodies were incubated over night at 4°C. After washing, the secondary antibody

was incubated at room temperature for 1h, followed by a further washing step. ECL prime detection reagent or ECL detection reagent (GE Healthcare) were added onto the membrane to detect chemiluminescence applying the Chemostar ECL Image (Intas Science Imaging). Primary antibodies against FOXR2 (Sigma-Aldrich, HPA057358), MYCN (Sigma-Aldrich, MABE333), MYC (abcam, ab32072), HA-tag (abcam, ab91110), β -actin (abcam, ab49900) were used and detected by chemiluminescence via secondary goat anti-rabbit and goat anti-mouse antibodies (Cell Signaling Technology) conjugated to horseradish peroxidase (HRP). Western blots were quantified using ImageJ.

2.1.8 CHX assay

Cells were plated in 6-well plates and incubated with 300 ng/ μ l cyclohexamide (CHX, Sigma-Aldrich) to stop translation. After 0h, 1h, 2h and 4h the cells were harvested. Protein levels were analyzed by western blot as described above.

2.1.9 Co-immunoprecipitation

Cells were lysed in NETN lysis buffer. Lysates were centrifuged at 14,000 rpm for 10 min at 4°C. Lysates were precleared by adding 10 μ l magnetic A/G beads and incubated of 1 h at 4°C. The beads were discarded and subsequently the precleared lysate was incubated with 2 μ g antibody for 1h at 4°C. In the next step 25 μ g magnetic beads were added. After three washing steps, the lysate, containing beads and antibodies, was incubated over night at 4°C. Subsequently, beads were washed and the target proteins were eluted using 40 μ l elution buffer. After boiling for 4 minutes, proteins were separated following the western blot protocol described above.

2.1.10 Gene expression analysis

Gene expression profiles of doxycycline-induced and non-induced SK-N-AS and SK-N-FI with *FOXR2* shRNA as well as with scrambled shRNA were generated on Affymetrix GeneChips® Human U133 Plus 2.0 arrays by the DKFZ Genomics and Proteomics Core Facility. Gene expression profiles can be accessed in Gene Expression Omnibus under accession number

GSE156092. CEL files were uploaded to the R2 platform (<http://r2.amc.nl>) for analysis and visualization. The Gene Set Enrichment Analysis (GSEA) software (Liberzon et al., 2011; Subramanian et al., 2005) was used to identify biological processes, which were associated with the *FOXR2* knockdown in SK-N-AS based on a background of 13,154 genes. Further pathway analyses on increased and decreased functions in the *FOXR2* knockdown cell lines SK-N-AS and SK-N-FI were conducted through the Ingenuity Pathway Analysis (IPA) software (QIAGEN Inc.).

2.1.11 Statistical analyses

Statistical comparison of *FOXR2* levels between shRNA knockdown cell lines was assessed by two-tailed t-test. Genes that were significantly differentially expressed in SK-N-AS and SK-N-FI after induction of the shRNA mediated *FOXR2* knockdown were defined by ANOVA (p -value < 0.05) and were corrected applying false discovery rate (FDR). For this analysis a minimal highest expression value of 50 units and minimal expression difference value of 50 units were defined in R2. To determine the difference in distribution of *FOXR2* cases over INSS stages and to assess the distribution of TERT positive cases over the groups *FOXR1*, *FOXR2*, *MYC*, *MYCN* and *OTHER* χ^2 analyses were performed. EFS and OS of the expression-based groups were analyzed and statistically compared applying log-rank tests performed by R2. SPSS was applied to perform multivariable Cox regression analyses in order to analyze the expression of *FOXR2* as a prognostic marker compared to other established risk factors including INSS stage, *MYCN* amplification, age at diagnosis or high-risk status. The distribution of these risk factors in each dataset is listed in Table 2. In general, p -values < 0.05 were considered statistically significant.

Table 2: Proportional distribution of risk factors and expression groups in the RNA-seq, NRC and TARGET dataset. Table from (Schmitt-Hoffner et al., 2021).

	RNA-seq dataset (n = 498)	NRC dataset (n = 283)	TARGET dataset (n = 249)	Total (n = 1030)
Age at diagnosis				
< 18 months	305 (61%)	145 (51%)	32 (13%)	482 (47%)
> 18 months	193 (39%)	133 (47%)	217 (87%)	543 (53%)
N/A	0 (0%)	5 (2%)	0 (0%)	5 (0%)
MYCN status				
amplified	92 (18%)	55 (19%)	68 (28%)	215 (21%)
non-amplified	401 (81%)	222 (79%)	175 (70%)	798 (77%)
N/A	5 (1%)	6 (2%)	6 (2%)	17 (2%)
INSS stage				
1	121 (24%)	50 (18%)	30 (12%)	201 (20%)
2	78 (16%)	36 (13%)	0 (0%)	114 (11%)
3	63 (13%)	43 (15%)	1 (0%)	107 (10%)
4	183 (37%)	124 (44%)	216 (87%)	523 (51%)
4s	53 (10%)	27 (9%)	0 (0%)	80 (8%)
N/A	0 (0%)	3 (1%)	2 (1%)	5 (0%)
Risk group				
non-high risk	318 (64%)	161 (57%)	30 (12%)	509 (50%)
high risk	175 (35%)	115 (41%)	217 (87%)	507 (49%)
N/A	5 (1%)	7 (2%)	2 (1%)	14 (1%)
Groups based on expression				
FOXR1	7 (1%)	4 (1%)	1 (0%)	12 (1%)
FOXR2	42 (8%)	17 (6%)	34 (14%)	93 (9%)
MYC	16 (3%)	5 (2%)	5 (2%)	26 (3%)
MYCN	92 (18%)	55 (20%)	63 (25%)	210 (20%)
OTHER	341 (70%)	202 (71%)	146 (59%)	689 (67%)

2.2 Material and methods based on “Therapeutic implications of improved molecular diagnostics for rare CNS-embryonal tumor entities – results of an international, retrospective study”

2.2.1 Study design and participants

Within this retrospective, international study, tumor samples and clinical data of patients, which were institutionally diagnosed with CNS-PNET, were collected and analyzed. In total twenty national groups and institutions contributed to this study, which has been approved by the ethics board of the coordinating institution as well as by the respective ethic boards of the participating institutions. Only cases that were histologically diagnosed as CNS-PNET or supratentorial PNET (cases diagnosed before the 2007 WHO classification of CNS tumors), for which formalin-fixed paraffin-embedded (FFPE) material for molecular analyses was available, were included in the cohort. For further clinical evaluation, additional 66 CNS NB-*FOXR2* cases with available DNA methylation data were added subsequently.

2.2.2 Histological and molecular re-evaluation

Histologically diagnosed CNS-PNET were molecularly re-evaluated using DNA methylation data. The “Heidelberg brain tumor classifier v11b4” (www.moleculareuropathology.org) was applied for classification based on entity specific DNA methylation pattern, as described in previous studies (Capper et al., 2018a; Capper et al., 2018b). A Maxscore of above 0.9 given by the classifier as well as clustering analyses by means of t-distributed stochastic neighbor embedding (t-SNE) were used to determine the molecular entity of the histologically diagnosed CNS-PNET cases. DNA methylation data was used to deduct copy number profiles applying the conumee package v1.3.0 (Hovestadt and Zapatka, 2017).

2.2.3 Cohort description and clinical data

DNA of 307 histologically diagnosed CNS-PNET was submitted for DNA methylation profiling. 74 out of 307 CNS-PNET cases and 44 of the 66 additional CNS NB-*FOXR2* patients have been described already in previous studies (Holsten et al., 2021; Hwang et al., 2018; Lambo et al., 2019b; Sturm et al., 2016). Patients of the cohort were diagnosed between 1988 and

2017. Clinical data was available for 292 patients. 204 patients received treatment within or according to clinical trials recruiting CNS-PNET patients (Aridgides et al., 2019; Dufour et al., 2014; Fangusaro et al., 2008; Friedrich et al., 2013; Gerber et al., 2014; Hwang et al., 2018; Massimino et al., 2006; Timmermann et al., 2006; von Hoff et al., 2009). Staging of the patients was determined based on the Chang classification (Chang et al., 1969).

2.3 Material and methods based on “Molecular analysis of pediatric CNS-PNET revealed nosologic heterogeneity and potent diagnostic markers for CNS neuroblastoma with *FOXR2*-activation”

2.3.1 Patient cohort

84 patients that were histologically diagnosed as CNS-PNET at the Burdenko Neurosurgical Institute in Moscow as well as the gene expression profiling dataset “Tumor Brain (DKFZ-public) - Kool - 2482 - MAS5.0 - u133p2” available on the R2 platform (<https://hgserver1.amc.nl/cgi-bin/r2/main.cgi>) containing 14 CNS NB-*FOXR2* were analyzed within this study. The age of the patients diagnosed at the Burdenko Neurosurgical Institute in Moscow ranged from 3 to 18 years and the patients were diagnosed between 01.01.2000 and 31.12.2016. Pineoblastoma (located in the pineal region) as well as atypical teratoid/rhabdoid tumor (AT/RT) and embryonal tumors with multilayered rosettes (ETMR), identified by LIN28A and INI1 immunohistochemistry (IHC), were excluded from the cohort.

2.3.2 DNA methylation array processing

Eighty-four FFPE tissue samples were available for DNA and RNA extraction. Using the Maxwell system (Promega, USA), 84 DNA samples and 53 RNA samples could be extracted with sufficient quality. The Illumina Human Methylation 450 k or 850 k/EPIC BeadChip array was used to generate DNA methylation data as described previously (Capper et al., 2018b; Korshunov et al., 2016; Pajtler et al., 2015; Reinhardt et al., 2019). Probes that are not represented in the 450k array but in the EPIC array were removed to allow comparability of the two arrays, resulting in 428,799 probes, which were processed and analyzed. The t-

distributed stochastic neighbor embedding (t-SNE) plots were generated using Rtsne (Van der Maaten and Hinton, 2008). The 84 cases were molecularly classified based on their characteristic methylation pattern applying the “Heidelberg brain tumor classifier v11b4” (www.moleculareuropathology.org). Maxscores of above 0.9 were defined as the lowest threshold to identify a specific entity. Thirty-two out of eighty-four cases (38%) were already included in previous studies (Capper et al., 2018a; Sturm et al., 2016).

2.3.3 RNA-sequencing and gene expression analyses

The NextSeq 500 sequencing system (Illumina) was used for RNA-sequencing of 53 samples as described in previous studies (Korshunov et al., 2020; Stichel et al., 2019). The alignment of reads as well as the elimination of samples with low quality was conducted as described previously (Korshunov et al., 2020; Okonechnikov et al., 2016). Molecular analyses by means of hierarchical clustering, principle component analysis (PCA) and t-SNE were performed using the 250, 500 and 1000 most differentially expressed genes, identified applying the DESeq 2 R package (adjusted p-value < 0.05) based on log₂ RPKM values (Love et al., 2014). Additionally the Affymetrix dataset “Tumor Brain (DKFZ-public) - Kool - 2482 - MAS5.0 - u133p2” containing 14 CNS NB-*FOXR2* cases was consulted. R2 was used for data analyses and the visualization of *SOX10* and *ANKRD55* gene expression of the distinct molecular entities of this cohort (<http://r2.amc.nl>).

2.3.4 Immunohistochemistry

To validate findings based on the molecular analyses, 4 µm sections of FFPE tumor tissue were mounted on slides by drying it for 15 minutes at 80°C. Immunohistochemical stainings were performed with a *SOX10* monoclonal antibody (Thermo Fisher Scientific Inc.; AB_2572892; clone 20B7) and an *ANKRD55* polyclonal antibody (Novus Biological; NBP2-14719). The automated immunostainer (Benchmark; Ventana XT) was applied to stain the slides with the *SOX10* antibody (dilution 1:100) and the *ANKRD55* antibody (dilution 1:20). Both antibodies were incubated at 37°C for 32 minutes. Staining intensities and numbers of nuclear *SOX10* and cytoplasmic *ANKRD55* positive cells were assessed and staged into the four categories: 1. Negative: no staining signal, 2. Low: 1-25% staining signal, 3. Moderate: 25-74% staining signal and 4. High: 75%-100% staining signal.

3 First chapter: The role of FOXR2 in peripheral neuroblastoma

3.1 Introduction

3.1.1 An overview on neuroblastoma

Neuroblastoma is a malignant embryonal tumor, derived from the neural crest during the development of the sympathetic nervous system (Johnsen et al., 2019). It occurs primarily in early childhood, where neuroblastoma constitutes the most common solid cancer diagnosed in children within their first year of life showing an incidence of 25 to 50 cases per million (American_Cancer_Society, accessed 12.11.2021; Heck et al., 2009; Matthay et al., 2016; Stiller and Parkin, 1992). The clinical outcome of neuroblastoma is highly variable and it accounts for 15% of all cancer deaths in children between the age 0 and 14 years (Ganeshan and Schor, 2011; Jiang et al., 2011; Swift et al., 2018). Most frequently neuroblastoma arises from the abdominal ganglia along the spine (60%) and from the adrenal medulla (30%), but it may also manifest in the sympathetic ganglia in the chest, pelvis as well as the head and neck region (Louis and Shohet, 2015; Maris, 2010). In adolescence and especially in adulthood, neuroblastoma is very rare and only 10% of neuroblastomas occur in children above 10 years of age (Conter et al., 2014; London et al., 2005; Matthay et al., 2016).

3.1.2 Risk stratification in neuroblastoma

Neuroblastoma patients show a broad spectrum of clinical outcomes, which ranges from spontaneous regression of the tumor to aggressive tumor progression and fatal outcome (Brodeur and Bagatell, 2014; Matthay et al., 2016; Pinto et al., 2015; Tolbert and Matthay, 2018). As a consequence of this, low-risk neuroblastoma shows favorable 5-year overall survival (OS) rates of above 95%, whereas high-risk neuroblastoma, which is primarily diagnosed in patients that harbor *MYCN*-amplifications in their tumor and/or are diagnosed after passing the age of 18 months in combination with INSS stage 4, show poor survival with a 5-year OS of below 50% (Maris, 2010; Meany, 2019; Pinto et al., 2015; Zhang et al., 2015). Over the last decades a variety of biological and clinical factors have been investigated aiming to improve the risk stratification of neuroblastoma patients and to identify targeted approaches to treat these patients. However, patient stratification between different countries and trials still varies, which challenges the comparability and the conclusions drawn from international multi-institutional collaborations. In order to establish an internationally concordant pretreatment risk

stratification, the International Neuroblastoma Risk Group (INRG) classification system was introduced in 2008, describing crucial risk factors in neuroblastoma based on which patients are classified in very low, low, intermediate and high pretreatment risk groups (Figure 5) (Ambros et al., 2009; Cohn et al., 2009; Monclair et al., 2009). These biological and clinical factors include age at diagnosis, histology, grade of tumor differentiation, *MYCN* amplification status, chromosome 11q aberration status, tumor cell ploidy and INRG stage, which comparably to the International Neuroblastoma Staging System (INSS) describes the disease stage (Sokol and Desai, 2019). On top of that over the last years several additional factors were identified that indicate a poor survival in neuroblastoma patients. These include telomerase maintenance mechanisms (TMM) and segmental chromosome aberrations (SCA) (Ackermann et al., 2018; Irwin et al., 2021). TMMs in neuroblastoma include alternative lengthening of telomeres (ALT), which is correlated with *ATRX* mutations (Clynes et al., 2015; Zeineldin et al., 2020), and the activation of telomerase reverse transcriptase (*TERT*), which is induced either by transcriptional activation through *MYCN* or by *TERT* rearrangements (Krämer, 2017; Mac et al., 2000; Peifer et al., 2015; Roderwieser et al., 2019; Stainczyk and Westermann, 2021; Valentijn et al., 2015a). SCAs that are associated with unfavorable outcome in neuroblastoma include chromosome 1p, 3p, 6q, and 11q deletion and 17q gain (Attiyeh et al., 2005; Depuydt et al., 2018; Schleiermacher et al., 2012; Spitz et al., 2003). Other SCA, such as 1p and 11p deletion were more recently evaluated in the context of the INRG classification system to improve risk stratification (Irwin et al., 2021). Identification and evaluation of new prognostic factors that were first described in recent years indicates the ongoing and dynamic process of improving risk stratification of patients in order to provide target- and risk-adjusted clinical care.

INRG Stage	Age (months)	Histologic Category	Grade of Tumor Differentiation	MYCN	11q Aberration	Ploidy	Pretreatment Risk Group		
L1/L2		GN maturing; GNB intermixed					A Very low		
L1		Any, except GN maturing or GNB intermixed		NA			B Very low		
				Amp			K High		
L2	< 18	Any, except GN maturing or GNB intermixed		NA	No		D Low		
					Yes		G Intermediate		
	≥ 18	GNB nodular; neuroblastoma	Differentiating	NA	No		E Low		
					Yes		H Intermediate		
					Poorly differentiated or undifferentiated	NA			
							Amp		N High
M	< 18			NA		Hyperdiploid	F Low		
	< 12			NA		Diploid	I Intermediate		
	12 to < 18			NA		Diploid	J Intermediate		
	< 18			Amp			O High		
	≥ 18						P High		
MS					No		C Very low		
	< 18			NA	Yes		Q High		
					Amp			R High	

Figure 5: INRG pretreatment classification scheme.

The INRG stratification into pretreatment risk groups based on biological and clinical factors was presented in 2008 in order to establish a consensus approach for pretreatment risk stratification. Figure from (Cohn et al., 2009).

3.1.3 Aim of this study

The clinical course of neuroblastoma patients varies substantially. To clearly distinguish the health risk of patients and to identify targets to treat neuroblastoma patients with specific molecular characteristics, the identification of prognostic markers that improve risk stratification and the understanding of mechanisms that cause oncogenesis and tumor progression in neuroblastoma is key.

The aim of this study was to investigate the clinical relevance and the mechanistic role of FOXR2 in neuroblastoma. Using three gene expression datasets that contained a total of 1030 neuroblastoma patients with full clinical annotation, a subset of neuroblastoma patients that express FOXR2, an oncogene that was previously identified to be activated in other pediatric cancers such as CNS NB-FOXR2 (Sturm et al., 2016), was identified. In this study, the clinical characteristics of these neuroblastoma patients were analyzed and the interaction between FOXR2 and MYCN was investigated *in vitro* and in patient samples to reveal the mechanism that might drive FOXR2-activated neuroblastoma.

3.2 Results

The Results (3.2) and Discussion (3.3) of the first chapter were published in the Journal of Clinical Oncology (Schmitt-Hoffner et al., 2021) and are based on this publication. Content, including figures, tables and text shown in this chapter was directly adopted or modified from the publication.

Publication:

Felix Schmitt-Hoffner*, Sjoerd van Rijn*, Umut H. Toprak, Monika Mauermann, Felix Rosemann, Anke Heit-Mondrzyk, Jens-Martin Hübner, Aylin Camgöz, Sabine Hartlieb, Stefan M. Pfister, Kai-Oliver Henrich, Frank Westermann*, Marcel Kool*; **“*FOXR2* Stabilizes *MYCN* Protein and Identifies Non-*MYCN*-Amplified Neuroblastoma Patients With Unfavorable Outcome”**, Journal of Clinical Oncology, 2021, DOI: 10.1200/JCO.20.02540

Felix Schmitt-Hoffner and Sjoerd van Rijn are co-first authors. Marcel Kool and Frank Westermann are co-senior authors.

3.2.1 Expression of *FOXR2* in peripheral neuroblastoma

In this study, a previously unreported subset of neuroblastoma expressing *FOXR2* was identified. In an RNA-seq cohort 8% (42 out of 498 cases) expressed this transcription factor (Figure 6A). All other cases did not show or showed only minimal levels of *FOXR2* expression (Figure 6B). Interestingly, the expression of *FOXR1*, present in 1% (7 out of 498 cases) and encoding a homologue of *FOXR2* that was previously reported in a small fraction of neuroblastomas (Katoh and Katoh, 2004c; Santo et al., 2012), as well as the expression of the proto-oncogenes *MYC* and *MYCN*, present in 3% (14 out of 498 cases) and 18% (92 out of 498 cases), respectively, were all observed in an almost mutually exclusive fashion (Figure 6B). High expression levels in the *MYCN* group were driven by amplifications of the *MYCN* gene in 98% (90 out of 92) of cases, which is a well established prognostic marker in neuroblastoma. The 341 remaining cases in this cohort, referred to as “OTHER”, were defined by the lack of *FOXR2*, *FOXR1*, *MYC* or *MYCN* expression. *FOXR2* expression was also analyzed in two non-overlapping neuroblastoma datasets based on Affymetrix gene expression arrays (Pugh et al., 2013; Rajbhandari et al., 2018). Analyses of the Neuroblastoma

Research Consortium (NRC) (n=283) as well as the TARGET series (n=249) revealed similar findings: *FOXR2* was expressed in 14% (34 out of 249) and 6% (17 out of 283) of cases, respectively. In both the NRC and the TARGET datasets the expression of *FOXR2* was again almost mutually exclusive with the groups expressing *FOXR1*, *MYC* or *MYCN* (Figure 6C, D). To analyze the distribution of the *FOXR2*-expressing group within the International Neuroblastoma Staging System (INSS), the cases with available INSS information of the three neuroblastoma datasets were combined (n=1025). The 90 cases (9%) of the combined cohort that expressed *FOXR2* were distributed over all INSS stages but showed a significant enrichment in stage 3 and 4 when compared to stage 1, 2 and 4s (χ^2 -test, *p*-value 0.001) (Figure 6E). Overrepresentation of *FOXR2* cases in more aggressive subtypes is in line with the higher percentages of *MYCN*-amplified cases in INSS4 (Figure 6E), which is not seen for the *MYC*- and *FOXR1*-expressing cases. Investigating the distribution of *FOXR2*-expressing cases between risk groups I observed that they are present in the high-risk (10%, 52 out of 507 cases) as well as in the non high-risk (8%, 39 out of 509 cases) subset (Figure 6F).

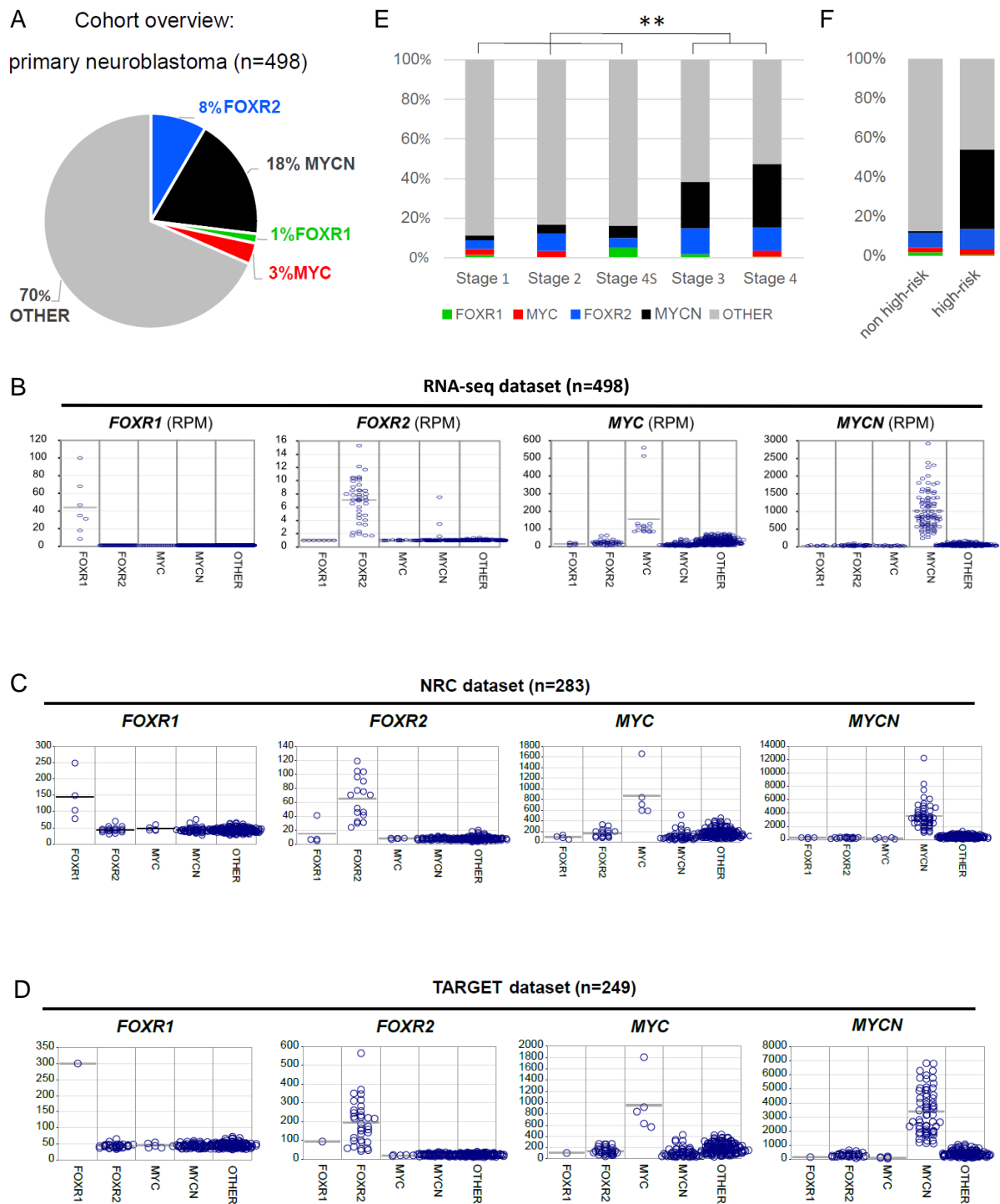


Figure 6: **FOXR2** expression in a subset of neuroblastoma.

(A) Proportion of *FOXR2*, *FOXR1*, *MYC* and *MYCN* expression in the RNA-seq dataset. (B) Mutually exclusive expression of *FOXR2*, *FOXR1*, *MYC* and *MYCN* in nearly all cases in the RNA-seq dataset. (C) Mutually exclusive expression of *FOXR2*, *FOXR1*, *MYC* and *MYCN* in nearly all cases in the NRC dataset. (D) Mutually exclusive expression of *FOXR2*, *FOXR1*, *MYC* and *MYCN* in nearly all cases in the TARGET dataset. (E) Distribution of *FOXR2*, *FOXR1*, *MYC* and *MYCN*-expressing cases in the stages of the INSS. (F) Distribution of the molecular groups in high-risk and non high-risk tumors. Figure modified from (Schmitt-Hoffner et al., 2021).

3.2.2 FOXR2-expressing cases do not show ALT phenotype but increased TERT expression

Besides *MYCN*-amplification, telomerase maintenance mechanisms like *TERT*-rearrangements or ALT phenotype are further prognostic markers that were investigated in the context of *FOXR2* expression (Koneru et al., 2020; Peifer et al., 2015; Valentijn et al., 2015b; Zeineldin et al., 2020). Status of the ALT phenotype was assessed via C-Circle assays (Hartlieb et al., 2021). When analyzing cases with available ALT status (174/498 cases), including 16 *FOXR2*-, 5 *FOXR1*-, 7 *MYC*-, 41 *MYCN*-expressing cases, and 105 OTHERs, it was observed that none of the *FOXR2*- or *FOXR1*-expressing neuroblastomas showed an ALT phenotype (Figure 7A). Furthermore, as previously reported, also the *MYCN* group did not include any ALT cases (Zeineldin et al., 2020). In the *MYC* group, only two cases with an ALT phenotype were observed (Figure 7A). Altogether, these data indicate that *FOXR2* expression, *FOXR1* expression, *MYCN* amplification, and largely *MYC* expression occurs in a mutually exclusive fashion with an ALT phenotype in neuroblastoma. To investigate the distribution of *TERT* activation in the different groups, a threshold of activated *TERT* expression was determined. As previously shown, *TERT* expression in neuroblastoma can be induced by *MYCN* or is activated by *TERT* rearrangements (Ackermann et al., 2018; Peifer et al., 2015). Therefore, the lowest expression level of *TERT* among *TERT*-rearranged cases was identified and used as a cut-off to annotate all *TERT*-activated cases. Based on these data, the *FOXR2* group showed a significant enrichment of *TERT*-activated cases (χ^2 -test, $P < 0.001$) (Figure 7B). As expected this was also the case for the *MYCN* group (χ^2 -test, $P < 0.001$). The *MYC*, *FOXR1* and OTHER group showed less *TERT*-activated cases than expected by chance (Figure 7B). In line with these findings high levels of *TERT* expression were observed in the *FOXR2* group whereas the overall *TERT* expression levels in the residual cases (*MYCN* group excluded) was clearly lower (Figure 7C).

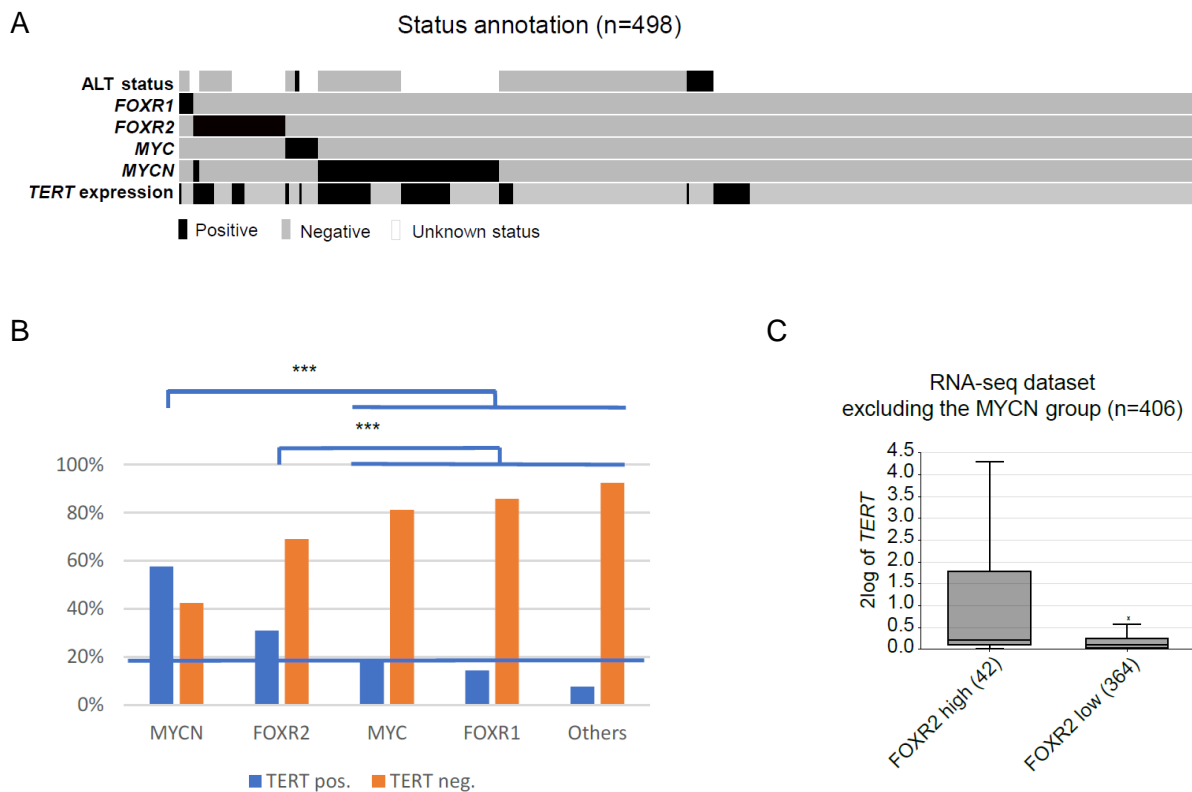


Figure 7: ***TERT***-expression is increased in the ***FOXR2*** group.

(A) Oncoprint of ALT status, *FOXR1*, *FOXR2*, *MYC*, *MYCN* and *TERT* expression in the RNA-seq dataset. (B) Distribution of *TERT* positive cases over the molecular groups. (C) *TERT* expression levels in cases expressing high levels of *FOXR2* and cases with low or absent levels of *FOXR2*. Figure modified from (Schmitt-Hoffner et al., 2021).

3.2.3 *FOXR2* expression identifies neuroblastoma patients with unfavorable outcome independent from established prognostic factors

To identify clinical implications of *FOXR2* in neuroblastoma, the clinical characteristics of the *FOXR2*-expressing neuroblastomas were compared to the remaining groups that show *FOXR1*, *MYC*, *MYCN* expression and all other neuroblastomas, not showing any of these characteristics. Overall survival (OS) and event-free survival (EFS) curves in the RNA-seq dataset indicated that the *FOXR2* group has a 5-year and 10-year OS of 67% (95% CI of 49-79) and 59% (95% CI of 38-75), respectively, and a 5- and 10-year EFS of 51% (95% CI of 35-65). This was in both cases significantly ($P < 0.01$) reduced compared to the OTHER group indicating a 5- and 10-year OS of 91% (95% CI of 87-93) and 88% (95% CI of 83-91),

respectively, and a 5- and 10-year EFS of 74% (95% CI of 69-78) and 72% (95% CI of 67-77) (Figure 8A). As expected also the *MYCN* group showed a significantly ($P<0.001$) worse outcome when compared to the OTHER group, but also a significantly ($P=0.002$) worse outcome than the *FOXR2* group with a 5- and 10-year OS of 37% (95% CI of 26-48) and a 5- and 10-year EFS of 29% (95% CI of 19-39) (Figure 8A). The small subset of patients with *FOXR1* expression showed a 5- and 10-year OS of 57% (95% CI of 17-84), which is similar to the OS of the *FOXR2* group ($P=0.715$). Primary neuroblastomas with elevated *MYC* expression revealed a relatively good outcome compared to the previously mentioned groups with a 5- and 10-year OS of 85% (95% CI of 52-96) (Figure 8A).

Consulting the independent NRC microarray dataset, similar findings to the RNA-seq dataset were made, showing that the *FOXR2*-expressing subset (5- and 10-year OS 53% (95% CI of 25-74)) forms a group with a significantly ($P<0.001$) worse outcome than the OTHER group (5-year OS 82% (95% CI of 74-87); 10-year OS 80% (95% CI of 71-86)) (Figure 8B). Consistent with the RNA-seq dataset, the *MYCN* group also showed a worse patient outcome than the *FOXR2* group in the NRC dataset with a 5- and 10-year OS of 26% (95% CI of 14-40) (Figure 8B). The third dataset investigated within this study (TARGET) was not used as a reference for the overall survival analysis due to the high proportion of high-risk tumors, but was investigated in the following analyses comparing exclusively high-risk subsets.

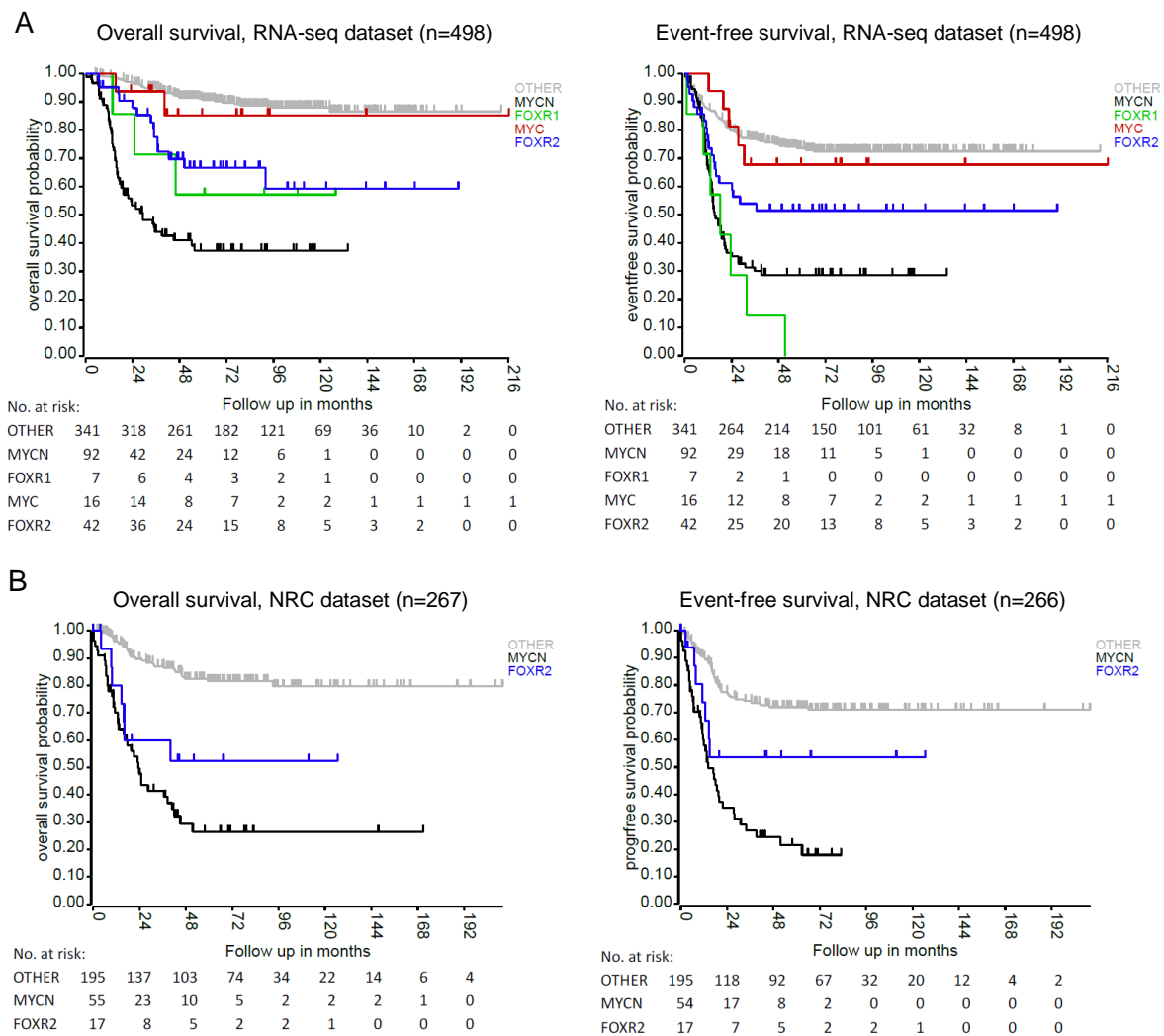


Figure 8: Survival analyses of the *FOXR2*, *FOXR1*, *MYC*, *MYCN* and *OTHER* group.

(A) Overall and event-free survival of the distinct molecular groups in the RNA-seq dataset (n=498). (B) Overall and event-free survival of the distinct molecular groups in the NRC dataset (n=267/n=266). The *FOXR1* and the *MYC* group were excluded due to low group numbers. Figure modified from (Schmitt-Hoffner et al., 2021).

Within the high-risk subsets of the RNA-seq, NRC and TARGET datasets the *FOXR2* group showed a very poor clinical outcome with a 5-year OS of 34% (95% CI of 11-60), 0% and 24% (95% CI of 11-40), respectively (Figure 9A, B, C). The OS of the *FOXR2* group in the RNA-seq dataset was comparable and in the NRC and the TARGET dataset slightly worse but not significantly different from the OS of the *MYCN* group (RNA-seq dataset $P=0.971$, NRC dataset $P=0.063$, TARGET dataset $P=0.172$). When *FOXR2*-expressing cases were compared to the *OTHER* group, they showed a significantly worse survival within the high-risk subsets of the NRC and the TARGET datasets with P -values below 0.001 and a P -value of 0.052 for the RNA-seq dataset (Figure 9A, B, C).

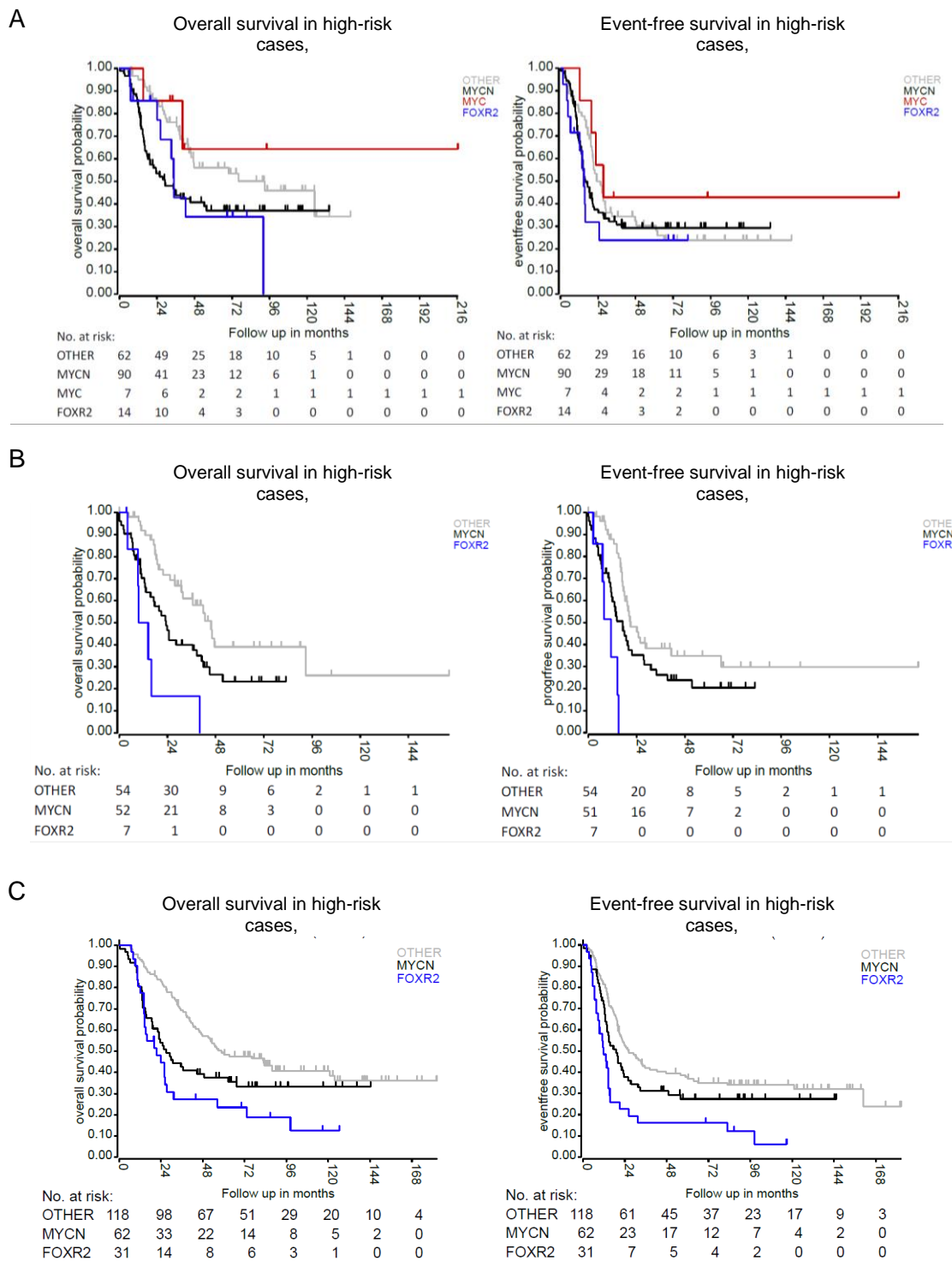


Figure 9: Survival analysis in the high-risk subsets of the RNA-seq, NRC and the TARGET dataset.

(A) Overall and event-free survival of the distinct molecular groups in the high-risk subset of the RNA-seq dataset (n=173). The *FOXR1* group was excluded due to low numbers. (B) Overall and event-free survival of the distinct molecular groups in the high-risk subset of the NRC dataset (n=113/n=112). The *FOXR1* and *MYC* group were excluded due to low numbers. (C) Overall and event-free survival of the distinct molecular groups in the high-risk subset of the TARGET dataset (n=211). The *FOXR1* and *MYC* group were excluded due to low numbers. Figure modified from (Schmitt-Hoffner et al., 2021).

The mutual exclusive manner of the *FOXR2* group and neuroblastomas that show an ALT phenotype allowed for a survival analysis comparing these two groups. Within the RNA-seq subset with available ALT status the *FOXR2* group and ALT positive cases showed a similar 5-year OS of 72% (95% CI of 41-88) for the *FOXR2* group and 61% (95% CI of 25-84) for the ALT group (Figure 10). Moreover, the EFS of the *FOXR2* group and the established risk factor ALT phenotype did not differ significantly ($P=0.253$) with a 5-year EFS of 47% (95% CI of 22-69) for the *FOXR2* group and 29% (95% CI of 9-53) for the ALT group (Figure 10).

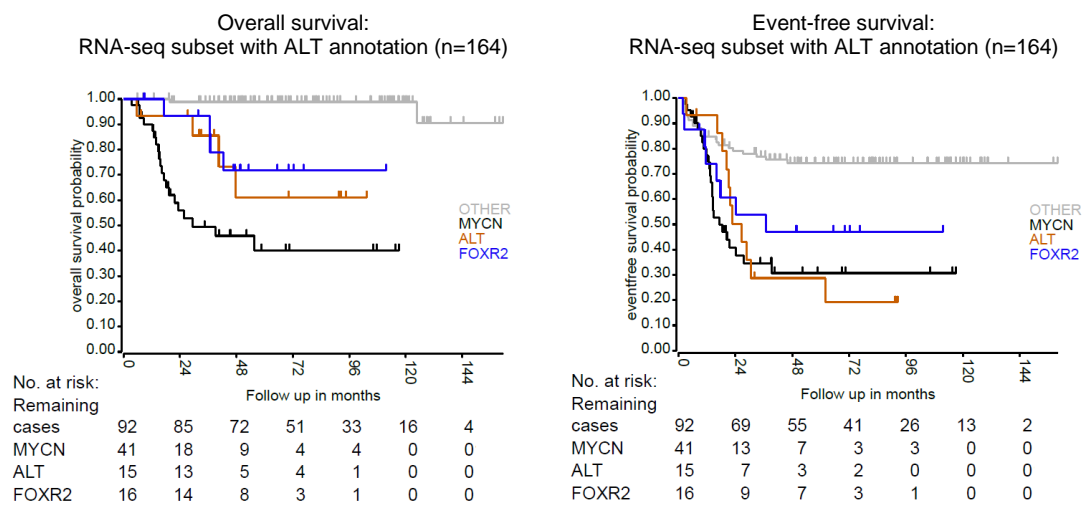


Figure 10: **Survival analyses of the ALT annotated subset of the RNA-seq dataset.**

Overall and event-free survival of the *FOXR2* group and cases with ALT phenotype in the ALT status annotated subset of the RNA-seq dataset (n=173). The *FOXR1* and the *MYC* group were excluded due to low numbers. Figure modified from (Schmitt-Hoffner et al., 2021).

Based on the results of the survival analyses showing a poor outcome of the *FOXR2* group the clinical relevance of *FOXR2* expression in neuroblastoma was evaluated and compared to previously established risk factors by multivariable analyses. *FOXR2* was found to be a significant independent prognostic factor when compared to INSS4, age at diagnosis above 18 months and *MYCN* amplification associated with a hazard ratio of 2.5 ($P=0.004$) in the RNA-seq dataset and 3.5 ($P=0.003$) in the NRC dataset (Figure 11A, B; Table 3). Strikingly, even when comparing *FOXR2* to the high-risk annotated cases of the RNA-seq dataset, defined by patients that show a *MYCN* amplification and/or INSS4 in combination with an age at diagnosis of above 18 months (Zhang et al., 2015), *FOXR2* remained to be a significant independent prognostic factor in both the RNA-seq ($P=0.033$) (Figure 11A) and in the NRC datasets

($P=0.004$) (Figure 11B). These results indicate that the expression of *FOXR2* identifies patients that would otherwise not have been identified as high-risk. Accordingly, *FOXR2* expressing cases in the non-high-risk subsets of the RNA-seq and the NRC datasets indicated a significantly lower survival ($P=0.012$ in the NRC and $P<0.001$ in the RNA-seq dataset) than cases without or very low *FOXR2* expression (Figure 11C).

Performing multivariable analyses on a subset of the RNA-seq dataset for which information on segmental chromosomal alterations (SCA) was available, *FOXR2* was confirmed as a prognostic factor when compared to previously described SCA related prognostic markers, such as 11q deletion, 1p deletion, 3p deletion and 17q gain (Figure 11D). The TARGET dataset was not evaluated due to the large proportion of high-risk tumors and its consequential bias on the analyses.

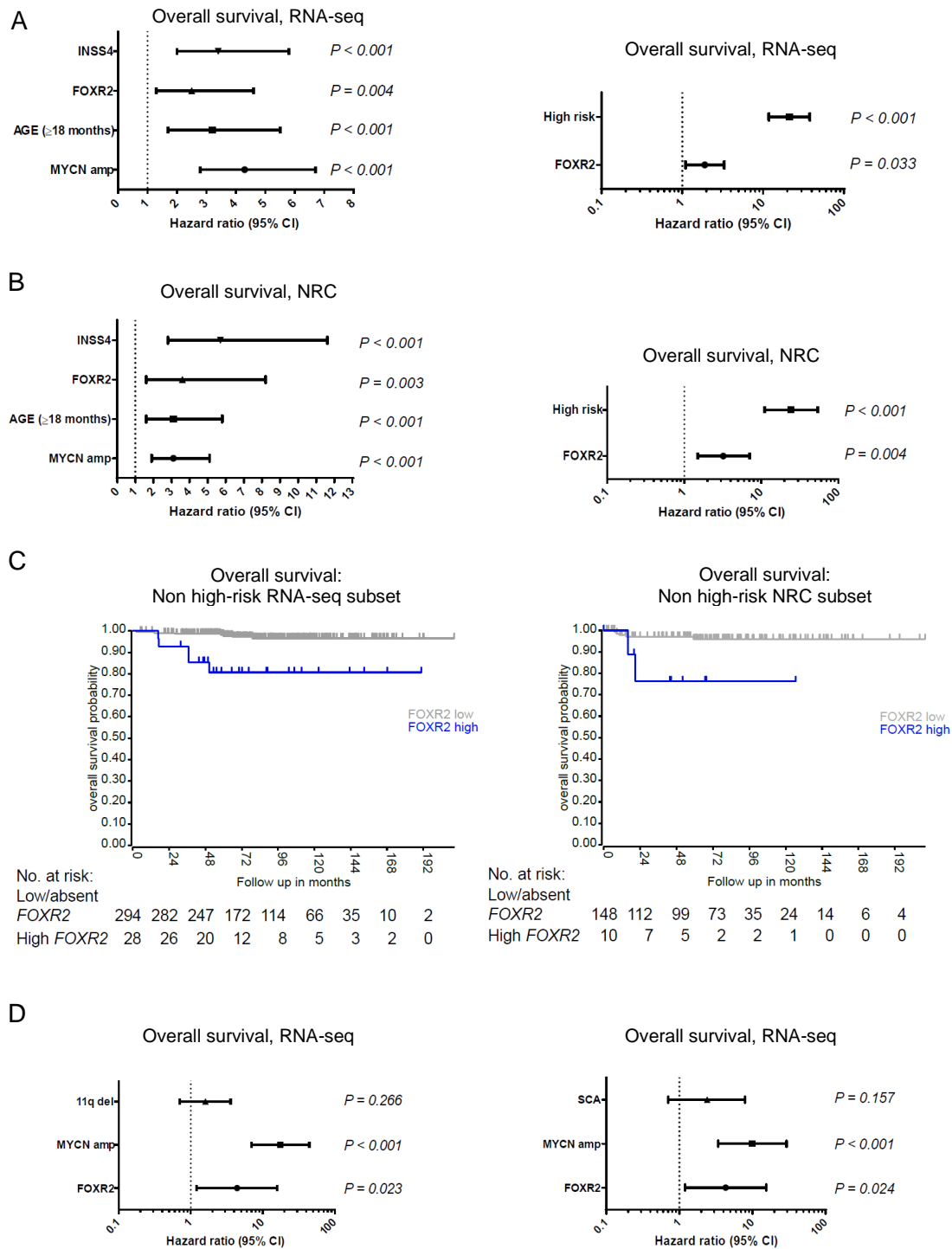


Figure 11: ***FOXR2* is a significant independent risk factor.**

(A) Multivariable analyses comparing *FOXR2* to the established risk factors *MYCN* amplification, age at diagnosis above 18 months, INSS 4 and high-risk status in the RNA-seq dataset. (B) Multivariable analyses comparing *FOXR2* to established risk factors in the NRC dataset. (C) Overall and event-free survival analyses showing that *FOXR2* identifies patients with poorer outcome in the non high-risk subset of the RNA-seq and of the NRC dataset. (D) Multivariable analyses comparing *FOXR2* to the established risk factors *MYCN* amplification, 11q deletion and segmental chromosome aberration (SCA) in the RNA-seq dataset. Figure modified from (Schmitt-Hoffner et al., 2021).

Table 3: Hazard ratios and 95% confidence intervals of the multivariable analyses on overall and event-/progression-free survival in the RNA-seq and the NRC dataset. Table from (Schmitt-Hoffner et al., 2021).

	Factor	Overall survival		Event/progression-free survival	
		HR (95% CI)	P-value	HR (95% CI)	P-value
RNA-seq dataset	INSS stage 4	3.4 (2.0-5.8)	< 0.001	2.4 (1.7-3.4)	< 0.001
	<i>FOXR2</i>	2.5 (1.3-4.6)	0.004	1.6 (1.0-2.6)	0.049
	Age > 18 months	3.2 (1.9-5.5)	< 0.001	1.8 (1.3-2.6)	< 0.001
	<i>MYCN</i> amp.	4.3 (2.8-6.7)	< 0.001	1.9 (1.4-2.8)	< 0.001
	high-risk status	21.6 (12.0-38.7)	< 0.001	5.2 (3.8-7.1)	< 0.001
	<i>FOXR2</i>	1.8 (1.1-3.2)	0.033	1.6 (1.0-2.6)	0.04
NRC dataset	INSS stage 4	6.0 (2.9-12.2)	< 0.001	3.3 (2.0-5.6)	< 0.001
	<i>FOXR2</i>	3.5 (1.5-7.9)	0.003	2.0 (0.9-4.5)	0.08
	Age > 18 months	2.8 (1.5-5.3)	< 0.001	2.1 (1.3-3.5)	0.003
	<i>MYCN</i> amp.	3.0 (1.8-4.9)	< 0.001	2.2 (1.4-3.4)	< 0.001
	high-risk status	24.4 (11.0-54.1)	< 0.001	7.9 (4.8-13.0)	< 0.001
	<i>FOXR2</i>	3.2 (1.4-7.0)	0.004	2.1 (1.0-4.6)	0.061

3.2.4 Mechanism of *FOXR2* activation in neuroblastoma

In CNS neuroblastoma with *FOXR2* activation (CNS NB-*FOXR2*) it was previously shown that the activation of *FOXR2* is caused by enhancer hijacking events where the entire *FOXR2* gene is fused to the promoter of a highly active gene that drives *FOXR2* expression in these tumors. However, in neuroblastoma, only one *FOXR2*-expressing case (out of 42) with a similar intrachromosomal (chromosome X) gene fusion was identified. In this case, *FOXR2* was fused to *USP9X*, a gene that is highly expressed in neuroblastoma and, like *FOXR2*, located on the p arm of chromosome X. For all other cases the mechanism of activation of *FOXR2* remains elusive.

3.2.5 *FOXR2* knockdown in neuroblastoma cell lines results in decreased proliferation

Two neuroblastoma cell lines, SK-N-AS and SK-N-FI, were selected to mechanistically investigate the role of *FOXR2* in neuroblastoma. Both cell lines express *FOXR2*, show no *MYCN* amplification and express either *MYCN* (SK-N-FI) or *MYC* (SK-N-AS) at relatively low levels. Using doxycycline-inducible shRNA constructs, a significant knockdown of *FOXR2* both

at the RNA and protein levels in both cell lines was induced (Figure 12A). Upon knockdown of FOXR2 a significantly reduced cell growth in SK-N-AS and SK-N-FI was observed when compared to mock shRNA (scrambled shRNA) transfected cells over a time course of 9 and 13 days, respectively (Figure 12B). To further analyze the consequences of the FOXR2 knockdown, transcription profiles of SK-N-AS and SK-N-FI cell lines with and without the induction of the FOXR2 knockdown were generated. In SK-N-AS and SK-N-FI 4,886 and 1,829 significantly differentially expressed genes (p-value: 0.05, ANOVA, minimal highest expression: 50 units, minimal expression difference: 50 units) were detected upon FOXR2 knockdown, respectively. Comparing these signatures of differentially expressed genes, an overlap of 1,155 genes was identified, which includes around 63% and 24% of genes contained in the signature of SK-N-FI and SK-N-AS, respectively (Figure 12C).

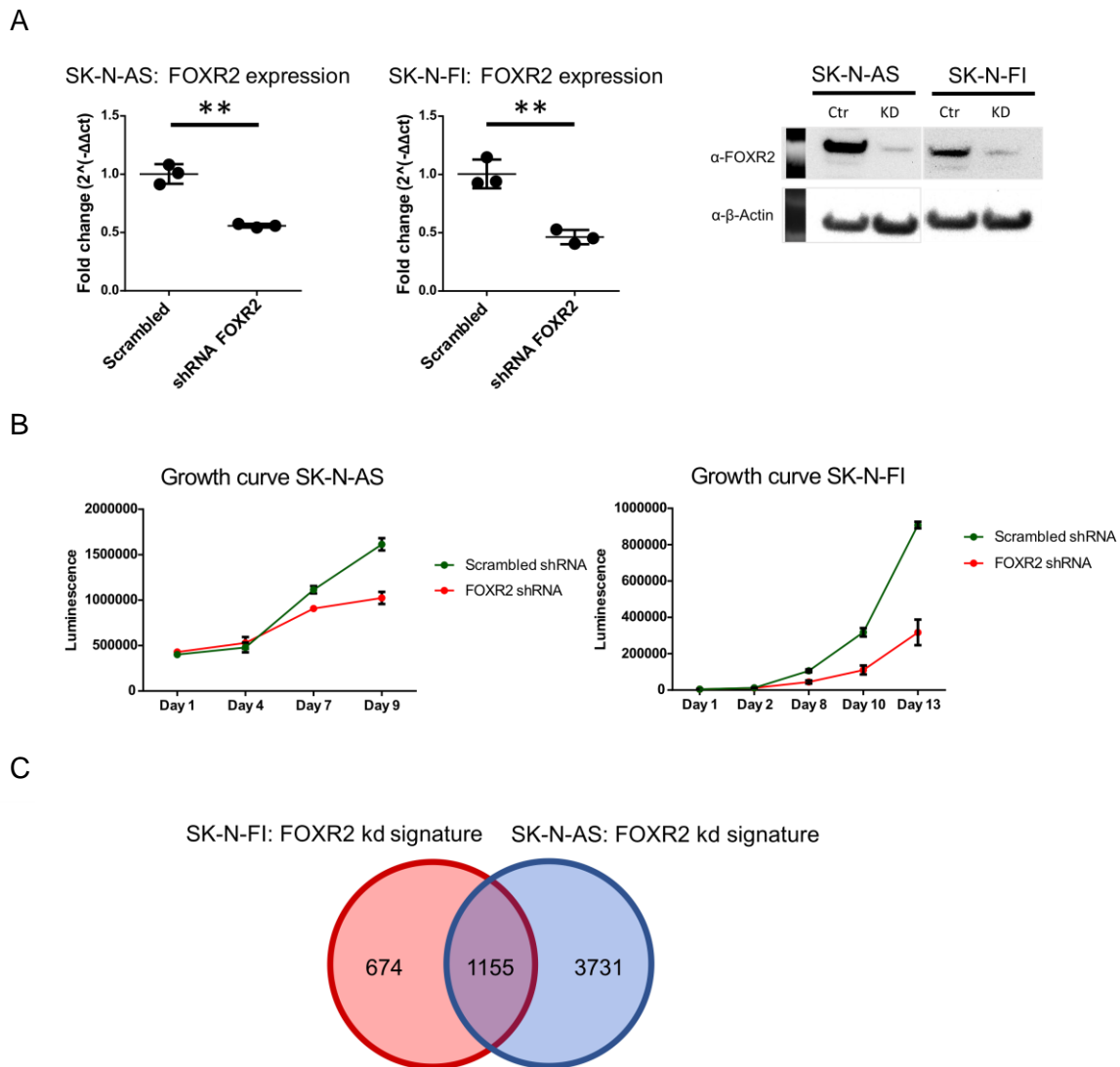
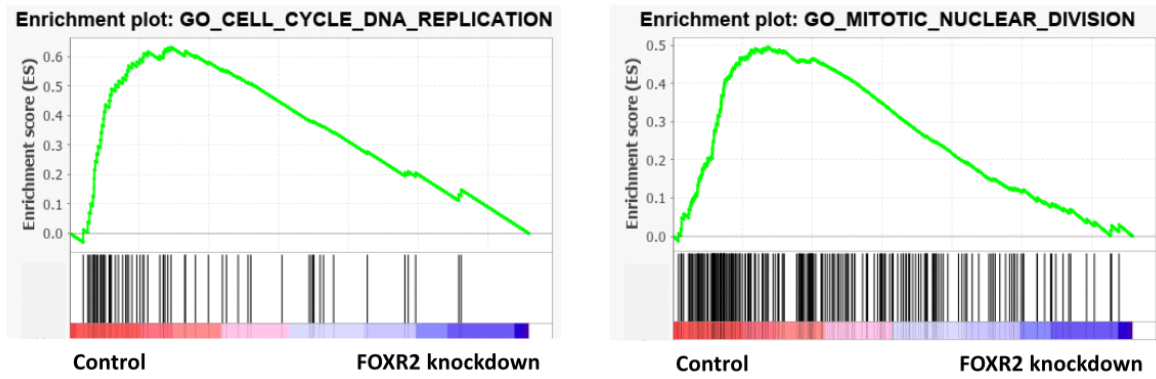


Figure 12: **Knockdown of FOXR2 results in decreased proliferation.**

(A) Knockdown of *FOXR2* in SK-N-AS and SK-N-FI on an mRNA and on a protein level. (B) Growth curves of SK-N-AS and SK-N-FI after induction of the FOXR2 knockdown and the scrambled shRNA (control). (C) Venn-diagram indicating the overlap of the knockdown signatures of SK-N-AS and SK-N-FI. Figure modified from (Schmitt-Hoffner et al., 2021).

Gene Set Enrichment Analyses (GSEA) and Ingenuity Pathway Analyses (IPA) after FOXR2 knockdown showed that biological processes related to cell cycle and cell proliferation such as “M-Phase” and “Cell survival” were downregulated in SK-N-AS as well as SK-N-FI, while processes related to cellular death, such as “apoptosis” or “necrosis” were upregulated in both cell lines upon FOXR2 knockdown (Figure 13A, B). Cell cycle and cell death analyses validated the FOXR2 knockdown being associated with cell cycle arrest and increased cell death in SK-N-AS and SK-N-FI (Figure 14A, B).

A



B

	Diseases or Functions Annotation	p-value	Predicted	Activation	# Molecules
SK-N-AS	M phase	1E-06	Decreased	-2.213	23
	Cell survival	2E-05	Decreased	-2.121	91
	Development of tumor cell lines	2E-05	Decreased	-2.599	32
SK-N-AS	Morbidity or mortality	8E-05	Increased	3.344	134
	Apoptosis	9E-05	Increased	3.236	140
	Organismal death	1E-04	Increased	3.199	132
SK-N-FI	Digestive system cancer	7,77E-16	Decreased	-2,640	401
	Cell survival	2,48E-06	Decreased	-2,452	84
	M phase	3,28E-06	Decreased	-2,774	21
SK-N-FI	Apoptosis	9,72E-10	Increased	2,238	146
	Necrosis	3,66E-09	Increased	2,324	144
	Organismal death	7,89E-09	Increased	2,630	133

Figure 13: Pathway analyses suggest oncogenic roles of FOXR2.

Pathway analysis upon FOXR2 knockdown in neuroblastoma cell lines shown by GSEA enrichment plots for SK-N-AS (A) and by IPA in SK-N-AS and SK-N-FI (B). Figure from (Schmitt-Hoffner et al., 2021).

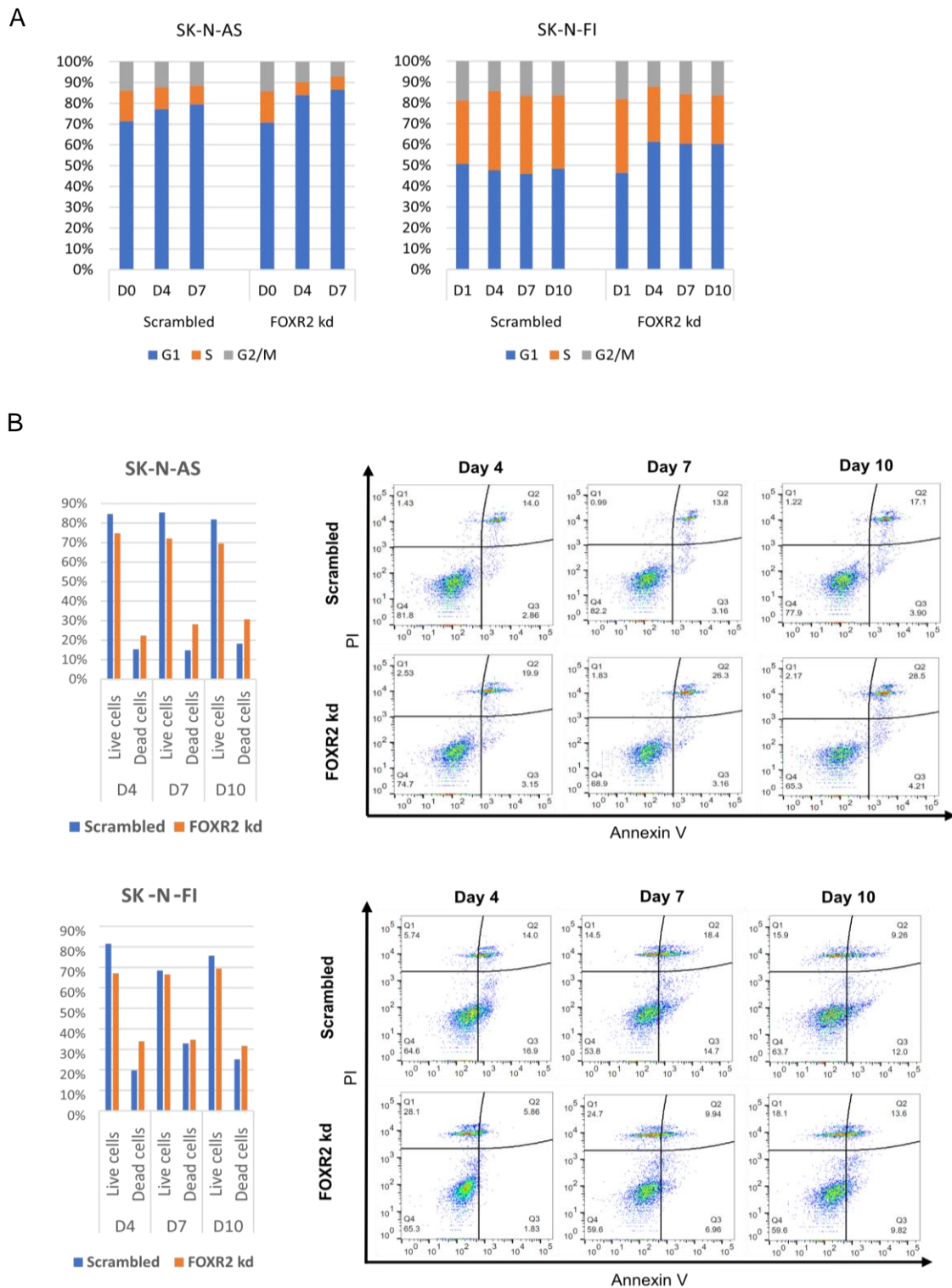


Figure 14: **FOXR2 knockdown is associated with cellular death and cell cycle arrest.**

(A) Cell cycle analysis shows the percentage of SK-N-AS and SK-N-FI cells in G1, S and G2/M phase upon FOXR2 knockdown over time. (B) Dot plots show cell populations based on PI and Annexin V stains (left). The bar chart quantifies live (quadrant 3 and 4) and dead (quadrant 1 and 2) cells based in PI staining (right). Figure from (Schmitt-Hoffner et al., 2021).

3.2.6 Transcriptome analyses of *FOXR2*-expressing neuroblastoma reveals similarities to the *MYCN* group

Since both the *FOXR2* and *MYCN* groups show reduced survival, I investigated in the next step whether these groups are related or transcriptionally distinct. First, when clustering all cases by t-SNE based on gene expression data, the *FOXR2* group did not cluster separately from the other groups (Figure 15A). However, when the differentially expressed genes between the *FOXR2* and the OTHER group were analyzed (Suppl. table 1) and when the resulting gene signature was applied on all other cases, the *FOXR2* and the *MYCN* groups cluster closely together. Furthermore, almost all genes from this signature were upregulated in both of these groups, which was not the case for all other groups (Figure 15B).

Similar results, indicating the transcriptional similarity of the *FOXR2* and the *MYCN* groups, were generated when applying a previously described *MYC(N)* signature (Westermann et al., 2008) to cluster the RNA-seq dataset (Figure 16A). Eventually, a *MYC(N)* activity score was generated based on the previously described *MYC(N)* signature, which was then plotted against the expression of *FOXR2*. In line with my previous findings almost all cases that expressed *FOXR2* showed a positive *MYC(N)* activity score, which in several cases was comparable to the *MYC(N)* activity score of the *MYCN* group (Figure 16B). Overall, these results show the transcriptional similarity of the *FOXR2* and *MYCN* groups and suggest that *MYCN* target genes are activated likewise in the *FOXR2* group even though the mRNA expression levels of *MYCN* itself are low in these tumors.

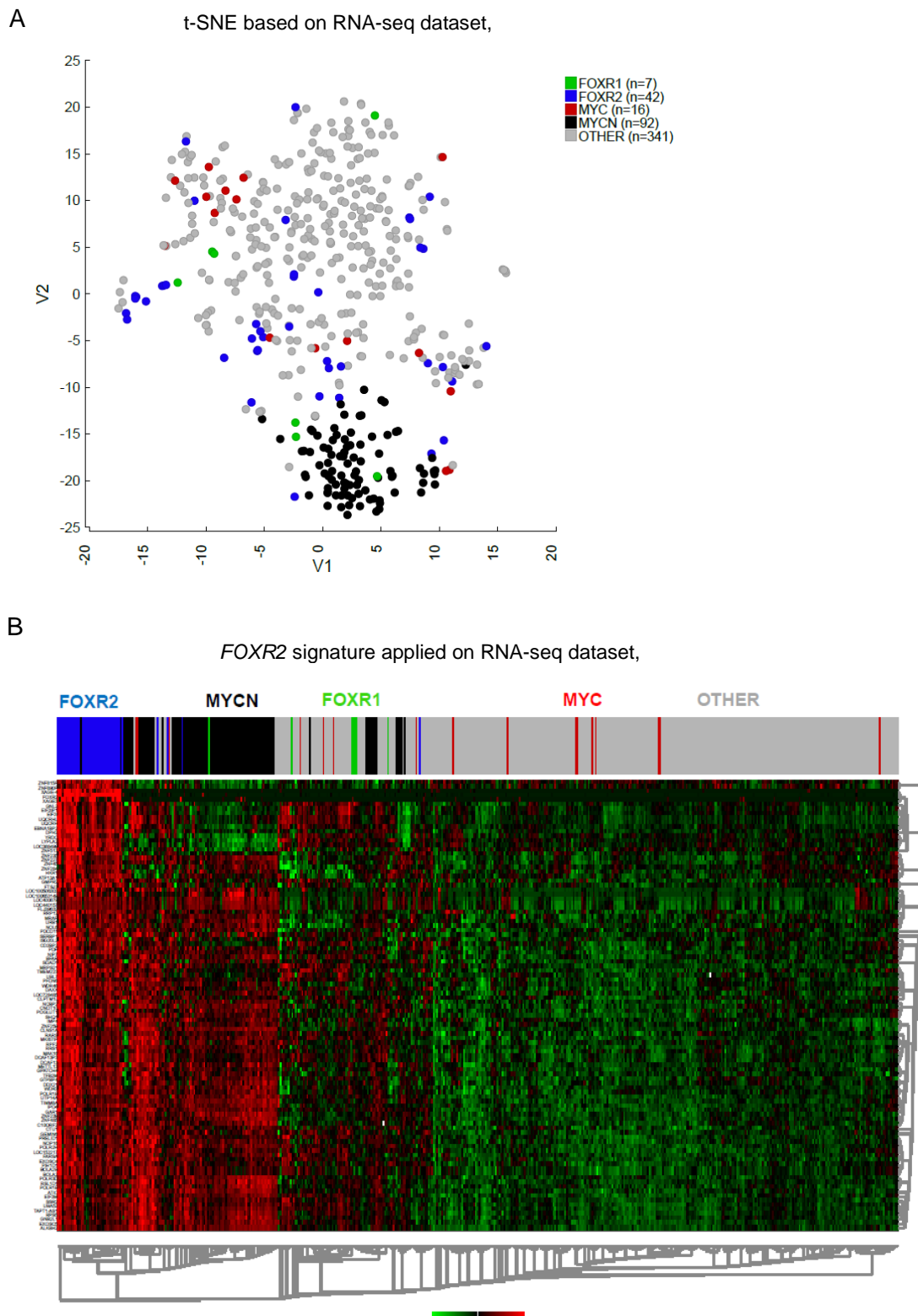


Figure 15: The *FOXR2* and the *MYCN* group are transcriptionally related.

(A) Gene expression based t-SNE analysis in the RNA-seq dataset. (B) Supervised hierarchical clustering of the RNA-seq dataset based on a *FOXR2* signature indicated similarities in gene activation of *FOXR2* and *MYCN*. Figure modified from (Schmitt-Hoffner et al., 2021).

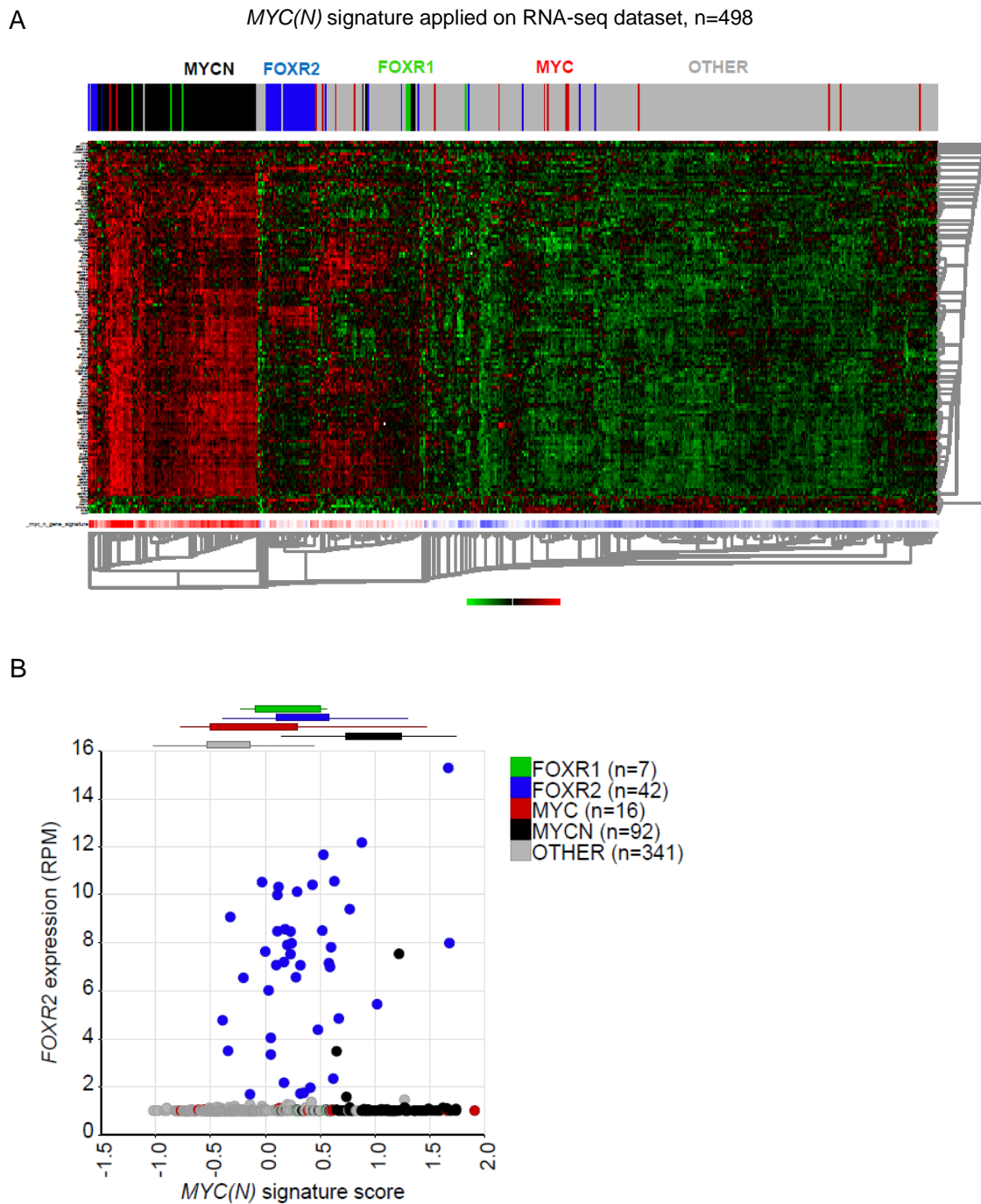


Figure 16: *FOXR2* cases show a positive *MYCN* activity score.

(A) Supervised hierarchical clustering of the RNA-seq dataset based on a *MYC(N)* signature indicated similarities in gene activation of *FOXR2* and *MYCN*. (B) The expression of *FOXR2* is plotted against a *MYC(N)* activity score, indicating a positive *MYC(N)* score for almost all *FOXR2* cases. Figure modified from (Schmitt-Hoffner et al., 2021).

3.2.7 MYCN and MYC is stabilized by FOXR2 on a protein level

Previously, it has been suggested that expression of FOXR2 stabilizes MYC protein levels in a human Schwann cell line (Beckmann et al., 2019). However, it is unclear whether FOXR2 can also stabilize MYCN protein levels. Therefore, 293T cell lines with (i) co-expression of HA-tagged FOXR2 with GFP, (ii) co-expression of MYCN with RFP, and (iii) co-expression of both FOXR2 and MYCN were generated. Expression of FOXR2 and MYCN was validated by fluorescence microscopy (Figure 17A). By means of Western blot analyses an increase in signal intensity by around two fold was shown for MYCN protein levels when MYCN and FOXR2 were both expressed in the cells compared to the cells exclusively expressing MYCN (Figure 17B). Analysis by quantitative RT-PCR demonstrated that this effect was not the result of elevated RNA expression levels of *MYCN* (Figure 17C). Performing co-immunoprecipitation assays using an HA-specific antibody to pull down FOXR2-HA it was demonstrated that FOXR2 binds to MYCN. Protein co-immunoprecipitation assays using a MYCN antibody to pull down MYCN in turn confirmed binding to FOXR2 (Figure 17D). Since the expression of FOXR2 results in increased MYCN protein levels, it was hypothesized that the binding of FOXR2 might result in stabilization of MYCN protein. Therefore, cycloheximide chase assays were conducted, disabling cellular translation to analyze protein turnover and degradation of the short-lived MYCN protein. When FOXR2 was co-expressed with MYCN, increased MYCN protein levels were found (Figure 17E), indicating that indeed binding of FOXR2 to MYCN results in increased stabilization of the MYCN protein. Using the FOXR2 knockdown cell line SK-N-FI this findings was confirmed, since less MYCN protein was observed when FOXR2 was knocked down (Figure 17F). Moreover, the degradation of MYCN was tracked over time. In both the FOXR2-overexpressing 293T cells as well as the FOXR2 knockdown neuroblastoma cell line SK-N-FI, an increased MYCN protein degradation was observed over a time course of 4h in the absence of FOXR2. On the other hand a stabilization of MYCN was observed in the presence of FOXR2 (Figure 17E, F). Following the stabilization experiment of FOXR2 and MYCN, it was further shown that the co-expression of FOXR2 and MYC in 293T cells leads to similar results indicating that FOXR2 stabilizes MYC protein (Figure 17E). Investigating the effect of MYC stabilization by FOXR2 in neuroblastoma, the knockdown of FOXR2 in the neuroblastoma cell line SK-N-AS increased MYC degradation, whereas the presence of FOXR2 resulted in increased MYC protein levels compared to the knockdown (Figure 17F). Overall, these *in vitro* results indicate that FOXR2 stabilizes both MYC and MYCN on protein level and emphasizes FOXR2's critical function in neuroblastoma.

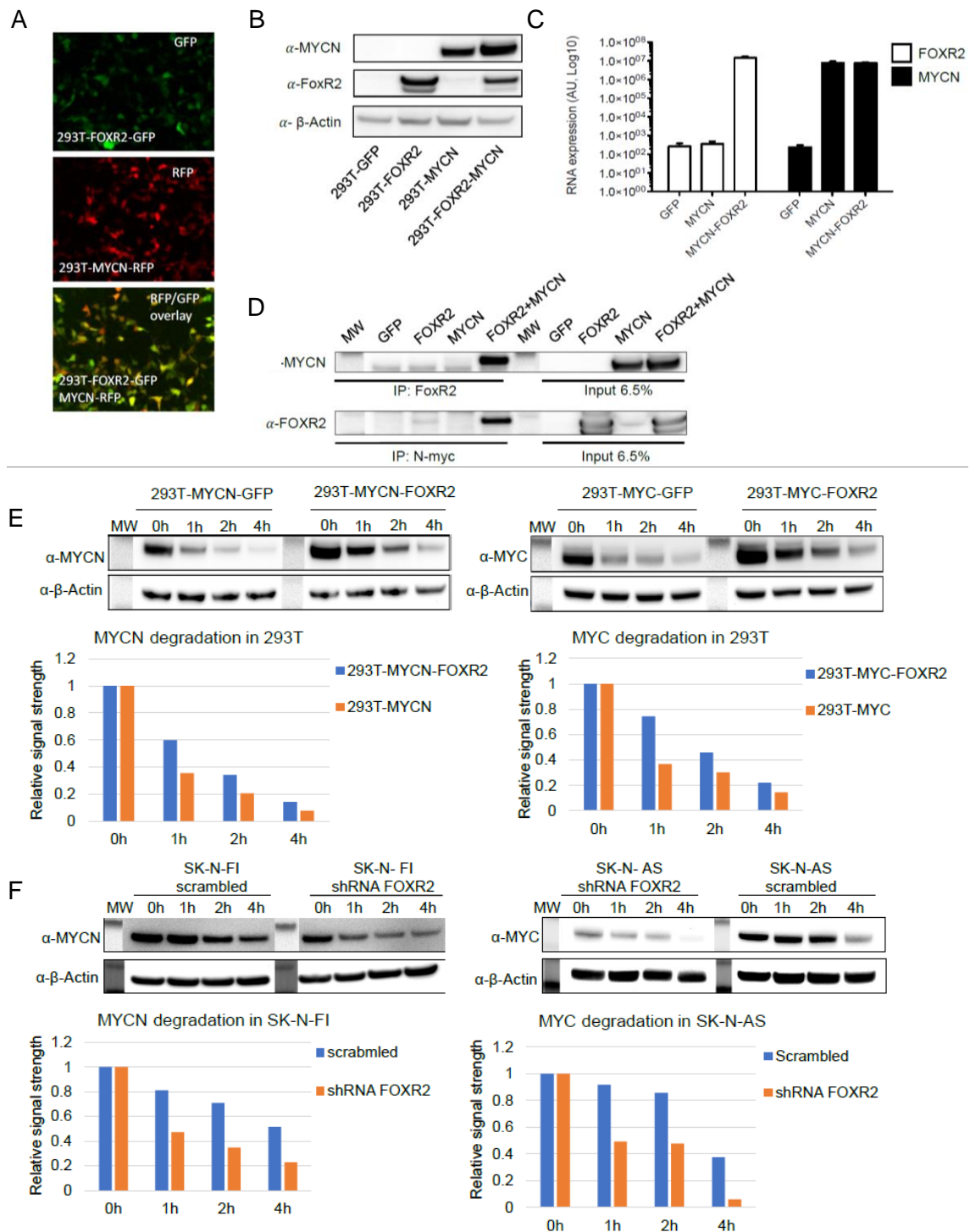


Figure 17: FOXR2 binds and stabilizes MYCN on a protein level.

(A) Co-expression of FOXR2-GFP and MYCN-RFP in HEK 293T cells shown by confocal microscopy. Expression of FOXR2, MYC and MYCN on a protein (B) and mRNA (C) level. (D) FOXR2 binds MYCN as shown by means of immunoprecipitation. (E) CHX assays show that FOXR2 stabilizes MYCN and MYC in 293T cells. Western blot bands intensities are quantified in the bar chart. (F) CHX assays show that FOXR2 stabilizes MYCN and MYC in SK-N-AS and SK-N-FI. Western blot bands intensities are quantified in the bar chart. Experiments shown in (A), (B), (C), (D), (E) were conducted by Sjoerd van Rijn. Figure modified from (Schmitt-Hoffner et al., 2021).

To investigate if the *in vitro* findings on the stabilization mechanism of FOXR2 and MYCN protein also apply to neuroblastoma patients, tissue samples were analyzed. Seven FOXR2-activated tumors that based on RNA levels showed increased FOXR2 expression and minimal MYCN expression were compared to three low-risk neuroblastoma tumors without FOXR2 expression and minimal MYCN expression levels and to three tumors that harbored a MYCN amplification and showed no FOXR2 expression. Despite the minimal MYCN RNA expression, five out of seven FOXR2-expressing cases showed high protein MYCN protein levels, which was not observed in the low risk tumors (Figure 18). Strikingly, NF2 and NF3, both belonging to the FOXR2-expressing cases, showed MYCN protein levels comparable to the cases with MYCN amplification (Figure 18). Only two of the FOXR2 samples showed low or no MYCN protein. By means of Western blot analysis, protein levels of FOXR2 could only be detected in two out of the seven FOXR2 mRNA expressing cases due to low signal intensities (Figure 18). Interestingly, these two cases also showed very high MYCN protein levels, which in line with my previous findings suggests that MYCN protein is high in the presence of FOXR2. Overall, these findings *in vitro* and in neuroblastoma tissue indicate that MYCN protein is stabilized by FOXR2, revealing a novel and clinically relevant stabilization mechanism in neuroblastoma patients.

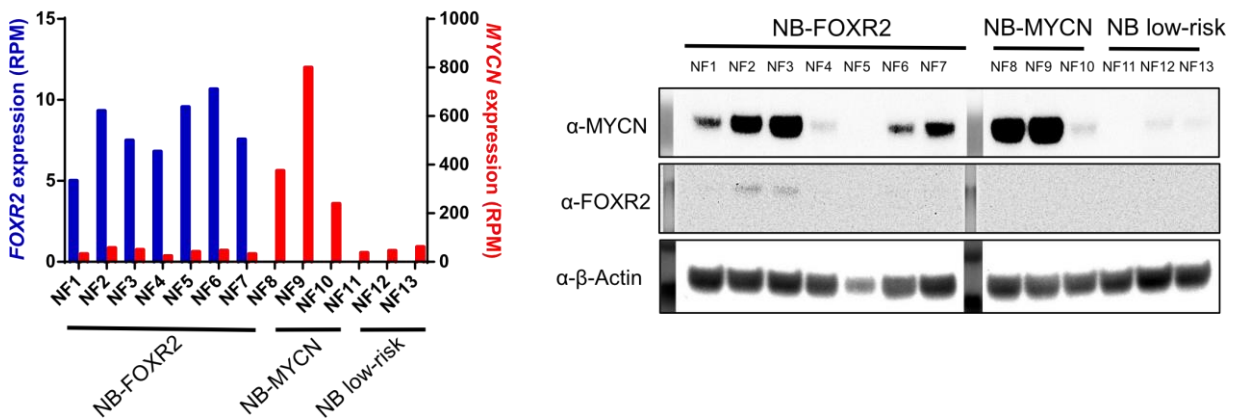


Figure 18: **FOXR2-expressing neuroblastoma show high MYCN protein levels.**

MYCN protein is high in five out of seven cases that express FOXR2 mRNA. Figure modified from (Schmitt-Hoffner et al., 2021).

3.3 Discussion

This study revealed the expression of *FOXR2* in neuroblastoma as a novel independent prognostic marker that indicates unfavorable survival of patients. Furthermore, an alternative mechanism to confer high MYCN protein levels, next to *MYCN* amplification, was identified, namely the stabilization of MYCN by FOXR2 at the protein level.

FOXR2 was previously identified to play a critical oncogenic role in subsets of specific adult and pediatric cancer types (Koso et al., 2014; Li et al., 2018; Liu et al., 2019; Lu et al., 2017; Sturm et al., 2016; Wang et al., 2016; Xu et al., 2017). For the first time in this study, a subset of *FOXR2*-expressing neuroblastomas was identified, which is mutually exclusive from a neuroblastoma subset expressing *FOXR1*, encoding a homologue of FOXR2 (Santo et al., 2012). Furthermore, almost no overlap is found to subsets expressing high levels of *MYCN* and *MYC*, which themselves form separate groups (Westermann et al., 2008). In line with findings in breast cancer and endometrial adenocarcinoma, *FOXR2*-activated neuroblastoma identifies a group of patients with an unfavorable clinical outcome (Deng et al., 2017; Song et al., 2016). Previously identified molecular markers indicating an unfavorable outcome for neuroblastoma patients, including amplified *MYCN*, *TERT* rearrangements and ALT phenotype, were found to be distinct markers rarely overlapping (Ikegaki et al., 2019; Peifer et al., 2015; Valentijn et al., 2015b; Zeineldin et al., 2020). Cases with elevated *TERT* expression, however, were enriched in the *FOXR2*-expressing group. It is known that transcriptional activation of *TERT* in neuroblastoma can be induced either by genomic rearrangements or as a transcriptional target of MYCN (Mac et al., 2000; Peifer et al., 2015). The increased *TERT* expression in *FOXR2* tumors is thus most likely a direct consequence of the increased MYCN protein levels in these tumors. Increased *TERT* expression is on the other hand known to predict unfavorable clinical outcome in high-risk neuroblastoma (Koneru et al., 2020), which was also observed for the *FOXR2*-activated group showing a 10-year OS of 59%, significantly reduced compared to a 10-year OS of 88% in the OTHER group that does not express *FOXR2*, *MYCN*, *MYC* or *FOXR1*. An enrichment of *FOXR2*-expressing patients in INSS stage 3 and 4, indicating intermediate and high-risk neuroblastoma, further affirms the unfavorable outcome of *FOXR2*-activated neuroblastoma. Comparable to the *FOXR2* group, similar findings were made on the clinical outcome in the smaller neuroblastoma group (n=7) with activation of *FOXR1* (10-year OS 57%), which encodes a homologue of FOXR2, that was previously shown to substitute MYC-driven proliferation and that is negatively correlated to cell cycle arrest and cell death (Santo et al., 2012). Patients with elevated *MYC* expression showed a comparably good overall survival in the RNA-seq dataset. Previous investigations by Zimmerman et al. and

Wang et al. (Wang et al., 2015; Zimmerman et al., 2018) found that MYC expression is associated with unfavorable survival, however these studies considered either only high-risk patients (Zimmerman et al., 2018) or analyzed MYC protein levels (Wang et al., 2015), which is not directly comparable to the mRNA expression based *MYC* group described in this study.

As mentioned previously there are well-established prognostic factors in neuroblastoma that identify patients with a poor survival. These risk factors include *MYCN* amplification, age at diagnosis above 18 months, INSS stage 4 (equivalent to INRG stage M), 11q aberration and several others (Pinto et al., 2015; Zhang et al., 2015). To investigate the clinical relevance of *FOXR2* expression in neuroblastoma as a prognostic marker for risk stratification multivariable analyses demonstrated that *FOXR2* expression forms a significant risk factor that independent from established prognostic markers indicates poor patient survival. Interestingly, *FOXR2* was found to still represent a significant and independent risk factor when compared to a pre-defined high-risk subset, indicating that *FOXR2* expression marks a yet unidentified subset of patients with poor survival not covered by the high-risk group. Affirmed by univariate analyses that showed a significantly lower survival of *FOXR2*-expressing patients in non high-risk subsets of the RNA-seq and NRC cohort, my results suggest that these patients with a poor survival are currently not being identified by established prognostic markers as patients with increased risk, which underlines the importance of *FOXR2* as a biomarker for risk stratification. Since risk stratification, primarily in patients with an unfavorable histology, INSS stage 3 and age at diagnosis above 18 months can differ depending on the country where the study was conducted, *FOXR2* might play an important role to distinguish intermediate and high-risk patients. To conduct a final evaluation of *FOXR2* expression in risk groups, further sub-classification of the non high-risk group into low- and intermediate-risk group will be necessary.

The clinical data presented in the RNA-seq dataset is in most cases based on the NB97 and the NB2004 treatment studies (420 out of 498 patients). To ensure survival analyses based on homogeneous data in the pooled trials the treatment studies were compared. It was observed that survival rates in both studies were highly similar in the RNA-seq dataset and that in both trials *FOXR2*-expressing patients showed a similarly poor survival (data not shown). Furthermore, differences in induction or consolidation treatment arms did result in comparable responses in high-risk patients of the RNA-seq data (Berthold et al., 2020). These observations suggest that the prognostic value of *FOXR2* expression is not biased by a specific treatment protocol within the analyzed dataset.

Mechanistically, it was shown that in line with findings in NSCL, breast, hepatocellular and prostate cancer cell lines, the knockdown of FOXR2 decreases cell proliferation also in neuroblastoma cell lines (Li et al., 2016; Wang et al., 2016; Xu et al., 2017; Xu et al., 2019). Supporting the crucial oncogenic role of FOXR2 in neuroblastoma, the FOXR2 knockdown changes the gene expression signature to a less aggressive one based on predictions of the pathway analysis tools GSEA and IPA, which was validated by *in vitro* experiments on cell cycle and cell death in FOXR2 knockdown cell lines. Comparing the transcriptional profiles of the FOXR2 and the MYCN groups based on differentially expressed genes of the FOXR2 vs. OTHER group, MYCN-activated neuroblastomas strongly resembled the FOXR2 cases. Furthermore, FOXR2-activated cases transcriptionally resembled the MYCN group when applying the MYC(N) signature, which was confirmed by a high MYC(N) signature score assigned to the majority of FOXR2-expressing cases. In line with these findings, already in 2008 and in 2012 a non-MYCN-amplified group of neuroblastoma with activated MYCN expression signature, showing low MYCN expression but high nuclear MYCN levels was identified by (Westermann et al., 2008) and (Valentijn et al., 2012), which could potentially overlap with the FOXR2 group identified in the current study. Interestingly, brain tumors like CNS NB-FOXR2, glioblastoma and medulloblastoma that express FOXR2 also had a positive MYC(N) signature, suggesting that FOXR2 may have a similar role in stabilizing MYC(N) proteins in these tumors as well.

These observations at the transcriptional level indicate a similar oncogenic mechanism in the FOXR2 and MYCN group. Indeed, MYCN as well as MYC is stabilized by FOXR2 on a protein level in neuroblastoma cell lines and I demonstrated in neuroblastoma tissue with low MYCN RNA levels that MYCN protein is increased in the presence of FOXR2. Preventing the short-lived MYCN protein from degradation, these results suggest that neuroblastoma with FOXR2 expression remain in the proliferative cell state by increased MYCN protein levels (Huang and Weiss, 2013; Zhang et al., 2016). The mechanistic study as well as the gene signatures of the FOXR2 and MYCN group therefore indicate that the stabilization of MYCN by FOXR2 is an alternative mechanism to MYCN amplification in neuroblastoma resulting in high MYCN protein levels and leading to an unfavorable outcome in patients (Figure 19).

Since also a subset of non high-risk neuroblastoma was observed with FOXR2 activation and since the FOXR2 group overall shows a better outcome than the MYCN group, I speculate that for some FOXR2-activated neuroblastomas further mechanisms besides MYCN stabilization may play a role. While this study provides insights into the mechanistic relation of FOXR2 and

MYCN, the function of FOXR2, e.g. as a transcription factor, needs to be addressed in further studies.

The current study has several limitations that have to be considered when interpreting the presented data. The clinical analyses and evaluation of *FOXR2*-expression as a prognostic marker are based on three independent cohorts of retrospective nature. This might lead to potential confounding, e.g. related to a selection bias or variable treatment of patients. To compensate for these potential shortcomings associated with the retrospective character of the evaluated datasets three independent cohorts were analyzed, which contained clinical information for a total of 1011 patients. Furthermore, the NB97 and NB2004 trials in the RNA-seq dataset were compared to demonstrate the high similarity and comparability of treatments. Moreover, this study was limited by the available annotations for the three cohorts. To conduct a precise risk stratification further information on ALT status, *TERT* rearrangements, histologic category, grade of tumor differentiation and ploidy would be necessary. Finally, since only around 9% of neuroblastoma express elevated *FOXR2* mRNA levels, the clinical data available for the *FOXR2* group is limited. By investigating the three independent datasets a relatively high number of in total 90 *FOXR2* expressing cases were analyzed, but for further prospective studies that would be needed to investigate the *FOXR2* group in a cohort of uniformly treated patients classified as non high-risk, presumably an international collaboration would be required.

Taken together, this study reveals *FOXR2* expression as a novel prognostic marker that indicates an unfavorable survival in a subset of around 9% of neuroblastoma. Furthermore, a stabilization mechanism of MYCN was identified that leads to high MYCN protein levels, which very likely is correlated with the poor overall and event-free survival of patients in the *FOXR2* group and which provides crucial knowledge for targeted therapies of neuroblastoma patients with *FOXR2* expression.

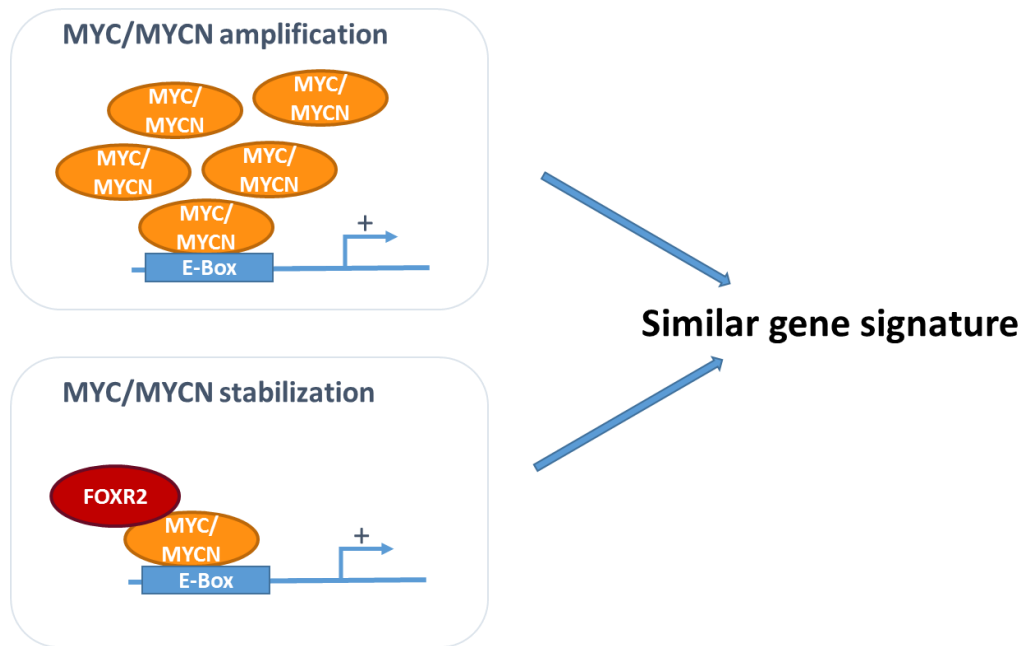


Figure 19: **Stabilization of MYCN by FOXR2 might function as an alternative mechanism to MYCN-amplifications.**

Based on the findings of this study tumors with *FOXR2* expression show a similar gene signature as *MYCN*-amplified tumors by a stabilization mechanism of FOXR2 and MYCN that alternatively to *MYCN* amplifications leads to high MYCN protein levels in neuroblastoma.

4 Second chapter: Molecular and clinical characterization of CNS NB-FOXR2

4.1 Introduction

4.1.1 Molecular re-evaluation of CNS-PNET

The classification of cancer types into biologically meaningful classes plays a key role for the treatment stratification of cancer patients. Histopathological characteristics of tumor classes have been exploited as a primary source for many decades to diagnose pediatric brain tumor entities (Armstrong and Giangaspero, 2003; Kleihues and Sobin, 2000; Pfister et al., 2009). Advances in modern sequencing methods, however, have substantially improved the classification and characterization of pediatric brain tumor entities and has led to a significant increase in newly identified distinct tumor entities and the identification of entity-specific therapeutic targets (Cacciotti et al., 2020; Capper et al., 2018a; Gajjar et al., 2014; Gröbner, 2017; Guerreiro Stucklin et al., 2018; Koelsche et al., 2021; Pajtler et al., 2015; Perez and Capper, 2020; Sturm et al., 2016). Hence, in the updated 2021 WHO Classification of Tumors of the Central Nervous System, molecular characteristics play an increasingly important role and many novel pediatric brain tumor entities and subgroups are introduced, which were often identified primarily based on DNA methylation profiling (Gritsch et al., 2021; Louis et al., 2021). Amongst these newly introduced entities is CNS neuroblastoma with *FOXR2* activation (CNS NB-*FOXR2*), which was identified by Sturm et al. in 2016 as a fraction of institutionally diagnosed primitive neuroectodermal tumors of the central nervous system (CNS-PNET) (Louis et al., 2021; Sturm et al., 2016). CNS-PNETs were described in the 2007 WHO Classification of Tumors of the Central Nervous System as a heterogeneous group of embryonal tumors that arise primarily during childhood or adolescence (Louis et al., 2007). Histologically, they are predominantly defined by small and poorly differentiated cells, but in parts they show a propensity for histological characteristics diverging into neuronal or glial differentiation phenotypes, (Louis et al., 2007; Sturm et al., 2016; Vogel and Fuller, 2003). The clinical outcome of CNS-PNET patients was thought to be generally poor and 5-year overall survival rates of 50% were observed (Lester et al., 2014; Massimino et al., 2013; Peris-Bonet et al., 2006; Schwalbe et al., 2013b). Importantly, however, several studies have now shown that CNS-PNETs represent a variety of different molecular entities (Danielsson et al., 2015; Picard et al., 2012; Schwalbe et al., 2013b), which resulted in the removal of the term CNS-PNET from the 2016 update of the WHO Classification of Tumors of the Central Nervous System (Louis et al., 2007; Louis et al., 2016). Underlining the need for an improved molecular

classification and more differentiated therapeutic approaches, also the clinical outcome of patients with CNS-PNETs was shown to be highly heterogeneous in retrospectively re-evaluated CNS-PNET cohorts and that poor outcome of CNS-PNETs might be mainly caused by misclassification of high grade gliomas (HGG) (Hwang et al., 2018). A comprehensive study by Sturm et al., revealed by means of DNA methylation profiling that a high percentage (196/323; 61%) of CNS-PNETs can be molecularly re-classified into established pediatric brain tumor entities such as embryonal tumors with multilayered rosettes (ETMR), HGG, ependymomas, or atypical teratoid/rhabdoid tumors (ATRT) (Figure 20). Furthermore, novel molecular entities emerged from the molecular classification of this CNS-PNET cohort (77/323; 24%), including CNS tumors with BCOR internal tandem duplication (former CNS HGNET-BCOR) and Astroblastoma, MN1 altered (former CNS-HNGET-MN1) and the previously mentioned CNS NB-FOXR2, which are all represented in the updated 2021 WHO Classification of Tumors of the Central Nervous System (Louis et al., 2021; Sturm et al., 2016). Overall, this indicates the importance of using molecular classification methods to identify biologically and clinically meaningful entities. Further molecular and clinical characterization is needed, especially for these newly described entities to identify specific therapeutic targets and to enable a differentiated clinical view on these tumors.

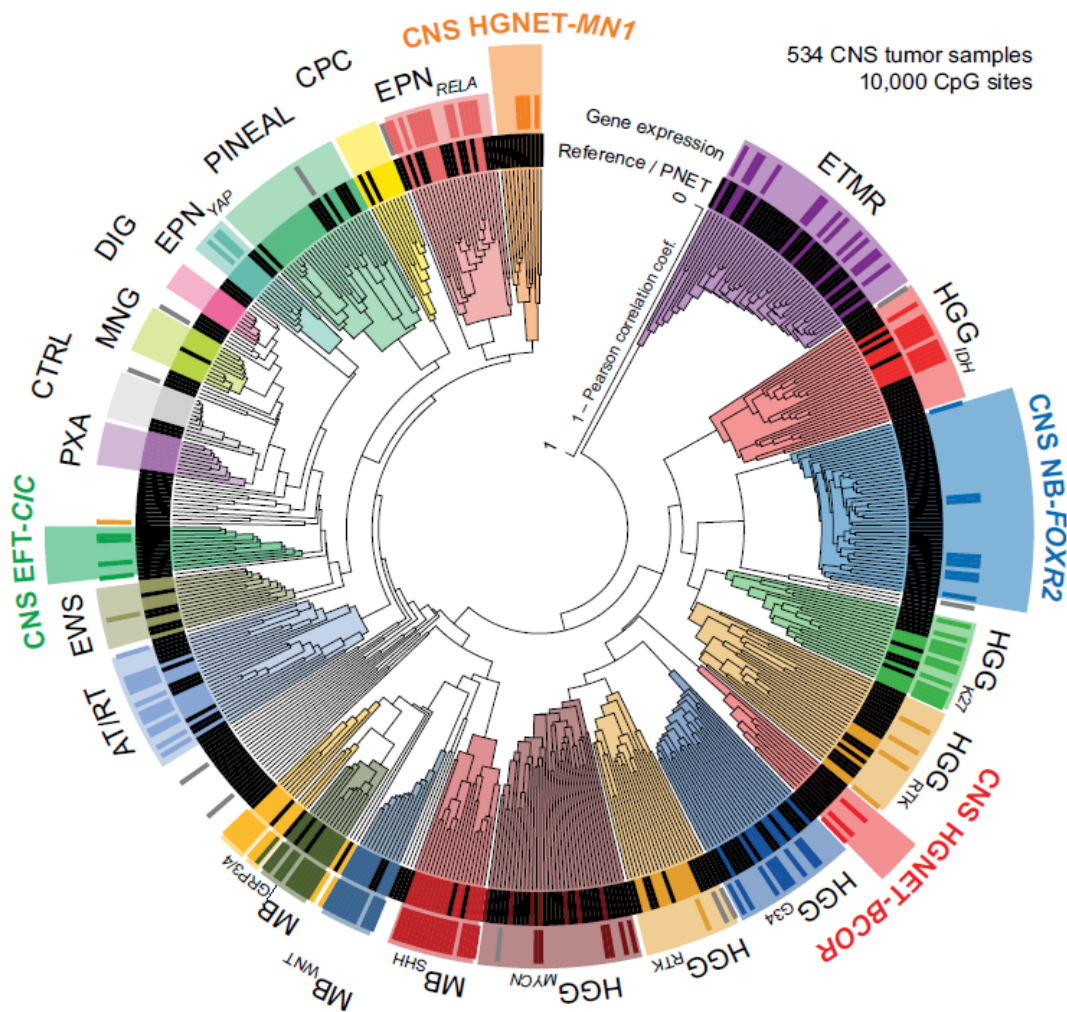


Figure 20: **DNA methylation profiling based classification of institutionally diagnosed CNS-PNET.**

By means of DNA methylation profiling, institutionally diagnosed CNS-PNETs were molecularly classified into established and novel pediatric brain tumor entities. Figure from (Sturm et al., 2016).

4.1.2 CNS NB-FOXR2

CNS NB-FOXR2 were initially described by Sturm and colleagues in 2016 and due to the rarity of this entity the molecular and clinical characterization has since then been ongoing (Sturm et al., 2016). It is estimated that approximately 10% of previously diagnosed CNS-PNET are comprised of CNS NB-FOXR2 (Hwang et al., 2018; Sturm et al., 2016). CNS NB-FOXR2 are embryonal tumors that primarily occur in childhood, slightly enriched in female patients (Sturm et al., 2016). Histologically, this entity is characterized by poorly differentiated, round to oval cells with a high nuclear to cytoplasmic ratio, resembling histological characteristics of CNS-

PNET (Lastowska et al., 2020; Sturm et al., 2016). CNS NB-FOXR2 are exclusively found in supratentorial regions of the brain, typically located in the cerebral hemispheres (Furuta et al., 2020; Sturm et al., 2016). Almost all CNS NB-FOXR2 show a gain of chromosome 1q and in approximately half of the cases a loss of chromosome 16q (Sturm et al., 2016). Furthermore, the activation of the *FOXR2* gene is observed in almost all cases, typically caused by inter- or intrachromosomal rearrangements that lead to fusions between the *FOXR2* gene and different gene partners (Sturm et al., 2016). This leads to the high expression levels of *FOXR2*, which are likely facilitated by promoters of active genes (Sturm et al., 2016). By *in-vivo* experiments it has been demonstrated that the expression of *FOXR2* can under specific conditions lead to tumorigenesis, however, the *FOXR2*-related function and the mechanism that drives these tumors still needs to be investigated (Poh et al., 2019). Clinical observations in small cohorts suggest that patients with CNS NB-FOXR2 have a favorable clinical outcome but further clinical analyses in datasets with larger patient numbers and molecularly classified CNS NB-FOXR2 cases are needed to get a differentiated clinical view on this entity (Hwang et al., 2018; Lastowska et al., 2020; Sturm et al., 2016).

4.1.3 Aim of this study

CNS NB-FOXR2 is a novel molecular pediatric brain tumor entity that was identified in a fraction of historically diagnosed CNS-PNETs. They were molecularly characterized and clinical characteristics were described for single patients and small cohorts. Yet, the molecular re-evaluation of further histologically diagnosed CNS-PNET cohorts is needed to identify additional molecular characteristics and to validate initial findings. Moreover, clinical analyses of CNS NB-FOXR2 in large cohorts are needed to analyze treatment response and patient survival of this new molecular entity. The aim of this study was the molecular and clinical characterization of CNS NB-FOXR2. Therefore, the so far largest clinical cohort of CNS NB-FOXR2 was collected and analyzed. Furthermore, CNS NB-FOXR2 were molecularly analyzed in order to identify diagnostic markers for this new entity.

4.2 Results

The molecular and clinical characterization of CNS NB-FOXR2 was conducted in two joint projects with Katja von Hoff et al. and with Andrey Korshunov et al. The Results (4.2) and Discussion (4.3) of the second chapter are based on collaborative publications together with Katja von Hoff et al. and Andrey Korshunov et al. (Korshunov et al., 2021; von Hoff et al., 2021). Katja von Hoff et al. collected the cases and data for the CNS-PNET cohort and performed the clinical analyses. I performed the molecular re-evaluation of the CNS-PNET cohort, analyzed molecular and patient characteristics and provided figures. Andrey Korshunov et al. analyzed the CNS-PNET cohort and the RNA-seq dataset. In parallel, I analyzed the Affymetrix dataset and provided figures. Our collaborative findings were validated by stainings performed by Andrey Korshunov et al. Some content, including figures, tables and text that is shown in this chapter was directly adopted or modified from these publications.

Publications:

“Therapeutic implications of improved molecular diagnostics for rare CNS-embryonal tumor entities – results of an international, retrospective study”

Katja von Hoff, Christine Haberler, **Felix Schmitt-Hoffner**, Elizabeth Schepke, Teresa de Rojas, Sandra Jacobs, Michal Zapotocky, David Sumerauer, Marta Perek-Polnik, Christelle Dufour, Dannis van Vuurden, Irene Slavc, Johannes Gojo, Jessica C. Pickles, Nicolas U. Gerber, Maura Massimino, Maria Joao Gil-da-Costa, Miklos Garami, Ella Kumirova, Astrid Sehested, David Scheie, Ofelia Cruz, Lucas Moreno, Jaeho Cho, Bernward Zeller, Niels Bovenschen, Michael Grotzer, Daniel Alderete, Matija Snuderl, Olga Zheludkova, Andrey Golanov, Konstantin Okonechnikov, Martin Mynarek, B. Ole Juhnke, Stefan Rutkowski, Ulrich Schüller, Barry Pizer, Barbara v. Zezschwitz, Robert Kwiecien, Maximilian Wechsung, Frank Konietzschke, Eugene I. Hwang, Dominik Sturm, Stefan M. Pfister, Andreas von Deimling, Elisabeth J. Rushing, Marina Ryzhova, Peter Hauser, Maria Łastowska, Pieter Wesseling, Felice Giangaspero, Cynthia Hawkins, Dominique Figarella-Branger, Charles Eberhart, Peter Burger, Marco Gessi, Andrey Korshunov, Tom S. Jacques, David Capper, Torsten Pietsch, Marcel Kool;

Neuro-Oncology; 2021; <https://doi.org/10.1093/neuonc/noab136>

“Molecular analysis of pediatric CNS-PNET revealed nosologic heterogeneity and potent diagnostic markers for CNS neuroblastoma with FOXR2-activation”

Andrey Korshunov, Konstantin Okonechnikov, **Felix Schmitt-Hoffner**, Marina Ryzhova, Felix Sahm, Damian Stichel, Daniel Schrimpf, David E. Reuss, Philipp Sievers, Abigail Kora Suwala, Ella Kumirova, Olga Zheludkova, Andrey Golanov, David T. W. Jones, Stefan M. Pfister, Marcel Kool, Andreas von Deimling;

Acta Neuropathologica Communications; 2021; <https://doi.org/10.1186/s40478-021-01118-5>

4.2.1 Methylation-based characterization of the CNS-PNET cohort

The molecular re-classification of CNS-PNET cohorts and early analyses of small series with clinical data suggested that the poor outcome is largely driven by misclassification of HGG (Hwang et al., 2018; Sturm et al., 2016). To further investigate the clinical outcome of CNS NB-FOXR2 and other entities that were histologically classified and treated as CNS-PNET, 307 institutionally diagnosed CNS-PNET samples with clinical data were collected and molecularly analyzed (von Hoff et al., 2021). DNA methylation profiling differentiated the cohort into five major groups: 12% (36) CNS NB-FOXR2, 19% (58) ETMRs, 18% (57) HGG, 22% (89) Others and 22% (67) cases, which were unclassifiable by DNA methylation analysis (Figure 21B). Methylation based t-SNE analysis of the re-evaluation cohort (n=307) and 66 additional CNS NB-FOXR2 cases (Figure 21A), added based on their methylation profiles matching CNS NB-FOXR2, showed that CNS NB-FOXR2 as well as ETMR form two distinct clusters from the remaining groups, namely Other, HGG and unclassifiable cases (Figure 21C). Based on the methylation classifier it was observed that the Other group primarily included Ependymoma (mostly of the RELA subtype (23)), atypical teratoid/rhabdoid tumor (mostly of subclass SHH (10)), Pineoblastoma (mostly classified as group B (7)), CNS HGNET-BCOR (6), CNS EFT-CIC (6) and pleomorphic xanthoastrocytoma (5) and the HGG group mostly included HGG not otherwise specified (19), Glioblastoma IDH wild-type H3.3 G34 mutant (10), infantile hemispheric glioma (7), diffuse midline glioma H3 K27M mutant (6) and glioblastoma, IDH wildtype subclass midline (6) (Figure 21D).

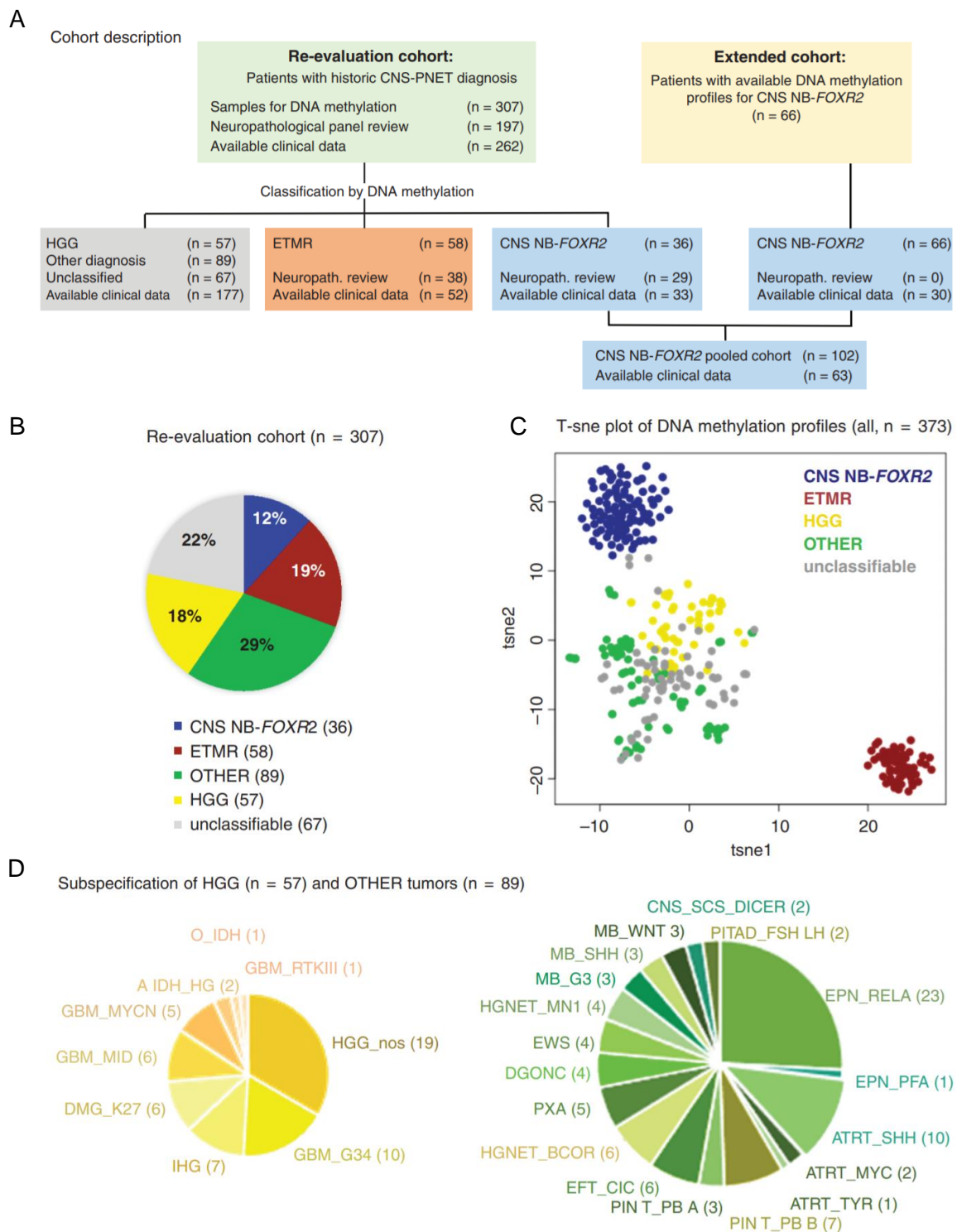


Figure 21: Classification of the CNS-PNET cohort based on methylation data.

(A) Cohort overview of 307 cases of the CNS-PNET re-evaluation cohort and additional 66 CNS NB-FOXR2, (B) Methylation data based classification of the CNS-PNET cohort. (C) t-SNE analysis of the combined cohort based on methylation profiles. (D) Allocation of the HGG and OTHER group into molecular entities and subgroups. This figure was jointly generated with the authors and is taken from the collaborative publication (von Hoff et al., 2021).

4.2.2 Molecular and patient characteristics of CNS NB-FOXR2

In line with previous findings (Sturm et al., 2016) in smaller datasets of CNS NB-FOXR2, in the combined molecular cohort of in total 102 CNS-NB-FOXR2 cases a slight bias to female gender (56 out of 102) and an age range of 1 to 20 years with an median age at diagnosis of 5 years was observed (Figure 22A, B). Data on the location of the tumor, available for 87 cases, clearly indicated that CNS NB-FOXR2 occur exclusively supratentorially with a majority of cases located in the frontal and the temporal lobe (Figure 22C). Copy number profiles, which were generated based on DNA methylation data showed a characteristic gain of chromosome 1q in 94% of cases and further frequent gains of chromosome 3q (21%), 8p (21%), 8p (28%) and 17q (49%). The most prominent loss was observed in chromosome 16q in 56% of cases but also chromosome 3p (34%), 6q (24%), and 10q (25%), showed relatively frequent losses in the CNS NB-FOXR2 cohort (Figure 22D).

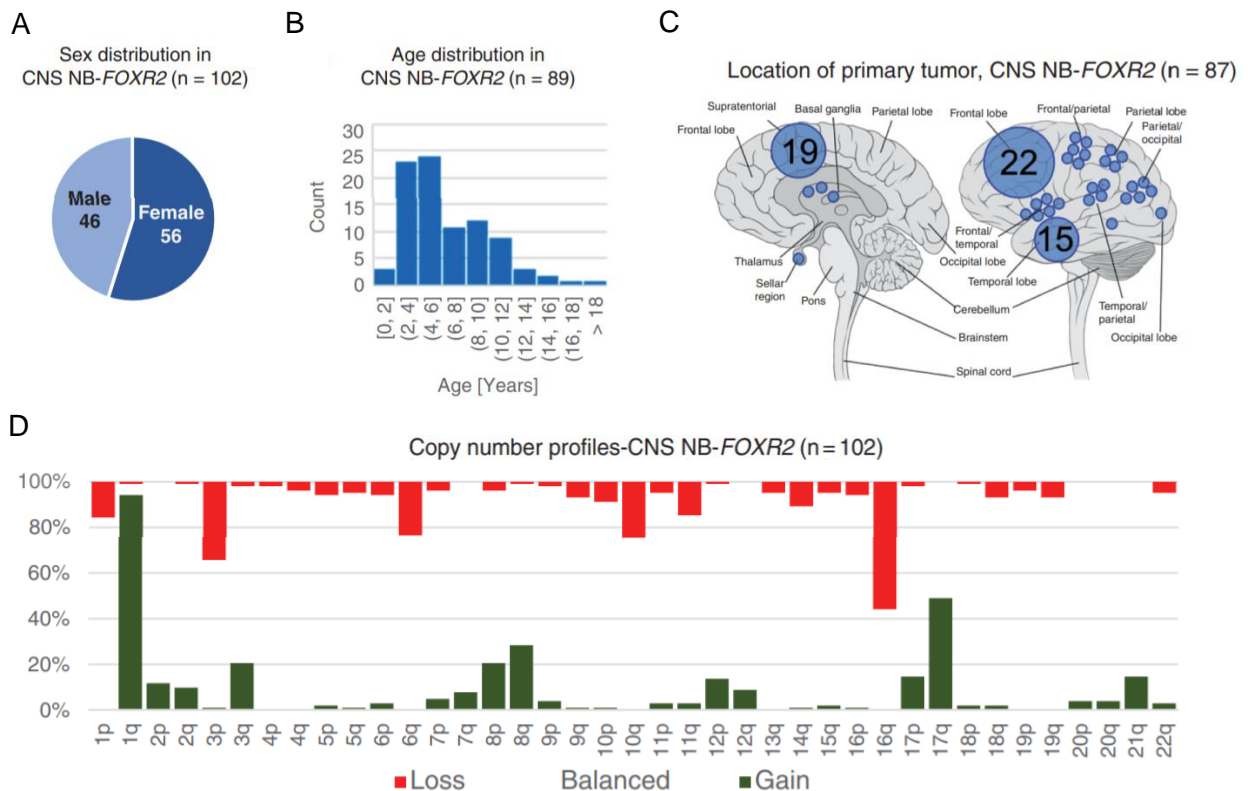


Figure 22: Molecular and patient characteristics of CNS NB-FOXR2.

(A) Gender distribution of 102 CNS NB-FOXR2 cases. (B) Age distribution of 89 CNS NB-FOXR2 cases. (C) Tumor location in different brain regions of 87 CNS NB-FOXR2 cases. (D) Copy number profiles of 102 CNS NB-FOXR2 cases showing frequent chromosomal gains and losses. This figure was jointly generated with the authors and is taken from the collaborative publication (von Hoff et al., 2021).

4.2.3 Survival analyses of CNS NB-FOXR2 in comparison to other entities originally classified as CNS-PNET

Analyzing 247/307 CNS-PNET cases for which full clinical data was available, showed 5-year OS rates of 51% and 5-year PFS rates of 40%, which is in line with previous CNS-PNET cohorts (Figure 23A, B). In contrast to the relatively poor survival of the CNS-PNETs as a mixed bag, the 33 cases classified as CNS NB-FOXR2 showed high survival rates with a 5-year OS survival of 86% and a 5-year PFS of 69% (Figure 23C, D). Extending the clinical cohort by an additional 30 CNS NB-FOXR2 samples identified by methylation profiling confirmed the relatively good prognosis of CNS NB-FOXR2 patients, with a 5-year OS of 85% and a 5-year PFS of 57% in the extended cohort and a 5-year OS of 85% and a 5-year PFS of 63% for the entire CNS NB-FOXR2 cohort (n = 63). As previously concluded, the low overall survival in the CNS-PNET cohort can in large parts be attributed to CNS-PNETs reclassified as embryonal tumors with multilayered rosettes (ETMR; 49/247) or high grade gliomas (HGG; 44/274), which showed 5-year OS rates of 24% and 25% and 5 year PFS rates of 18% and 22%, respectively (Figure 23C, D). OS and PFS analyses of initial staging did not result in significant differences between metastatic disease (M+), localized disease with complete resection (M0R0) and localized disease with incomplete or unknown resection (M0R+/M0Rx) (Figure 23E, F). Overall, these findings demonstrate the clinical importance of molecular diagnostics and clearly indicate a relatively favorable outcome of CNS NB-FOXR2.

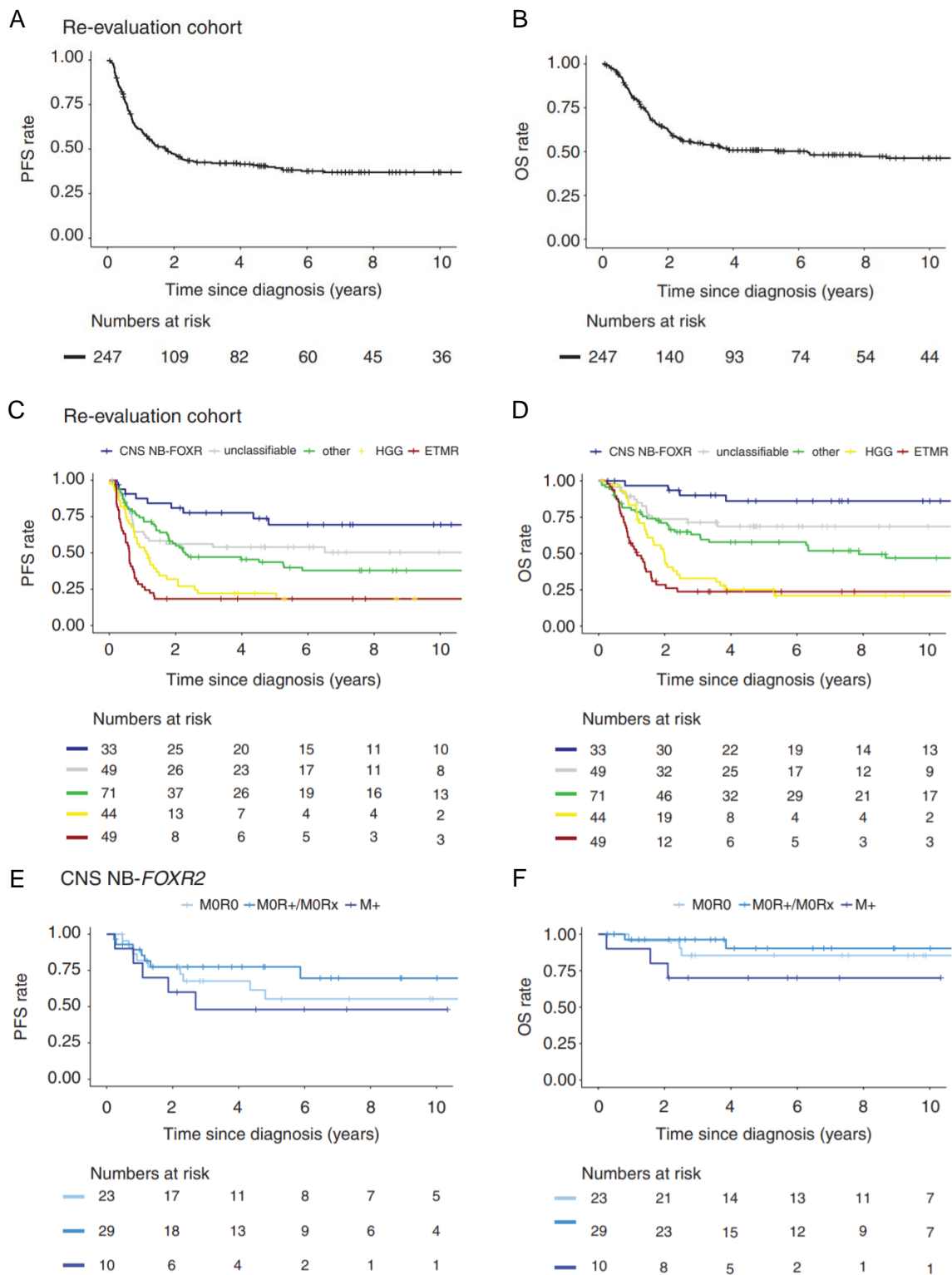


Figure 23: Survival analyses of molecular groups with a focus on CNS NB-FOXR2.

(A) Overall and progression-free survival of CNS-PNET re-evaluation cohort. (B) Overall and progression-free survival of the five distinct groups CNS NB-FOXR2, ETMR, HGG, OTHER and unclassifiable cases. (C) Overall and progression-free survival of CNS NB-FOXR2 by initial staging. This Figure was jointly generated with the authors, and is taken from the collaborative publication (von Hoff et al., 2021).

4.2.4 Diagnostic markers for CNS NB-FOXR2

As described in 4.2.1 the standard identification method of CNS NB-FOXR2 is based on molecular analyses including DNA methylation profiling. However immunohistochemical markers, representing an alternative in case methylation profiling is not available or material is very limited, were so far not described for this entity. To discriminate CNS NB-FOXR2 from morphological mimics represented by neoplasms that are microscopically poorly differentiated, characterized by small cells with an oval or round nucleus and a high nuclear-cytoplasmic ratio (Figure 24), a cohort of 84 pediatric brain tumors that were histologically diagnosed as CNS-PNET was investigated.

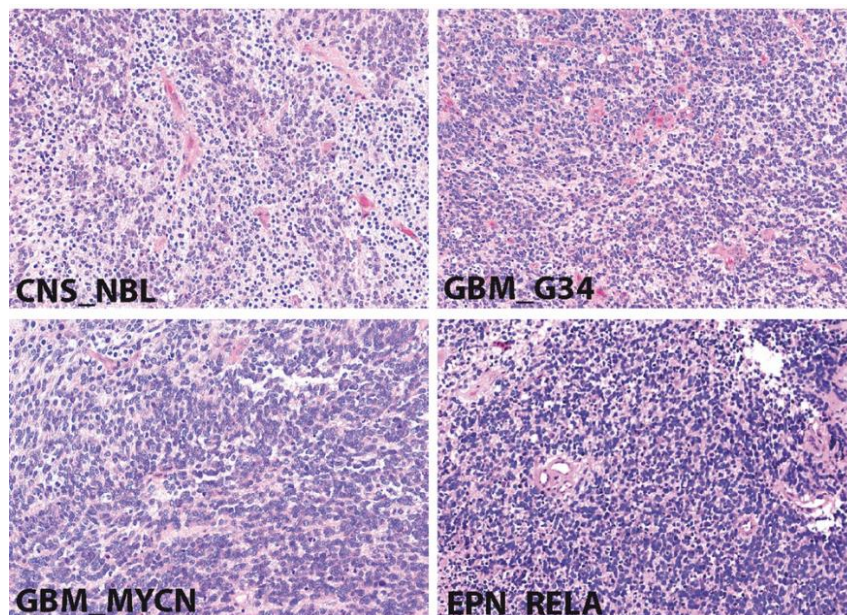


Figure 24: Histopathological analyses of CNS-PNET.

Molecularly distinct entities show similar histopathological characteristics. Figure from collaborative publication, generated by Korshunov et al. (Korshunov et al., 2021).

For molecular characterization DNA methylation profiles were investigated by t-SNE analysis. Using a reference dataset of around 68.500 tumors representing various tumor entities, 84 preselected CNS-PNET cases that matched to four established methylation based entities were observed: 20 (24%) cases were identified as CNS NB-FOXR2, 22 (26%) Glioblastoma IDH wild-type subtype H3.3 G34 mutant (GBM-G34), 18 (21%) Glioblastoma IDH wild-type

subtype MYCN (GBM-MYCN) as well as 24 (29%) Ependymoma with RELA:C11orf95 fusion (EPN-RELA) (Figure 25A, B). Significant histopathological differences between the molecularly defined entities were not observed (Figure 24).

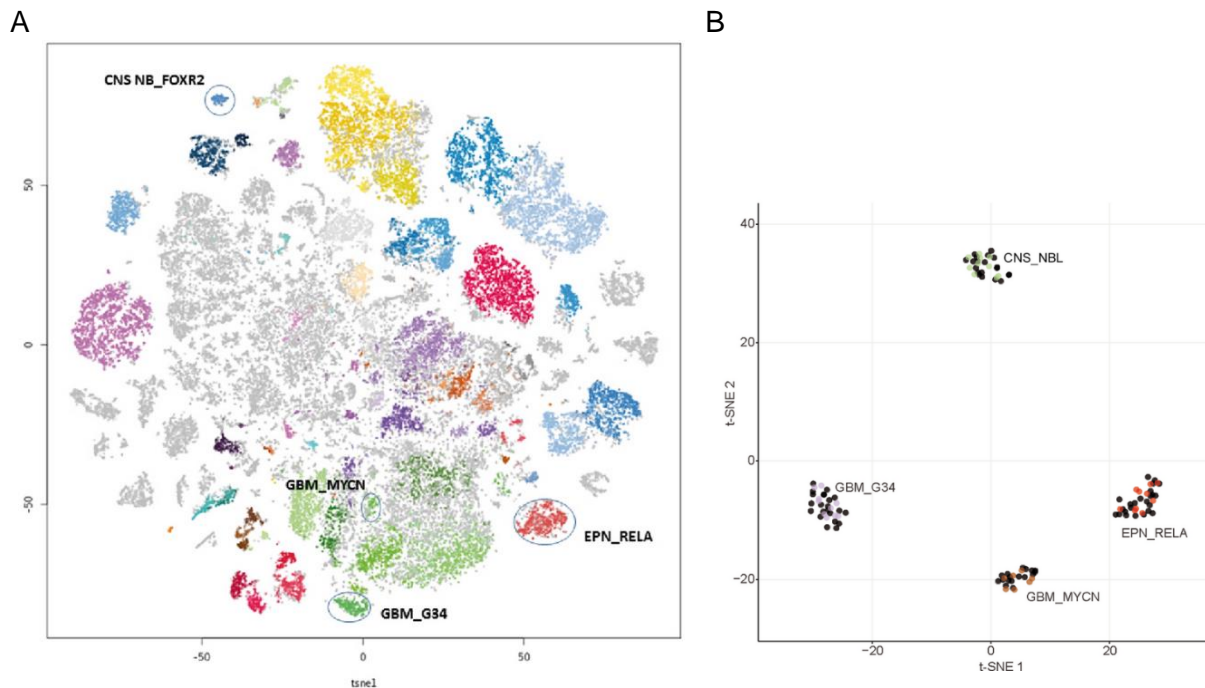


Figure 25: **Methylation data based classification of CNS-PNET cohort.**

(A) Reference dataset of around 68.500 cases containing EPN-RELA, GBM-MYCN, GBM-G34 and CNS NB-FOXR2 displayed by methylation profile based t-SNE clustering. (B) t-SNE analysis of the 84 CNS-PNET cases. Figure modified from collaborative publication, generated by Korshunov et al. (Korshunov et al., 2021).

Transcriptome analyses based on 53 samples, 13 of them CNS NB-FOXR2, 12 GBM-MYCN, 8 GBM-34 and 20 EPN-RELA, showed by means of unsupervised hierarchical clustering, principal component analysis (PCA) and t-SNE analysis that CNS NB-FOXR2 tumors cluster distinctly from EPN-RELA, GBM-MYCN and GBM-G34 tumors based on the top 500 differentially expressed genes (Figure 26A, B, C). This also holds true for the EPN-RELA, whereas GBM-MYCN and GBM-G34 indicated a transcriptionally more similar group indicated by the proximity of the two clusters (Figure 26B, C).

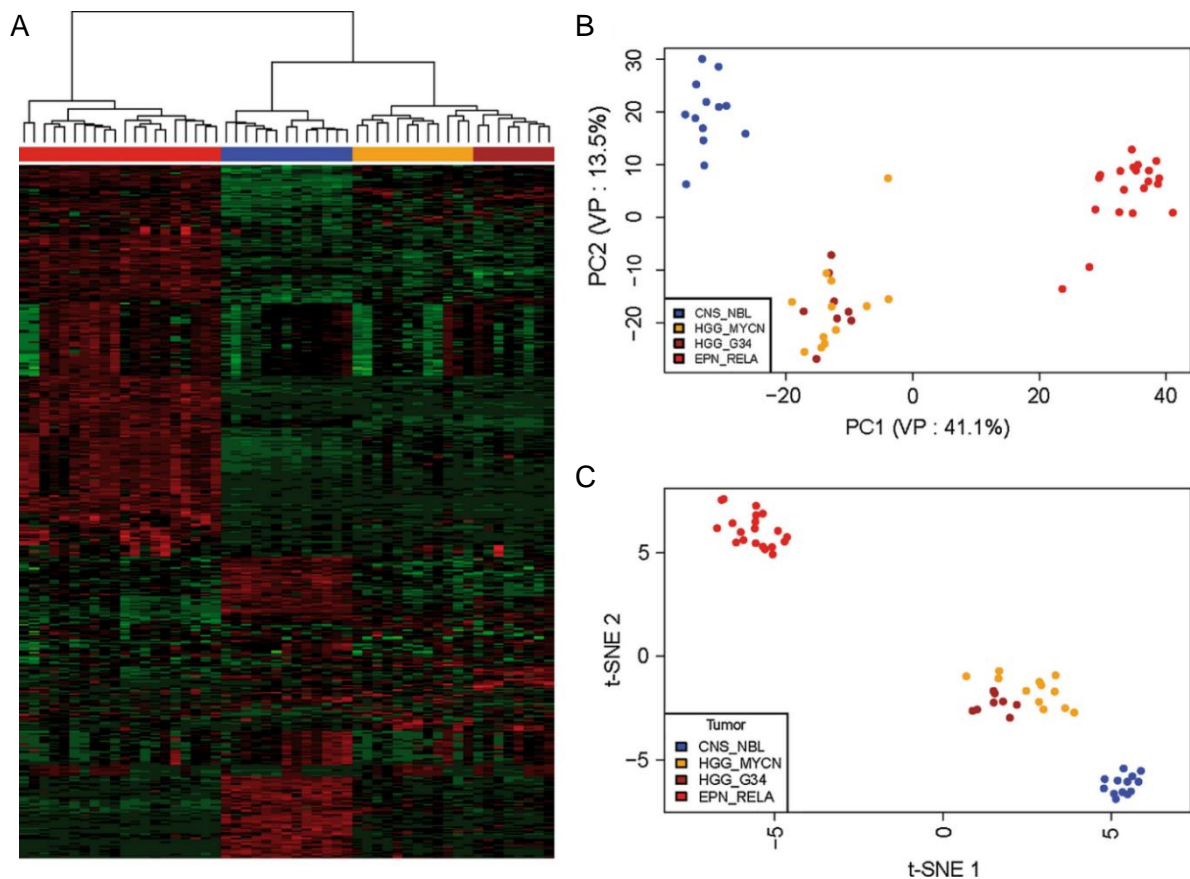


Figure 26: **Transcriptomic analyses of EPN-RELA, GBM-MYCN, GBM-G34 and CNS NB-FOXR2.**

(A) Unsupervised hierarchical clustering based on gene expression data of the four distinct entities. Principle component analysis (PCA) (B) and t-SNE analysis (C) based on top 500 most differentially expressed genes. Figure from collaborative publication, generated by Korshunov et al. (Korshunov et al., 2021).

Investigating the RNA-seq data of the CNS-PNET cohort for potential marker genes, the 30 most differentially expressed genes of CNS NB-FOXR2 compared to the other entities were analyzed. CNS NB-FOXR2 exclusively expressed high levels of *FOXR2* and *SOX10* (Figure 27A, B). In line with the expected mechanism driving EPN-RELA and GBM-MYCN these entities expressed high levels of *RELA* and *MYCN*, respectively. Performing differential gene expression analyses on the independent Affymetrix gene expression dataset consisting of 14 CNS NB-FOXR2 and other brain tumor entities occurring in institutionally diagnosed CNS-PNETs, including glioblastoma, ependymoma, atypical teratoid rhabdoid tumor (ATRT), embryonal tumor with multilayered rosettes (ETMR) and three further recently identified entities originating from CNS-PNETs (Sturm et al., 2016), *SOX10* expression was also identified to be highly expressed in CNS NB-FOXR2 when compared to the other entities, confirming the findings of the RNA-seq dataset (Figure 27C).

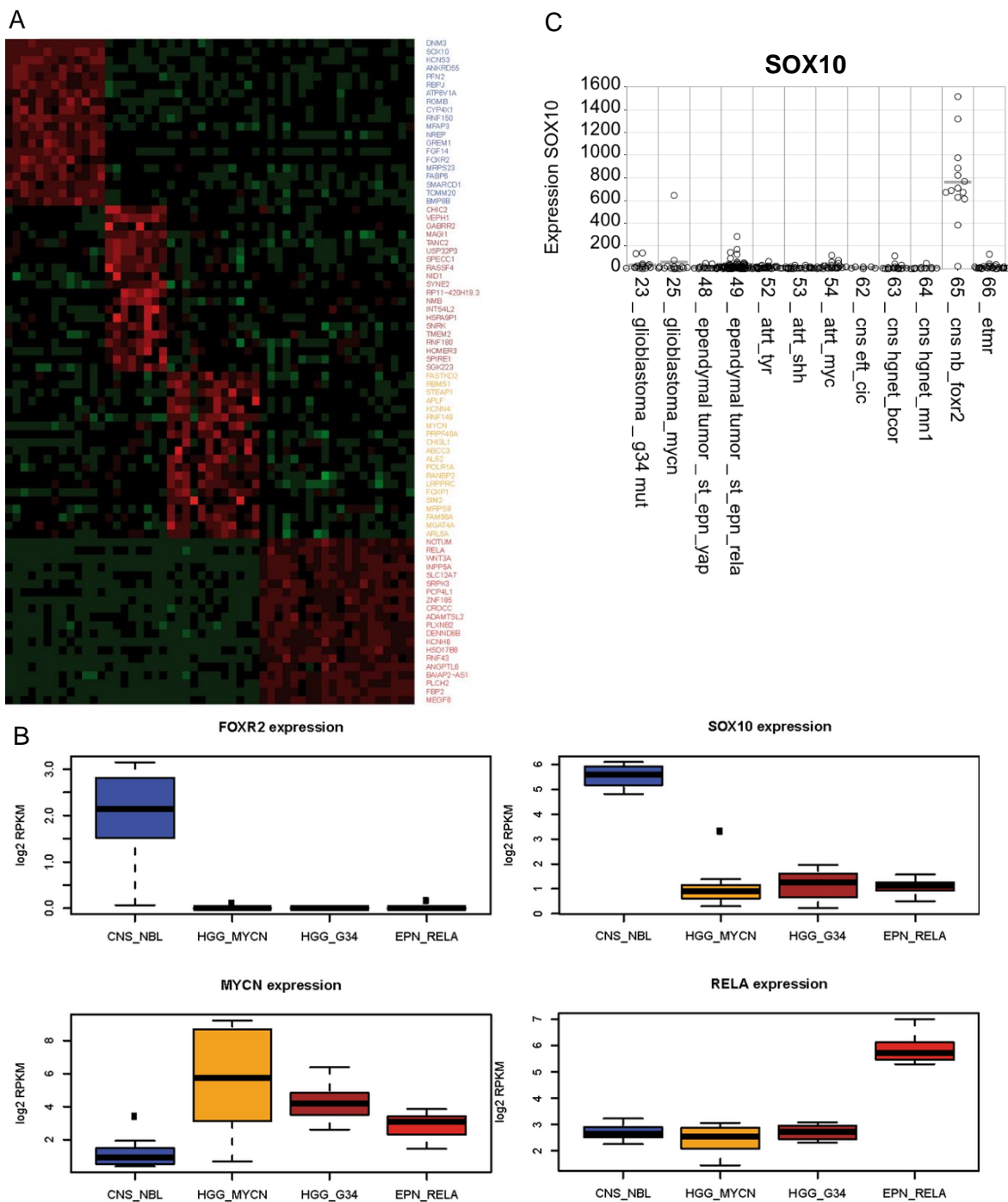


Figure 27: Identification of marker genes for CNS NB-FOXR2 based on expression data.

(A) Analysis of differentially expressed genes between the distinct molecular groups. (B) Expression levels of *FOXR2*, *SOX10*, *MYCN* and *RELA* in the four molecular groups. (C) Expression analysis of *SOX10* in the Affymetrix dataset comparing several CNS-PNET derived entities. This figure was jointly generated with the authors and is modified from the collaborative publication (Korshunov et al., 2021).

To establish a reliable immunohistochemical marker for CNS NB-FOXR2 tumors, the 84 CNS-PNET samples and additional 263 pediatric high-grade CNS tumors showing a variety of molecular diagnoses were stained with a SOX10 antibody. All (100%) of the CNS NB-FOXR2 cases showed a high proportion of cells with intense nuclear SOX10 expression (>75%), whereas EPN-RELA, GBM-MYCN and GBM-G34 as well as embryonal tumors like ETMR, ATRT or the recently identified Astroblastoma, *MN1* altered (former CNS HGNET-*MN1*), CNS tumors with *BCOR* ITD (former CNS HGNET-*BCOR*) and CNS Ewing sarcoma family tumor with *CIC* alteration (CNS EFT-*CIC*) were SOX10 negative (Figure 28; Table 4). Hence, SOX10 identifies a diagnostic marker to distinguish CNS NB-FOXR2 from almost all other histologically diagnosed CNS-PNET with the exception of single cases of malignant gliomas.

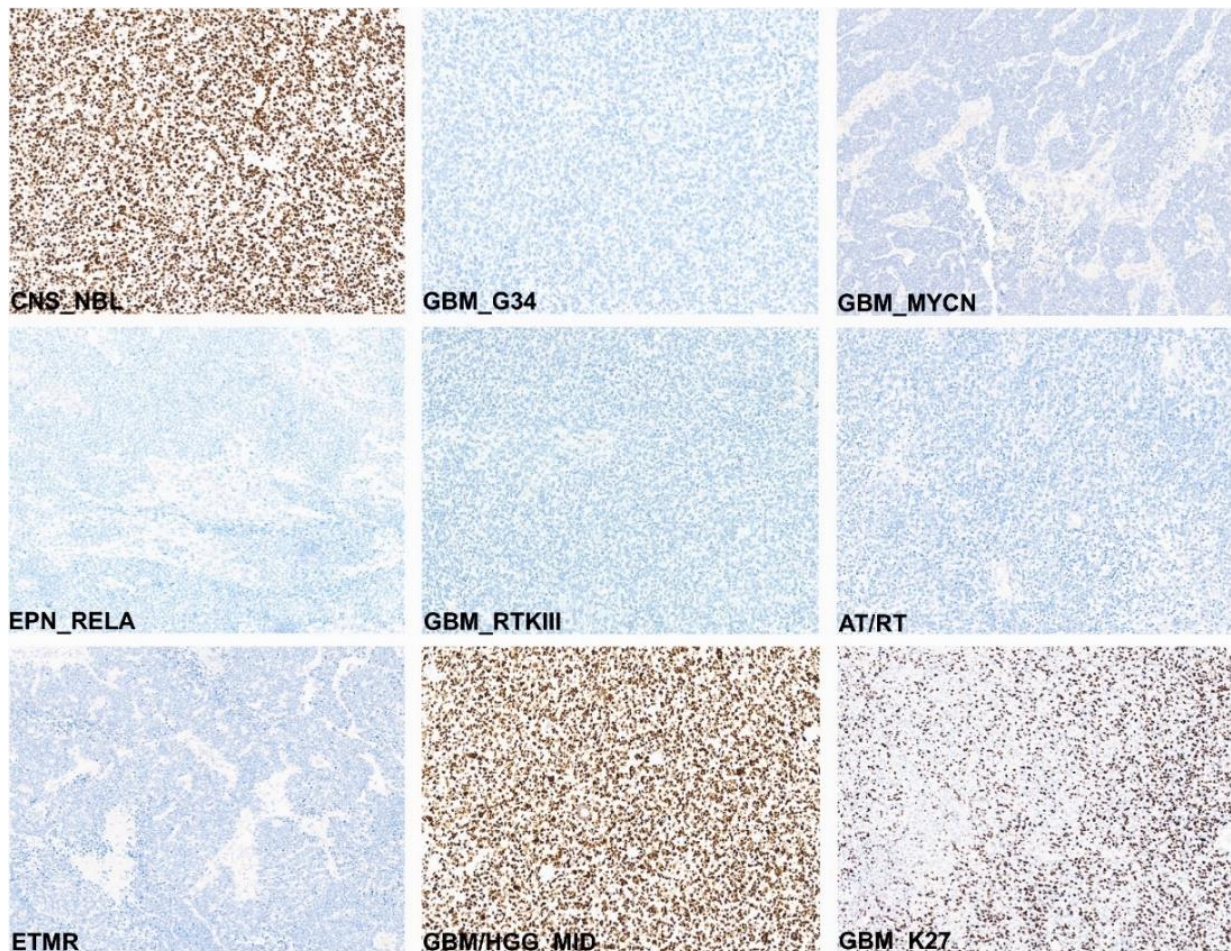


Figure 28: **SOX10 as a immunohistochemical marker for CNS NB-FOXR2.**

SOX10 IHC of entities with CNS-PNET like histologies. Figure from collaborative publication, generated by Korshunov et al. (Korshunov et al., 2021).

Table 4: Percentage of entities with a potential CNS-PNET like histology that show no, low, intermediate or high signal intensity for SOX10 IHC. Table from collaborative publication, generated by Korshunov et al. (Korshunov et al., 2021).

Tumor entity	> 75%	25–74%	1–24%	Negative
CNS neuroblastoma with <i>FOXR2</i> activation (n = 20)	100%	0	0	0
Pediatric glioblastoma with G34 mutation (n = 25)	0	0	0	100%
Pediatric glioblastoma; MYCN (n = 20)	0	0	0	100%
Supratentorial ependymoma; <i>RELA</i> fusion (n = 40)	0	0	0	100%
Diffuse midline glioma, H3 K27-altered (n = 30)	0	40%	30%	30%
Pediatric glioblastoma, RTKI (pGBM_MID; n = 30)	25%	35%	20%	20%
Pediatric glioblastoma, RTKIII (n = 12)	0	0	0	100%
Adult glioblastoma, IDH-wildtype (n = 40)	0	20%	40%	40%
Adult glioblastoma; IDH-mutant (n = 20)	10%	30%	40%	20%
Anaplastic oligodendroglioma, IDH-mutant (n = 20)	10%	40%	30%	20%
Embryonal tumor with multilayered rosettes (n = 30)	0	0	0	100%
Atypical teratoid/rhabdoid tumor (n = 20)	0	0	0	100%
CNS neuroepithelial tumor; MN1-altered (n = 18)	0	0	0	100%
CNS neuroepithelial tumor; BCOR-altered (n = 8)	0	0	0	100%
CNS neuroepithelial tumor; CIC-altered (n = 5)	0	0	0	100%
Intracranial Ewing sarcoma (n = 4)	0	0	0	100%
Diffuse leptomeningeal glioneuronal tumor (n = 5)	0	0	0	100%

Since some malignant gliomas showed SOX10 expression (Table 4) and in order to reliably distinguish CNS NB-*FOXR2* also from these cases, differential gene expression analysis was performed between these groups. Top hits included ANKRD55, OBSCN and GPC3 (Figure 29A, B). Since ANKRD55 was also identified as a promising marker when consulting the Affymetrix dataset (Figure 29C), this candidate was investigated by means of IHC. CNS NB-*FOXR2* showed a clear ANKRD55 signal in all 20 cases, whereas all other cases with the exception of ETMR showed no ANKRD55 signal (Figure 29D, Table 5). Hence, the combined expression of SOX10 and ANKRD55 precisely discriminates CNS NB-*FOXR2* from other morphologically similar hemispheric CNS neoplasms.

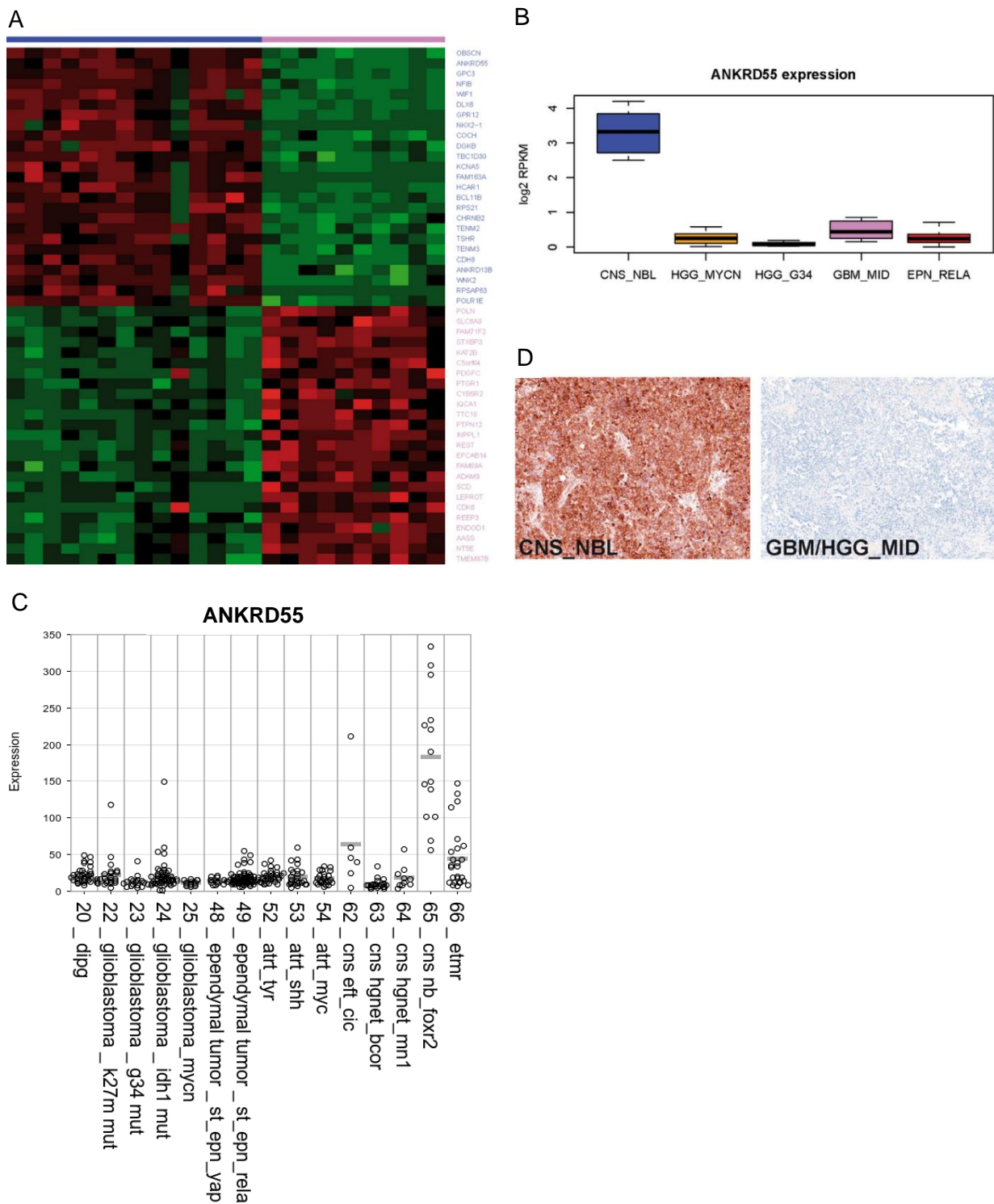


Figure 29: **ANKRD55 is a marker to distinguish CNS NB-FOXR2 from GBM-MID.**

(A) Differential expression analysis of CNS NB-FOXR2 and GBM-MID. (B) Expression levels of *ANKRD55* in CNS NB-FOXR2, HGG-MYCN, HGG-G34, GBM-MID and EPN-RELA. (C) Expression levels of *ANKRD55* in several entities molecularly classified from former CNS-PNET. (D) *ANKRD55* IHC on CNS NB-FOXR2 and HGG-MID. This figure was jointly generated with the authors and is modified from the collaborative publication (Korshunov et al., 2021).

Table 5: Percentage of entities with a potential CNS-PNET like histology that show no, low, intermediate or high signal intensity for ANKRD55 IHC. Table from collaborative publication, generated by Korshunov et al. (Korshunov et al., 2021).

Tumor entity	> 75%	25–74%	1–24%	Negative
CNS neuroblastoma with <i>FOXR2</i> activation (n = 20)	100%	0	0	0
Pediatric glioblastoma with G34 mutation (n = 25)	0	0	0	100%
Pediatric glioblastoma; MYCN (n = 20)	0	0	0	100%
Supratentorial ependymoma; <i>RELA</i> fusion (n = 40)	0	0	0	100%
Diffuse midline glioma, H3 K27-altered (n = 30)	0	0	0	100%
Pediatric glioblastoma, RTKI (pGBM_MID; n = 30)	0	0	0	100%
Pediatric glioblastoma, RTKIII (n = 12)	0	0	0	100%
Adult glioblastoma, IDH-wildtype (n = 40)	0	0	0	100%
Adult glioblastoma; IDH-mutant (n = 20)	0	0	0	100%
Anaplastic oligodendroglioma, IDH-mutant (n = 20)	0	0	0	100%
Embryonal tumor with multilayered rosettes (n = 30)	0	0	30%	70%
Atypical teratoid/rhabdoid tumor (n = 20)	0	0	0	100%
CNS neuroepithelial tumor; MN1-altered (n = 18)	0	0	0	100%
CNS neuroepithelial tumor; BCOR-altered (n = 8)	0	0	0	100%
CNS neuroepithelial tumor; CIC-altered (n = 5)	0	0	0	100%
Intracranial Ewing sarcoma (n = 4)	0	0	0	100%
Diffuse leptomeningeal glioneuronal tumor (n = 5)	0	0	0	100%

4.3 Discussion

Historical cohorts of CNS-PNET are molecularly and clinically highly heterogeneous. They were therefore molecularly re-classified by Sturm et al. in 2016 into several established and four new entities, amongst them CNS NB-FOXR2 (Sturm et al., 2016). In the context of this thesis, two studies were conducted (Korshunov et al., 2021; von Hoff et al., 2021) where CNS-PNET cohorts were re-evaluated by methylation data based classification. Identified molecular entities were clinically and molecularly characterized with a focus on CNS NB-FOXR2. In 307 CNS-PNET cases of the von Hoff cohort a representation of 12% CNS NB-FOXR2, 19% ETMR, 18% HGG and 29% of other entities not covered by the previous groups, including mainly ependymoma, ATRT, pineoblastoma and medulloblastoma were identified (von Hoff et al., 2021). Within the Korshunov cohort 84 histologically diagnosed CNS-PNET were molecularly analyzed and re-classified into 24% CNS NB-FOXR2, 26% glioblastoma H3.3 G34 mutant, 29% glioblastoma MYCN and 29% ependymoma RELA (Korshunov et al., 2021). Astroblastoma, *MN1* altered (former CNS HGNET-*MN1*), CNS tumors with *BCOR* internal tandem duplication (former CNS HGNET-*BCOR*) as well as CNS EFT-*CIC* were not detected in this cohort. Furthermore, no ETMR, ATRT or pineoblastoma were identified since cases showing positive LIN28A or lack of INI1 staining in tumor cells as well as tumors of the pineal region were excluded from the cohort.

In line with previous studies the distribution of molecular entities in the two cohorts demonstrated that a high proportion of CNS-PNET cannot be considered embryonal tumors since only around 24% of the Korshunov cohort and around 41% of the von Hoff cohort, including mainly CNS NB-FOXR2, ETMR and smaller subsets of ATRT, pineoblastoma and medulloblastoma, are thought to have an embryonal origin (Hwang et al., 2018; Schwalbe et al., 2013a; Sturm et al., 2016). Other tumors classified as HGG and ependymoma are all considered to have a glial origin (Jiang and Uhrbom, 2012; Kristensen et al., 2019; Poppleton and Gilbertson, 2007). The description of patient characteristics of the identified CNS NB-FOXR2 revealed characteristic features such as the exclusively supratentorial location of the tumors, a median age of 5 years and a slight bias to female patients, which is relevant for diagnosis and differs from other embryonal tumors such as ETMR that show a younger patient age and highly variable tumor location (Lambo et al., 2019a; von Hoff et al., 2021; Wang et al., 2018). Furthermore, a gain of chromosome 1q in almost all cases, a loss of chromosome 16q as well as a gain of chromosome 17q is highly characteristic for CNS NB-FOXR2, which was not only reported in the studies described here but also by previous publications (Chiang and Ellison, 2017; Sturm et al., 2016).

At this stage, the gold standard for identifying CNS NB-*FOXR2* and various other pediatric cancer types may be DNA methylation analysis (Capper et al., 2018a; Capper et al., 2018b; Korshunov et al., 2016; Pajtler et al., 2015; Reinhardt et al., 2019; Sturm et al., 2016). Institutions without access to this technology, however, rely on specific immunohistochemical markers to identify the constantly increasing number of pediatric brain tumor entities. Several entities, including glioblastoma H3.3 G34 mutant or ependymoma *RELA* can be identified using established antibodies against H3.3 G34 or p65-*RelA* and *L1CAM* (Gessi et al., 2019), however no specific immunohistochemical identification for CNS NB-*FOXR2* was possible so far. Hence, gene expression data was generated for 53 CNS-PNET of the Korshunov cohort, including 13 CNS NB-*FOXR2* cases. The four identified molecular entities showed distinct transcriptional signatures, especially for the CNS NB-*FOXR2* and ependymoma *RELA*, which allowed for the investigation of marker genes by differential gene expression analyses. *SOX10* and *ANKRD55* were identified as promising candidates highly expressed almost exclusively in CNS NB-*FOXR2*. Conducting this analysis in an independent Affymetrix gene expression dataset containing a variety of entities that can potentially be diagnosed as CNS-PNET, *SOX10* was again identified as a top hit and also *ANKRD55* was found to be exclusively expressed in CNS NB-*FOXR2* and ETMR. SRY-Box Transcription Factor 10 (*SOX10*) is essential for the development of various neural crest derived cells and is highly expressed in melanomas and Schwann cells tumors (Bannykh et al., 2006; Miettinen et al., 2015). For Ankyrin Repeat Domain-Containing Protein 55 (*ANKRD55*) the biological function has not yet been identified, however, SNPs in the *ANKRD55* gene were associated with a risk for multiple sclerosis (James et al., 2018; Ugidos et al., 2019). Furthermore, recent data suggests a role in forming multi-protein complexes and influencing mitosis, but the presence of *ANKRD55* in pediatric brain tumors has not been systematically investigated, yet (James et al., 2018; Ugidos et al., 2019). By means of immunohistochemical analyses using commercially available antibodies against *SOX10* and *ANKRD55* these potential CNS NB-*FOXR2* markers were investigated. *ANKRD55* was detected exclusively in CNS NB-*FOXR2* and ETMR by IHC and *SOX10* was found in all CNS NB-*FOXR2* but also in some malignant gliomas. Therefore, *SOX10* IHC can be applied to distinguish CNS NB-*FOXR2* from other embryonal tumors. For discrimination of this entity from other histologically diagnosed CNS-PNET/morphological mimics, including small subsets of malignant glioma, immunopositivity for *SOX10* and *ANKRD55* represents a specific diagnostic marker for CNS NB-*FOXR2*.

The importance of clearly identifying CNS NB-*FOXR2* becomes particularly relevant when taking into account findings related to their clinical outcome. Within CNS-PNET that show a highly heterogeneous but overall very poor survival of patients (Davidson et al., 2011; Hwang

et al., 2018; Picard et al., 2012; Stensvold et al., 2017; Sturm et al., 2016), we observed in the so far largest cohort of clinically analyzed CNS NB-FOXR2 that these patients have a favorable overall survival (5-year OS of 85%). These observations are in line with previous reports in smaller cohorts (Hwang et al., 2018; Lastowska et al., 2020; Sturm et al., 2016; von Hoff et al., 2018). The overall poor patient outcome in CNS-PNET is clearly associated to CNS-PNET subsets that were molecularly classified as either high-grade glioma or ETMR, showing 5-year OS rates of 25% and 24%, respectively. These results underline the need of differentiated therapeutic approaches to treat the molecularly re-evaluated subsets of CNS-PNET. Prospective clinical trials will be necessary to investigate a potential de-escalation of treatment, which is currently conducted according to relatively aggressive CNS-PNET protocols (Fangusaro et al., 2008; Friedrich et al., 2013; Gerber et al., 2014; Geyer et al., 2005; Massimino et al., 2013).

Since CNS NB-FOXR2 is a rare disease, presumably an international collaboration would be required to conduct a prospective clinical trial. Within this context, the diagnostic algorithm for immunohistochemical identification of CNS NB-FOXR2 could be confirmed as well. Furthermore, a long-term follow-up of a prospective trial will be relevant due to late relapses that were observed in CNS NB-FOXR2.

Altogether, the clinical and molecular characterization of CNS NB-FOXR2, which was conducted on historically diagnosed CNS-PNET that were molecularly re-evaluated, revealed diagnostic markers, namely SOX10 and ANKRD55, to immunohistochemically identify CNS NB-FOXR2. Moreover, the analyses demonstrated that CNS NB-FOXR2 patients have a relatively favorable outcome, which has a high clinical relevance in the context of the aggressively treated CNS-PNET and that prospective trials are necessary to identify a differentiated therapeutic approach to treat this distinct entity.

5 Concluding discussion and outlook

In the first chapter (3), this study revealed the clinical and mechanistic role of *FOXR2* in peripheral neuroblastoma and in the second chapter (4) the recently identified entity CNS NB-*FOXR2* was molecularly and clinically characterized. *FOXR2* expression in peripheral neuroblastoma was for the first time described as a prognostic risk factor and the findings on the stabilization of the most prominent risk factor in neuroblastoma, *MYCN*, by *FOXR2* sheds light on an alternative mechanism driving these tumors. Furthermore, this study has shown that the recently described entity of CNS NB-*FOXR2* have a relatively favorable outcome, which is in stark contrast to the poor survival of CNS-PNETs under which most CNS NB-*FOXR2* tumors were previously histologically diagnosed (Sturm et al., 2016). To enable the identification of CNS NB-*FOXR2* from CNS-PNETs also for centers without access to molecular classification tools such as DNA methylation profiling, an immunohistochemical algorithm was developed that allows for specific identification of CNS NB-*FOXR2* by *SOX10* and *ANRKD55* staining.

Interestingly, in CNS NB-*FOXR2* and in the subset of peripheral neuroblastoma with *FOXR2* expression divergent clinical outcomes were observed, with 5-year OS rates of 85% and 67%, respectively. Factors that determine how prone different tumors are to the stabilization of *MYC* or *MYCN* might play a role. Based on the literature that has previously related *FOXR2* to the survival of patients, *FOXR2* is in all cases, including breast cancer, endometrial adenocarcinoma and ovarian cancer (Deng et al., 2017; Li et al., 2018; Song et al., 2016), associated with a poor clinical outcome. What causes the poor outcome and what might lead to differences in CNS NB-*FOXR2* is currently being investigated. From preliminary investigations it is known that not only *FOXR2*-expressing neuroblastoma but also *FOXR2*-expressing subsets of other pediatric malignancies such as glioblastoma, medulloblastoma and CNS NB-*FOXR2* are associated with a *MYC(N)* signature (Westermann et al., 2008), which might indicate increased *MYC/MYCN* protein levels also in these entities. To investigate the role of *FOXR2* in these entities, a deeper understanding on *MYC/MYCN* protein levels in various pediatric cancer types with and without *FOXR2* expression and knowledge on the precise mechanism of *MYC/MYCN* stabilization is therefore needed. The stabilization of *MYC* or *MYCN* is besides *FOXR2* also mediated by further proteins and the stabilization is observed in other malignancies as well. In T-cell leukemia Aurora B kinase (*AURKB*) phosphorylates *MYC* at serine 62 (S62) and thereby stabilizes the protein (Jiang et al., 2020; Malempati et al., 2006) and in neuroblastoma Aurora A kinase (*AURKA*) binds and stabilizes *MYCN* (Otto et al., 2009). During its lifecycle, *MYC/MYCN* undergoes different phosphorylation states that initially

lead to a stabilization via phosphorylation of S62. In a subsequent step, the phosphorylation of Threonine 58 (T58) targets MYC/MYCN for proteasomal degradation via FBW7 ubiquitin ligase (Gustafson and Weiss, 2010; Junttila and Westermarck, 2008; Laurenti et al., 2009; Welcker et al., 2004). Therefore, the precise investigation of the interaction between FOXR2 and MYC/MYCN is needed, since depending on the MYC/MYCN phosphorylation state that FOXR2 binds to, other tumor specific interaction partners involved in the MYC/MYCN lifecycle might play a role. Moreover, preliminary results in mice suggest an important role of FOXR2 per se in tumorigenesis since the expression of FOXR2 in neural stem cells (NSCs) injected into the mouse brain leads to the formation of tumors, which naïve NSCs are not capable of. In addition, it was observed that tumors were even more aggressive when NSCs expressing both FOXR2 and MYC/MYCN were injected into mice. To identify genes which are directly activated by the transcription factor FOXR2, and to compare these to genes activated by MYC and MYCN, CHIP sequencing is currently being conducted for FOXR2, MYC and MYCN using these tumor tissues from mice to identify the genomic binding sites for the three transcription factors. This approach may provide more insight on what drives FOXR2 activated tumors and how this correlates to tumors driven by MYC and MYCN. Together with the molecular analysis of the *FOXR2*-expressing pediatric brain tumors it may help to understand further functions of FOXR2 besides the stabilization of MYC/MYCN in these tumors. Findings of this study on the prognostic value of *FOXR2* expression in neuroblastoma may further be investigated in the context of prospective clinical trials to further improve risk stratification of this clinically heterogeneous tumor. Furthermore, the mechanistic interaction of FOXR2 and MYCN, which was revealed in this study, may in the future be exploited to identify therapeutic approaches, specifically targeting the stabilization or downstream effects of MYCN. This was already previously done in *MYCN*-amplified neuroblastoma and could therefore be highly efficient also in the *FOXR2* group due to the high MYCN protein levels (Barone et al., 2013; Huang and Weiss, 2013). Furthermore, *FOXR2* is not expressed in healthy tissue except for testis, but represents a strong marker for subsets of several cancer types, which makes FOXR2 itself a promising target of intervention with little on target associated side effects. Since FOXR2 is a transcription factor, which were historically viewed as “undruggable”, novel approaches such as proteolysis targeting chimaeras (PROTACs) may be an option to specifically target FOXR2 (Bushweller, 2019).

Overall, based on these ongoing investigations I aim to shed light on oncogenic mechanisms and functions of FOXR2 in pediatric cancer, which enables the identification of targets to identify novel and more specific treatment strategies for FOXR2 driven pediatric tumors.

6 References

- Ackermann, S., Cartolano, M., Hero, B., Welte, A., Kahlert, Y., Roderwieser, A., Bartenhagen, C., Walter, E., Gecht, J., Kerschke, L., *et al.* (2018). A mechanistic classification of clinical phenotypes in neuroblastoma. *362*, 1165-1170.
- Ambros, P.F., Ambros, I.M., Brodeur, G.M., Haber, M., Khan, J., Nakagawara, A., Schleiermacher, G., Speleman, F., Spitz, R., London, W.B., *et al.* (2009). International consensus for neuroblastoma molecular diagnostics: report from the International Neuroblastoma Risk Group (INRG) Biology Committee. *British journal of cancer* *100*, 1471-1482.
- American_Cancer_Society (accessed 12.11.2021). Key Statistics for Childhood Cancers <https://www.cancer.org/cancer/cancer-in-children/key-statistics.html>. In Key Statistics for Childhood Cancers (cancer.org).
- Aridgides, P., Kang, G., Mazewski, C., and Merchant, T.J.I.J.o.R.O., Biology, Physics (2019). Outcomes after radiation therapy for very young children with high-risk medulloblastoma or supratentorial primitive neuroectodermal tumor treated on COG ACNS0334. *105*, S109.
- Armstrong, D.D., and Giangaspero, F. (2003). Pediatric brain tumors: introduction. *Brain pathology (Zurich, Switzerland)* *13*, 373-375.
- Attiyeh, E.F., London, W.B., Mossé, Y.P., Wang, Q., Winter, C., Khazi, D., McGrady, P.W., Seeger, R.C., Look, A.T., Shimada, H., *et al.* (2005). Chromosome 1p and 11q Deletions and Outcome in Neuroblastoma. *353*, 2243-2253.
- Aubrey, B.J., Strasser, A., and Kelly, G.L. (2016). Tumor-Suppressor Functions of the TP53 Pathway. *Cold Spring Harbor perspectives in medicine* *6*, a026062.
- Bannykh, S.I., Stolt, C.C., Kim, J., Perry, A., and Wegner, M. (2006). Oligodendroglial-specific transcriptional factor SOX10 is ubiquitously expressed in human gliomas. *Journal of neuro-oncology* *76*, 115-127.
- Barone, G., Anderson, J., Pearson, A.D.J., Petrie, K., and Chesler, L. (2013). New Strategies in Neuroblastoma: Therapeutic Targeting of MYCN and ALK. *Clinical Cancer Research* *19*, 5814.
- Beckmann, P.J., Larson, J.D., Larsson, A.T., Ostergaard, J.P., Wagner, S., Rahrmann, E.P., Shamsan, G.A., Otto, G.M., Williams, R.L., Wang, J., *et al.* (2019). Sleeping Beauty Insertional Mutagenesis Reveals Important Genetic Drivers of Central Nervous System Embryonal Tumors. *Cancer Research* *79*, 905.
- Behjati, S., Gilbertson, R.J., and Pfister, S.M. (2021). Maturation Block in Childhood Cancer. *Cancer Discov* *11*, 542-544.
- Bender, S., Tang, Y., Lindroth, A.M., Hovestadt, V., Jones, D.T., Kool, M., Zapatka, M., Northcott, P.A., Sturm, D., Wang, W., *et al.* (2013). Reduced H3K27me3 and DNA hypomethylation are major drivers of gene expression in K27M mutant pediatric high-grade gliomas. *Cancer cell* *24*, 660-672.

- Berthold, F., Faldum, A., Ernst, A., Boos, J., Dilloo, D., Eggert, A., Fischer, M., Frühwald, M., Henze, G., Klingebiel, T., *et al.* (2020). Extended induction chemotherapy does not improve the outcome for high-risk neuroblastoma patients: results of the randomized open-label GPOH trial NB2004-HR. *Annals of Oncology* 31, 422-429.
- Brodeur, G.M., and Bagatell, R. (2014). Mechanisms of neuroblastoma regression. *Nature Reviews Clinical Oncology* 11, 704-713.
- Bushweller, J.H. (2019). Targeting transcription factors in cancer — from undruggable to reality. *Nature Reviews Cancer* 19, 611-624.
- Cacciotti, C., Fleming, A., and Ramaswamy, V. (2020). Advances in the molecular classification of pediatric brain tumors: a guide to the galaxy. *The Journal of Pathology* 251, 249-261.
- Capper, D., Jones, D.T.W., Sill, M., Hovestadt, V., Schrimpf, D., Sturm, D., Koelsche, C., Sahm, F., Chavez, L., Reuss, D.E., *et al.* (2018a). DNA methylation-based classification of central nervous system tumours. *Nature* 555, 469-474.
- Capper, D., Stichel, D., Sahm, F., Jones, D.T.W., Schrimpf, D., Sill, M., Schmid, S., Hovestadt, V., Reuss, D.E., Koelsche, C., *et al.* (2018b). Practical implementation of DNA methylation and copy-number-based CNS tumor diagnostics: the Heidelberg experience. *Acta Neuropathol* 136, 181-210.
- Chang, C.H., Housepian, E.M., and Herbert, C.J.R. (1969). An operative staging system and a megavoltage radiotherapeutic technic for cerebellar medulloblastomas. 93, 1351-1359.
- Chiang, J.C.H., and Ellison, D.W. (2017). Molecular pathology of paediatric central nervous system tumours. *The Journal of Pathology* 241, 159-172.
- Clynes, D., Jelinska, C., Xella, B., Ayyub, H., Scott, C., Mitson, M., Taylor, S., Higgs, D.R., and Gibbons, R.J. (2015). Suppression of the alternative lengthening of telomere pathway by the chromatin remodelling factor ATRX. *Nat Commun* 6, 7538.
- Cohn, S.L., Pearson, A.D.J., London, W.B., Monclair, T., Ambros, P.F., Brodeur, G.M., Faldum, A., Hero, B., Iehara, T., Machin, D., *et al.* (2009). The International Neuroblastoma Risk Group (INRG) classification system: an INRG Task Force report. *J Clin Oncol* 27, 289-297.
- Conter, H.J., Gopalakrishnan, V., Ravi, V., Ater, J.L., Patel, S., and Araujo, D.M. (2014). Adult versus Pediatric Neuroblastoma: The M.D. Anderson Cancer Center Experience. *Sarcoma* 2014, 375151.
- Cooper (2000). *The Cell: A Molecular Approach*. 2nd edition.
- Cozzio, A., Passegué, E., Ayton, P.M., Karsunky, H., Cleary, M.L., and Weissman, I.L. (2003). Similar MLL-associated leukemias arising from self-renewing stem cells and short-lived myeloid progenitors. *Genes & development* 17, 3029-3035.
- Danielsson, A., Nemes, S., Tisell, M., Lannering, B., Nordborg, C., Sabel, M., and Carén, H.J.C.e. (2015). MethPed: a DNA methylation classifier tool for the identification of pediatric brain tumor subtypes. 7, 1-9.

- Davidson, T.B., Ji, L., Haley, K., Dhall, G., Grimm, J.P., Gilles, F.H., Gardner, S.L., Allen, J.C., Bedros, A.A., Ettl, M.M., *et al.* (2011). Outcome of Head Start III multinational protocol for newly diagnosed central nervous system (CNS) primitive neuroectodermal tumors (pnet) of young children. *Journal of Clinical Oncology* 29, 9519-9519.
- Deng, X., Hou, C., Liang, Z., Wang, H., Zhu, L., and Xu, H. (2017). miR-202 Suppresses Cell Proliferation by Targeting FOXR2 in Endometrial Adenocarcinoma. *Disease markers* 2017, 2827435.
- Depuydt, P., Boeva, V., Hocking, T.D., Cannoodt, R., Ambros, I.M., Ambros, P.F., Asgharzadeh, S., Attiyeh, E.F., Combaret, V., and Defferrari, R.J.J.J.o.t.N.C.I. (2018). Genomic amplifications and distal 6q loss: novel markers for poor survival in high-risk neuroblastoma patients. *110*, 1084-1093.
- Dufour, C., Kieffer, V., Varlet, P., Raquin, M.A., Dhermain, F., Puget, S., Valteau-Couanet, D., Grill, J.J.P.b., and cancer (2014). Tandem high-dose chemotherapy and autologous stem cell rescue in children with newly diagnosed high-risk medulloblastoma or supratentorial primitive neuro-ectodermic tumors. *61*, 1398-1402.
- Dupain, C., Harttrampf, A.C., Urbinati, G., Geoerger, B., and Massaad-Massade, L. (2017). Relevance of Fusion Genes in Pediatric Cancers: Toward Precision Medicine. *Molecular Therapy - Nucleic Acids* 6, 315-326.
- Fangusaro, J., Finlay, J., Sposto, R., Ji, L., Saly, M., Zacharoulis, S., Asgharzadeh, S., Abromowitch, M., Olshefski, R., Halpern, S., *et al.* (2008). Intensive chemotherapy followed by consolidative myeloablative chemotherapy with autologous hematopoietic cell rescue (AuHCR) in young children with newly diagnosed supratentorial primitive neuroectodermal tumors (sPNETs): report of the Head Start I and II experience. *Pediatr Blood Cancer* 50, 312-318.
- Filbin, M., and Monje, M. (2019). Developmental origins and emerging therapeutic opportunities for childhood cancer. *Nature Medicine* 25, 367-376.
- Friedrich, C., von Bueren, A.O., von Hoff, K., Gerber, N.U., Ottensmeier, H., Deinlein, F., Benesch, M., Kwiecien, R., Pietsch, T., Warmuth-Metz, M., *et al.* (2013). Treatment of young children with CNS-primitive neuroectodermal tumors/pineoblastomas in the prospective multicenter trial HIT 2000 using different chemotherapy regimens and radiotherapy. *Neuro Oncol* 15, 224-234.
- Funato, K., Major, T., Lewis, P.W., Allis, C.D., and Tabar, V. (2014). Use of human embryonic stem cells to model pediatric gliomas with H3.3K27M histone mutation. *Science (New York, NY)* 346, 1529-1533.
- Furuta, T., Moritsubo, M., Muta, H., Koga, M., Komaki, S., Nakamura, H., Morioka, M., Ohshima, K., and Sugita, Y. (2020). Central nervous system neuroblastic tumor with FOXR2 activation presenting both neuronal and glial differentiation: a case report. *Brain Tumor Pathology* 37, 100-104.
- Gajjar, A., Pfister, S.M., Taylor, M.D., and Gilbertson, R.J. (2014). Molecular Insights into Pediatric Brain Tumors Have the Potential to Transform Therapy. *Clinical Cancer Research* 20, 5630.

- Ganeshan, V.R., and Schor, N.F. (2011). Pharmacologic Management of High-Risk Neuroblastoma in Children. *Pediatric Drugs* 13, 245-255.
- Gaspar, N., Hartmann, O., Munzer, C., Bergeron, C., Millot, F., Cousin-Lafay, L., Babin-Boilletot, A., Blouin, P., Pajot, C., and Coze, C. (2003). Neuroblastoma in adolescents. 98, 349-355.
- Gerber, N.U., von Hoff, K., Resch, A., Ottensmeier, H., Kwiecien, R., Faldum, A., Matuschek, C., Hornung, D., Bremer, M., Benesch, M., *et al.* (2014). Treatment of children with central nervous system primitive neuroectodermal tumors/pinealoblastomas in the prospective multicentric trial HIT 2000 using hyperfractionated radiation therapy followed by maintenance chemotherapy. *International journal of radiation oncology, biology, physics* 89, 863-871.
- Gessi, M., Giagnacovo, M., Modena, P., Elefante, G., Gianni, F., Buttarelli, F.R., Arcella, A., Donofrio, V., Diomedi Camassei, F., Nozza, P., *et al.* (2019). Role of Immunohistochemistry in the Identification of Supratentorial C11ORF95-RELA Fused Ependymoma in Routine Neuropathology. *The American journal of surgical pathology* 43, 56-63.
- Geyer, J.R., Sposto, R., Jennings, M., Boyett, J.M., Axtell, R.A., Breiger, D., Broxson, E., Donahue, B., Finlay, J.L., Goldwein, J.W., *et al.* (2005). Multiagent Chemotherapy and Deferred Radiotherapy in Infants With Malignant Brain Tumors: A Report From the Children's Cancer Group. *Journal of Clinical Oncology* 23, 7621-7631.
- Gritsch, S., Batchelor, T.T., and Gonzalez Castro, L.N. (2021). Diagnostic, therapeutic, and prognostic implications of the 2021 World Health Organization classification of tumors of the central nervous system. *Cancer* *n/a*.
- Gröbner, S. (2017). The landscape of genomic alterations and drug targets across childhood cancers. In *Pediatric Neurooncology* (Heidelberg University).
- Gröbner, S.N., Worst, B.C., Weischenfeldt, J., Buchhalter, I., Kleinheinz, K., Rudneva, V.A., Johann, P.D., Balasubramanian, G.P., Segura-Wang, M., Brabetz, S., *et al.* (2018). The landscape of genomic alterations across childhood cancers. *Nature* 555, 321-327.
- Guerreiro Stucklin, A.S., Ramaswamy, V., Daniels, C., and Taylor, M.D. (2018). Review of molecular classification and treatment implications of pediatric brain tumors. *Current opinion in pediatrics* 30, 3-9.
- Gustafson, W.C., and Weiss, W.A. (2010). Myc proteins as therapeutic targets. *Oncogene* 29, 1249-1259.
- Hanahan, D., and Weinberg, Robert A. (2011). Hallmarks of Cancer: The Next Generation. *Cell* 144, 646-674.
- Hanahan, D., and Weinberg, R.A.J.c. (2000). The hallmarks of cancer. 100, 57-70.
- Hartlieb, S.A., Sieverling, L., Nadler-Holly, M., Ziehm, M., Toprak, U.H., Herrmann, C., Ishaque, N., Okonechnikov, K., Gartlgruber, M., Park, Y.-G., *et al.* (2021). Alternative lengthening of telomeres in childhood neuroblastoma from genome to proteome. *Nature Communications* 12, 1269.

- Heck, J.E., Ritz, B., Hung, R.J., Hashibe, M., and Boffetta, P. (2009). The epidemiology of neuroblastoma: a review. *Paediatric and Perinatal Epidemiology* 23, 125-143.
- Holsten, T., Lubieniecki, F., Spohn, M., Mynarek, M., Bison, B., Löbel, U., Rutkowski, S., and Schüller, U. (2021). Detailed Clinical and Histopathological Description of 8 Cases of Molecularly Defined CNS Neuroblastomas. *J Neuropathol Exp Neurol* 80, 52-59.
- Hovestadt, V., and Zapatka, M.J.R.p.v. (2017). Conumee: enhanced copy-number variation analysis using Illumina DNA methylation arrays. 1.
- <http://r2.amc.nl>, R.G.A.a.V.P.
- Huang, M., and Weiss, W.A.J.C.S.H.p.i.m. (2013). Neuroblastoma and MYCN. 3, a014415.
- Hübner, J.-M. (2019). Investigating the genomic landscape of posterior fossa ependymoma. In DKFZ (Heidelberg University).
- Hübner, J.-M., Müller, T., Papageorgiou, D.N., Mauermann, M., Krijgsveld, J., Russell, R.B., Ellison, D.W., Pfister, S.M., Pajtler, K.W., and Kool, M. (2019). EZHIP/CXorf67 mimics K27M mutated oncohistones and functions as an intrinsic inhibitor of PRC2 function in aggressive posterior fossa ependymoma. *Neuro-oncology* 21, 878-889.
- Hwang, E.I., Kool, M., Burger, P.C., Capper, D., Chavez, L., Brabetz, S., Williams-Hughes, C., Billups, C., Heier, L., Jaju, A., *et al.* (2018). Extensive Molecular and Clinical Heterogeneity in Patients With Histologically Diagnosed CNS-PNET Treated as a Single Entity: A Report From the Children's Oncology Group Randomized ACNS0332 Trial. *J Clin Oncol*, Jco2017764720.
- Hwang, W.L., Wolfson, R.L., Niemierko, A., Marcus, K.J., DuBois, S.G., and Haas-Kogan, D. (2019). Clinical Impact of Tumor Mutational Burden in Neuroblastoma. *JNCI: Journal of the National Cancer Institute* 111, 695-699.
- Ikegaki, N., Shimada, H., and Committee, f.t.I.N.P. (2019). Subgrouping of Unfavorable Histology Neuroblastomas With Immunohistochemistry Toward Precision Prognosis and Therapy Stratification. 1-7.
- Irwin, M.S., Naranjo, A., Zhang, F.F., Cohn, S.L., London, W.B., Gastier-Foster, J.M., Ramirez, N.C., Pfau, R., Reshmi, S., Wagner, E., *et al.* (2021). Revised Neuroblastoma Risk Classification System: A Report From the Children's Oncology Group. *Journal of Clinical Oncology* 39, 3229-3241.
- James, T., Lindén, M., Morikawa, H., Fernandes, S.J., Ruhrmann, S., Huss, M., Brandi, M., Piehl, F., Jagodic, M., Tegnér, J., *et al.* (2018). Impact of genetic risk loci for multiple sclerosis on expression of proximal genes in patients. *Human molecular genetics* 27, 912-928.
- Jiang, J., Wang, J., Yue, M., Cai, X., Wang, T., Wu, C., Su, H., Wang, Y., Han, M., Zhang, Y., *et al.* (2020). Direct Phosphorylation and Stabilization of MYC by Aurora B Kinase Promote T-cell Leukemogenesis. *Cancer cell* 37, 200-215.e205.
- Jiang, M., Stanke, J., and Lahti, J.M. (2011). Chapter 4 - The Connections Between Neural Crest Development and Neuroblastoma. In *Current Topics in Developmental Biology*, M.A. Dyer, ed. (Academic Press), pp. 77-127.

- Jiang, Y., and Uhrbom, L. (2012). On the origin of glioma. *Upsala Journal of Medical Sciences* 117, 113-121.
- Johnsen, J.I., Dyberg, C., and Wickstrom, M. (2019). Neuroblastoma-A Neural Crest Derived Embryonal Malignancy. *Front Mol Neurosci* 12, 9.
- Johnson, K.J., Cullen, J., Barnholtz-Sloan, J.S., Ostrom, Q.T., Langer, C.E., Turner, M.C., McKean-Cowdin, R., Fisher, J.L., Lupo, P.J., Partap, S., *et al.* (2014). Childhood brain tumor epidemiology: a brain tumor epidemiology consortium review. *Cancer Epidemiol Biomarkers Prev* 23, 2716-2736.
- Junttila, M.R., and Westermarck, J. (2008). Mechanisms of MYC stabilization in human malignancies. *Cell cycle (Georgetown, Tex)* 7, 592-596.
- Katoh, M., Igarashi, M., Fukuda, H., Nakagama, H., and Katoh, M. (2013). Cancer genetics and genomics of human FOX family genes. *Cancer Letters* 328, 198-206.
- Katoh, M., and Katoh, M. (2004a). Human FOX gene family (Review). *International journal of oncology* 25, 1495-1500.
- Katoh, M., and Katoh, M. (2004b). Identification and characterization of human FOXN5 and rat Foxn5 genes in silico. *International journal of oncology* 24, 1339-1344.
- Katoh, M., and Katoh, M. (2004c). Identification and characterization of human FOXN6, mouse Foxn6, and rat Foxn6 genes in silico. *International journal of oncology* 25, 219-223.
- Kattner, P., Strobel, H., Khoshnevis, N., Grunert, M., Bartholomae, S., Pruss, M., Fitzel, R., Halatsch, M.-E., Schilberg, K., Siegelin, M.D., *et al.* (2019). Compare and contrast: pediatric cancer versus adult malignancies. *Cancer and Metastasis Reviews* 38, 673-682.
- Kleihues, P., and Sobin, L.H. (2000). World Health Organization classification of tumors. *Cancer* 88, 2887-2887.
- Koelsche, C., Schrimpf, D., Stichel, D., Sill, M., Sahm, F., Reuss, D.E., Blattner, M., Worst, B., Heilig, C.E., Beck, K., *et al.* (2021). Sarcoma classification by DNA methylation profiling. *Nature Communications* 12, 498.
- Koneru, B., Lopez, G., Farooqi, A., Conkrite, K.L., Nguyen, T.H., Macha, S.J., Modi, A., Rokita, J.L., Urias, E., Hindle, A., *et al.* (2020). Telomere Maintenance Mechanisms Define Clinical Outcome in High-Risk Neuroblastoma. *Cancer Res* 80, 2663-2675.
- Korshunov, A., Capper, D., Reuss, D., Schrimpf, D., Ryzhova, M., Hovestadt, V., Sturm, D., Meyer, J., Jones, C., Zheludkova, O., *et al.* (2016). Histologically distinct neuroepithelial tumors with histone 3 G34 mutation are molecularly similar and comprise a single nosologic entity. *Acta Neuropathol* 131, 137-146.
- Korshunov, A., Okonechnikov, K., Sahm, F., Ryzhova, M., Stichel, D., Schrimpf, D., Ghasemi, D.R., Pajtler, K.W., Antonelli, M., Donofrio, V., *et al.* (2020). Transcriptional profiling of medulloblastoma with extensive nodularity (MBEN) reveals two clinically relevant tumor subsets with VSNL1 as potent prognostic marker. *Acta Neuropathol* 139, 583-596.

- Korshunov, A., Okonechnikov, K., Schmitt-Hoffner, F., Ryzhova, M., Sahm, F., Stichel, D., Schrimpf, D., Reuss, D.E., Sievers, P., Suwala, A.K., *et al.* (2021). Molecular analysis of pediatric CNS-PNET revealed nosologic heterogeneity and potent diagnostic markers for CNS neuroblastoma with FOXR2-activation. *Acta Neuropathol Commun* 9, 20.
- Koso, H., Tshako, A., Lyons, E., Ward, J.M., Rust, A.G., Adams, D.J., Jenkins, N.A., Copeland, N.G., and Watanabe, S. (2014). Identification of FoxR2 as an oncogene in medulloblastoma. *Cancer Res* 74, 2351-2361.
- Krämer, A. (2017). The prognostic and therapeutic relevance of TERT activation in neuroblastoma (Universität zu Köln, Kinderklinik, Exp. Kinderonkologie).
- Kristensen, B.W., Priesterbach-Ackley, L.P., Petersen, J.K., and Wesseling, P. (2019). Molecular pathology of tumors of the central nervous system. *Ann Oncol* 30, 1265-1278.
- Kyu, H.H., Stein, C.E., Boschi Pinto, C., Rakovac, I., Weber, M.W., Dannemann Purnat, T., Amuah, J.E., Glenn, S.D., Cercy, K., Biryukov, S., *et al.* (2018). Causes of death among children aged 5–14 years in the WHO European Region: a systematic analysis for the Global Burden of Disease Study 2016. *The Lancet Child & Adolescent Health* 2, 321-337.
- Lambo, S., Gröbner, S.N., Rausch, T., Waszak, S.M., Schmidt, C., Gorthi, A., Romero, J.C., Mauermann, M., Brabetz, S., Krausert, S., *et al.* (2019a). The molecular landscape of ETMR at diagnosis and relapse. *Nature* 576, 274-280.
- Lambo, S., Gröbner, S.N., Rausch, T., Waszak, S.M., Schmidt, C., Gorthi, A., Romero, J.C., Mauermann, M., Brabetz, S., Krausert, S., *et al.* (2019b). The molecular landscape of ETMR at diagnosis and relapse. *Nature* 576, 274-280.
- Lastowska, M., Trubicka, J., Sobocinska, A., Wojtas, B., Niemira, M., Szalkowska, A., Kretowski, A., Karkucinska-Wieckowska, A., Kaleta, M., Ejmont, M., *et al.* (2020). Molecular identification of CNS NB-FOXR2, CNS EFT-CIC, CNS HGNET-MN1 and CNS HGNET-BCOR pediatric brain tumors using tumor-specific signature genes. *Acta Neuropathol Commun* 8, 105.
- Laurenti, E., Wilson, A., and Trumpp, A. (2009). Myc's other life: stem cells and beyond. *Current Opinion in Cell Biology* 21, 844-854.
- Lee, E.Y., and Muller, W.J. (2010). Oncogenes and tumor suppressor genes. *Cold Spring Harbor perspectives in biology* 2, a003236.
- Lester, R.A., Brown, L.C., Eckel, L.J., Foote, R.T., NageswaraRao, A.A., Buckner, J.C., Parney, I.F., Wetjen, N.M., and Laack, N.N. (2014). Clinical outcomes of children and adults with central nervous system primitive neuroectodermal tumor. *Journal of neuro-oncology* 120, 371-379.
- Li, B., Huang, W., Cao, N., and Lou, G. (2018). Forkhead-box R2 promotes metastasis and growth by stimulating angiogenesis and activating hedgehog signaling pathway in ovarian cancer. *J Cell Biochem* 119, 7780-7789.
- Li, X., Wang, W., Xi, Y., Gao, M., Tran, M., Aziz, K.E., Qin, J., Li, W., and Chen, J. (2016). FOXR2 Interacts with MYC to Promote Its Transcriptional Activities and Tumorigenesis. *Cell Rep* 16, 487-497.

- Li, Z., Godinho, F.J., Klusmann, J.-H., Garriga-Canut, M., Yu, C., and Orkin, S.H. (2005). Developmental stage–selective effect of somatically mutated leukemogenic transcription factor GATA1. *Nature Genetics* 37, 613-619.
- Liberzon, A., Subramanian, A., Pinchback, R., Thorvaldsdottir, H., Tamayo, P., and Mesirov, J.P. (2011). Molecular signatures database (MSigDB) 3.0. *Bioinformatics* (Oxford, England) 27, 1739-1740.
- Liu, A.P.Y., Gudenas, B., Lin, T., Orr, B.A., Klimo, P., Jr., Kumar, R., Bouffet, E., Gururangan, S., Crawford, J.R., Kellie, S.J., *et al.* (2019). Risk-adapted therapy and biological heterogeneity in pineoblastoma: integrated clinico-pathological analysis from the prospective, multi-center SJMB03 and SJYC07 trials. *Acta Neuropathol.*
- Liu, X., Liu, N., Yue, C., Wang, D., Qi, Z., Tu, Y., Zhuang, G., Zhou, D., Gao, S., Niu, M., *et al.* (2017). FoxR2 promotes glioma proliferation by suppression of the p27 pathway. *Oncotarget* 8, 56255-56266.
- London, W.B., Castleberry, R.P., Matthay, K.K., Look, A.T., Seeger, R.C., Shimada, H., Thorner, P., Brodeur, G., Maris, J.M., Reynolds, C.P., *et al.* (2005). Evidence for an age cutoff greater than 365 days for neuroblastoma risk group stratification in the Children's Oncology Group. *J Clin Oncol* 23, 6459-6465.
- Louis, C.U., and Shohet, J.M. (2015). Neuroblastoma: Molecular Pathogenesis and Therapy. 66, 49-63.
- Louis, D.N., Ohgaki, H., Wiestler, O.D., Cavenee, W.K., Burger, P.C., Jouvet, A., Scheithauer, B.W., and Kleihues, P. (2007). The 2007 WHO Classification of Tumours of the Central Nervous System. *Acta Neuropathologica* 114, 97-109.
- Louis, D.N., Perry, A., Reifenberger, G., von Deimling, A., Figarella-Branger, D., Cavenee, W.K., Ohgaki, H., Wiestler, O.D., Kleihues, P., and Ellison, D.W. (2016). The 2016 World Health Organization Classification of Tumors of the Central Nervous System: a summary. *Acta Neuropathologica* 131, 803-820.
- Louis, D.N., Perry, A., Wesseling, P., Brat, D.J., Cree, I.A., Figarella-Branger, D., Hawkins, C., Ng, H.K., Pfister, S.M., Reifenberger, G., *et al.* (2021). The 2021 WHO Classification of Tumors of the Central Nervous System: a summary. *Neuro-Oncology* 23, 1231-1251.
- Love, M.I., Huber, W., and Anders, S. (2014). Moderated estimation of fold change and dispersion for RNA-seq data with DESeq2. *Genome Biol* 15, 550.
- Lu, S.Q., Qiu, Y., Dai, W.J., and Zhang, X.Y. (2017). FOXR2 Promotes the Proliferation, Invasion, and Epithelial-Mesenchymal Transition in Human Colorectal Cancer Cells. *Oncol Res* 25, 681-689.
- Ma, X., Liu, Y., Liu, Y., Alexandrov, L.B., Edmonson, M.N., Gawad, C., Zhou, X., Li, Y., Rusch, M.C., Easton, J., *et al.* (2018). Pan-cancer genome and transcriptome analyses of 1,699 paediatric leukaemias and solid tumours. *Nature* 555, 371-376.
- Mac, S.M., D'Cunha, C.A., and Farnham, P.J. (2000). Direct recruitment of N-myc to target gene promoters. *Molecular Carcinogenesis* 29, 76-86.

- Madanat-Harjuoja, L.M., Pokhrel, A., Kivivuori, S.M., and Saarinen-Pihkala, U.M. (2014). Childhood cancer survival in Finland (1953–2010): A nation-wide population-based study. *International Journal of Cancer* 135, 2129-2134.
- Malempati, S., Tibbitts, D., Cunningham, M., Akkari, Y., Olson, S., Fan, G., and Sears, R.C. (2006). Aberrant stabilization of c-Myc protein in some lymphoblastic leukemias. *Leukemia* 20, 1572-1581.
- Maris, J.M. (2010). Recent advances in neuroblastoma. *N Engl J Med* 362, 2202-2211.
- Massimino, M., Gandola, L., Biassoni, V., Spreafico, F., Schiavello, E., Poggi, G., Pecori, E., Vajna De Pava, M., Modena, P., Antonelli, M., *et al.* (2013). Evolving of therapeutic strategies for CNS-PNET. *Pediatr Blood Cancer* 60, 2031-2035.
- Massimino, M., Gandola, L., Spreafico, F., Luksch, R., Collini, P., Giangaspero, F., Simonetti, F., Casanova, M., Cefalo, G., Pignoli, E., *et al.* (2006). Supratentorial primitive neuroectodermal tumors (S-PNET) in children: A prospective experience with adjuvant intensive chemotherapy and hyperfractionated accelerated radiotherapy. *International journal of radiation oncology, biology, physics* 64, 1031-1037.
- Matthay, K.K., Maris, J.M., Schleiermacher, G., Nakagawara, A., Mackall, C.L., Diller, L., and Weiss, W.A. (2016). Neuroblastoma. *Nature Reviews Disease Primers* 2, 16078.
- Matthay, K.K.J.O. (1997). Neuroblastoma: biology and therapy. *11*, 1857-1866; discussion 1869.
- Meany, H.J. (2019). Non-High-Risk Neuroblastoma: Classification and Achievements in Therapy. *Children (Basel)* 6.
- Miettinen, M., McCue, P.A., Sarlomo-Rikala, M., Biernat, W., Czapiewski, P., Kopczynski, J., Thompson, L.D., Lasota, J., Wang, Z., and Fetsch, J.F. (2015). Sox10--a marker for not only schwannian and melanocytic neoplasms but also myoepithelial cell tumors of soft tissue: a systematic analysis of 5134 tumors. *The American journal of surgical pathology* 39, 826-835.
- Monclair, T., Brodeur, G.M., Ambros, P.F., Brisse, H.J., Cecchetto, G., Holmes, K., Kaneko, M., London, W.B., Matthay, K.K., Nuchtern, J.G., *et al.* (2009). The International Neuroblastoma Risk Group (INRG) staging system: an INRG Task Force report. *J Clin Oncol* 27, 298-303.
- Mossé, Y.P., Deyell, R.J., Berthold, F., Nagakawara, A., Ambros, P.F., Monclair, T., Cohn, S.L., Pearson, A.D., London, W.B., and Matthay, K.K. (2014). Neuroblastoma in older children, adolescents and young adults: A report from the International Neuroblastoma Risk Group project. *61*, 627-635.
- Myatt, S.S., and Lam, E.W.F. (2007). The emerging roles of forkhead box (Fox) proteins in cancer. *Nature Reviews Cancer* 7, 847-859.
- Newman, E.A., Abdessalam, S., Aldrink, J.H., Austin, M., Heaton, T.E., Bruny, J., Ehrlich, P., Dasgupta, R., Baertschiger, R.M., Lautz, T.B., *et al.* (2019). Update on neuroblastoma. *Journal of Pediatric Surgery* 54, 383-389.

- Ng, J.M., Martinez, D., Marsh, E.D., Zhang, Z., Rappaport, E., Santi, M., and Curran, T. (2015). Generation of a mouse model of atypical teratoid/rhabdoid tumor of the central nervous system through combined deletion of Snf5 and p53. *Cancer Res* 75, 4629-4639.
- NIH (accessed 04.11.2021a). Cancer Statistics <https://www.cancer.gov/about-cancer/understanding/statistics>, N.C. Institute, ed.
- NIH (accessed 04.11.2021b). <https://www.cancer.gov/about-cancer/understanding/what-is-cancer>, N.C. Institute, ed.
- Okonechnikov, K., Imai-Matsushima, A., Paul, L., Seitz, A., Meyer, T.F., and Garcia-Alcalde, F. (2016). InFusion: Advancing Discovery of Fusion Genes and Chimeric Transcripts from Deep RNA-Sequencing Data. *PLoS one* 11, e0167417.
- Otto, T., Horn, S., Brockmann, M., Eilers, U., Schüttrumpf, L., Popov, N., Kenney, A.M., Schulte, J.H., Beijersbergen, R., Christiansen, H., *et al.* (2009). Stabilization of N-Myc Is a Critical Function of Aurora A in Human Neuroblastoma. *Cancer cell* 15, 67-78.
- Pajtler, K.W., Witt, H., Sill, M., Jones, D.T., Hovestadt, V., Kratochwil, F., Wani, K., Tatevossian, R., Punchihewa, C., Johann, P., *et al.* (2015). Molecular Classification of Ependymal Tumors across All CNS Compartments, Histopathological Grades, and Age Groups. *Cancer cell* 27, 728-743.
- Panditharatna, E., and Filbin, M.G. (2020). The growing role of epigenetics in childhood cancers. *Current opinion in pediatrics* 32, 67-75.
- Papanicolau-Sengos, A., and Aldape, K. (2021). DNA Methylation Profiling: An Emerging Paradigm for Cancer Diagnosis. *Annual Review of Pathology: Mechanisms of Disease*.
- Pathania, M., De Jay, N., Maestro, N., Harutyunyan, A.S., Nitarska, J., Pahlavan, P., Henderson, S., Mikael, L.G., Richard-Londt, A., Zhang, Y., *et al.* (2017). H3.3(K27M) Cooperates with Trp53 Loss and PDGFRA Gain in Mouse Embryonic Neural Progenitor Cells to Induce Invasive High-Grade Gliomas. *Cancer cell* 32, 684-700.e689.
- Peifer, M., Hirtwig, F., Roels, F., Dreidax, D., Gartlgruber, M., Menon, R., Kramer, A., Roncaioli, J.L., Sand, F., Heuckmann, J.M., *et al.* (2015). Telomerase activation by genomic rearrangements in high-risk neuroblastoma. *Nature* 526, 700-704.
- Perez, E., and Capper, D. (2020). Invited Review: DNA methylation-based classification of paediatric brain tumours. *Neuropathology and Applied Neurobiology* 46, 28-47.
- Peris-Bonet, R., Martínez-García, C., Lacour, B., Petrovich, S., Giner-Ripoll, B., Navajas, A., and Steliarova-Foucher, E. (2006). Childhood central nervous system tumours – incidence and survival in Europe (1978–1997): Report from Automated Childhood Cancer Information System project. *European Journal of Cancer* 42, 2064-2080.
- Pfister, S., Hartmann, C., and Korshunov, A. (2009). Histology and Molecular Pathology of Pediatric Brain Tumors. *Journal of Child Neurology* 24, 1375-1386.
- Picard, D., Miller, S., Hawkins, C.E., Bouffet, E., Rogers, H.A., Chan, T.S.Y., Kim, S.-K., Ra, Y.-S., Fangusaro, J., Korshunov, A., *et al.* (2012). Markers of survival and metastatic potential in childhood CNS primitive neuro-ectodermal brain tumours: an integrative genomic analysis. *The Lancet Oncology* 13, 838-848.

- Pinto, N.R., Applebaum, M.A., Volchenbom, S.L., Matthay, K.K., London, W.B., Ambros, P.F., Nakagawara, A., Berthold, F., Schleiermacher, G., Park, J.R., *et al.* (2015). Advances in Risk Classification and Treatment Strategies for Neuroblastoma. *J Clin Oncol* 33, 3008-3017.
- Poh, B., Koso, H., Momota, H., Komori, T., Suzuki, Y., Yoshida, N., Ino, Y., Todo, T., and Watanabe, S. (2019). Foxr2 promotes formation of CNS-embryonal tumors in a Trp53-deficient background. *Neuro Oncol*.
- Pollack, I.F., Agnihotri, S., and Broniscer, A. (2019). Childhood brain tumors: current management, biological insights, and future directions: JNSPG 75th Anniversary Invited Review Article. *Journal of Neurosurgery: Pediatrics PED* 23, 261-273.
- Poppleton, H., and Gilbertson, R.J. (2007). Stem cells of ependymoma. *British Journal of Cancer* 96, 6-10.
- Proteinatlas (accessed 12.11.2021). THE HUMAN PROTEIN ATLAS - FOXR2 <https://www.proteinatlas.org/ENSG00000189299-FOXR2/tissue>.
- Pugh, T.J., Morozova, O., Attiyeh, E.F., Asgharzadeh, S., Wei, J.S., Auclair, D., Carter, S.L., Cibulskis, K., Hanna, M., Kiezun, A., *et al.* (2013). The genetic landscape of high-risk neuroblastoma. *Nat Genet* 45, 279-284.
- QIAGEN Inc., h.w.q.c.p.i.-a.
- Rahrman, E.P., Watson, A.L., Keng, V.W., Choi, K., Moriarity, B.S., Beckmann, D.A., Wolf, N.K., Sarver, A., Collins, M.H., Moertel, C.L., *et al.* (2013). Forward genetic screen for malignant peripheral nerve sheath tumor formation identifies new genes and pathways driving tumorigenesis. *Nature Genetics* 45, 756-766.
- Rajbhandari, P., Lopez, G., Capdevila, C., Salvatori, B., Yu, J., Rodriguez-Barrueco, R., Martinez, D., Yarmarkovich, M., Weichert-Leahey, N., Abraham, B.J., *et al.* (2018). Cross-Cohort Analysis Identifies a TEAD4–MYCN Positive Feedback Loop as the Core Regulatory Element of High-Risk Neuroblastoma. 8, 582-599.
- Reinhardt, A., Stichel, D., Schrimpf, D., Koelsche, C., Wefers, A.K., Ebrahimi, A., Sievers, P., Huang, K., Casalini, M.B., Fernandez-Klett, F., *et al.* (2019). Tumors diagnosed as cerebellar glioblastoma comprise distinct molecular entities. *Acta Neuropathol Commun* 7, 163.
- Roderwieser, A., Sand, F., Walter, E., Fischer, J., Gecht, J., Bartenhagen, C., Ackermann, S., Otte, F., Welte, A., and Kahlert, Y.J.J.P.O. (2019). Telomerase is a prognostic marker of poor outcome and a therapeutic target in neuroblastoma. 3, 1-20.
- Santo, E.E., Ebus, M.E., Koster, J., Schulte, J.H., Lakeman, A., Van Sluis, P., Vermeulen, J., Gisselsson, D., Øra, I., and Lindner, S.J.O. (2012). Oncogenic activation of FOXR1 by 11q23 intrachromosomal deletion-fusions in neuroblastoma. 31, 1571-1581.
- Schleiermacher, G., Mosseri, V., London, W.B., Maris, J.M., Brodeur, G.M., Attiyeh, E., Haber, M., Khan, J., Nakagawara, A., Speleman, F., *et al.* (2012). Segmental chromosomal alterations have prognostic impact in neuroblastoma: a report from the INRG project. *British Journal of Cancer* 107, 1418-1422.

- Schmitt-Hoffner, F., van Rijn, S., Hübner, J.-M., Lambo, S., Mauermann, M., Mack, N., Schwalm, B., Pfister, S., and Kool, M.J.N.-O. (2020). ETMR-03. The role of FOXR2 in pediatric brain cancer. *22*, iii323.
- Schmitt-Hoffner, F., van Rijn, S., Toprak, U.H., Mauermann, M., Rosemann, F., Heit-Mondrzyk, A., Hübner, J.-M., Camgöz, A., Hartlieb, S., Pfister, S.M., *et al.* (2021). FOXR2 Stabilizes MYCN Protein and Identifies Non-MYCN-Amplified Neuroblastoma Patients With Unfavorable Outcome. *Journal of Clinical Oncology*, JCO.20.02540.
- Schwalbe, E.C., Hayden, J.T., Rogers, H.A., Miller, S., Lindsey, J.C., Hill, R.M., Nicholson, S.-L., Kilday, J.-P., Adamowicz-Brice, M., Storer, L., *et al.* (2013a). Histologically defined central nervous system primitive neuro-ectodermal tumours (CNS-PNETs) display heterogeneous DNA methylation profiles and show relationships to other paediatric brain tumour types. *Acta Neuropathologica* *126*, 943-946.
- Schwalbe, E.C., Hayden, J.T., Rogers, H.A., Miller, S., Lindsey, J.C., Hill, R.M., Nicholson, S.L., Kilday, J.P., Adamowicz-Brice, M., Storer, L., *et al.* (2013b). Histologically defined central nervous system primitive neuro-ectodermal tumours (CNS-PNETs) display heterogeneous DNA methylation profiles and show relationships to other paediatric brain tumour types. *Acta Neuropathol* *126*, 943-946.
- Schwartzentruber, J., Korshunov, A., Liu, X.Y., Jones, D.T., Pfaff, E., Jacob, K., Sturm, D., Fontebasso, A.M., Quang, D.A., Tönjes, M., *et al.* (2012). Driver mutations in histone H3.3 and chromatin remodelling genes in paediatric glioblastoma. *Nature* *482*, 226-231.
- Siegel, D.A., Li, J., Ding, H., Singh, S.D., King, J.B., and Pollack, L.A. (2019). Racial and ethnic differences in survival of pediatric patients with brain and central nervous system cancer in the United States. *Pediatric Blood & Cancer* *66*, e27501.
- Siegel, R.L., Miller, K.D., Fuchs, H.E., and Jemal, A. (2021). Cancer Statistics, 2021. *CA: A Cancer Journal for Clinicians* *71*, 7-33.
- Siegel, R.L., Miller, K.D., and Jemal, A. (2018). Cancer statistics, 2018. *68*, 7-30.
- Siegel, R.L., Miller, K.D., and Jemal, A. (2020). Cancer statistics, 2020. *CA: A Cancer Journal for Clinicians* *70*, 7-30.
- Sokol, E., and Desai, A.V. (2019). The Evolution of Risk Classification for Neuroblastoma. *Children (Basel)* *6*, 27.
- Song, H., He, W., Huang, X., Zhang, H., and Huang, T. (2016). High expression of FOXR2 in breast cancer correlates with poor prognosis. *Tumour Biol* *37*, 5991-5997.
- Spitz, R., Hero, B., Ernestus, K., and Berthold, F. (2003). Deletions in chromosome arms 3p and 11q are new prognostic markers in localized and 4s neuroblastoma. *Clinical cancer research : an official journal of the American Association for Cancer Research* *9*, 52-58.
- Stainczyk, S.A., and Westermann, F.J.I.j.o.c. (2021). Neuroblastoma–telomere maintenance, deregulated signalling transduction and beyond.

- Stefan M. Pfister, M.R.-M., John K.C. Chan, Henrik Hasle, Alexander J., Lazar, S.R., Andrea Ferrari, Jason A. Jarzembowski, Kathy Pritchard-Jones, D., Ashley Hill, T.S.J., Pieter Wesseling, Dolores López Terrada, Andreas, and von Deimling, C.P.K., Ian Cree and Rita Alaggio (2021, in press). A summary of the inaugural WHO Classification of Pediatric Tumors: Transitioning from the optical into the molecular era. *Cancer Discov*.
- Stensvold, E., Krossnes, B.K., Lundar, T., Due-Tønnessen, B.J., Frič, R., Due-Tønnessen, P., Bechensteen, A.G., Myklebust, T., Johannesen, T.B., and Brandal, P. (2017). Outcome for children treated for medulloblastoma and supratentorial primitive neuroectodermal tumor (CNS-PNET) - a retrospective analysis spanning 40 years of treatment. *Acta oncologica* (Stockholm, Sweden) *56*, 698-705.
- Stichel, D., Schrimpf, D., Casalini, B., Meyer, J., Wefers, A.K., Sievers, P., Korshunov, A., Koelsche, C., Reuss, D.E., Reinhardt, A., *et al.* (2019). Routine RNA sequencing of formalin-fixed paraffin-embedded specimens in neuropathology diagnostics identifies diagnostically and therapeutically relevant gene fusions. *Acta Neuropathol* *138*, 827-835.
- Stiller, C.A., and Parkin, D.M. (1992). International variations in the incidence of neuroblastoma. *International Journal of Cancer* *52*, 538-543.
- Sturm, D., Orr, B.A., Toprak, U.H., Hovestadt, V., Jones, D.T.W., Capper, D., Sill, M., Buchhalter, I., Northcott, P.A., Leis, I., *et al.* (2016). New Brain Tumor Entities Emerge from Molecular Classification of CNS-PNETs. *Cell* *164*, 1060-1072.
- Sturm, D., Witt, H., Hovestadt, V., Khuong-Quang, D.A., Jones, D.T., Konermann, C., Pfaff, E., Tönjes, M., Sill, M., Bender, S., *et al.* (2012). Hotspot mutations in H3F3A and IDH1 define distinct epigenetic and biological subgroups of glioblastoma. *Cancer cell* *22*, 425-437.
- Su, Z., Fang, H., Hong, H., Shi, L., Zhang, W., Zhang, W., Zhang, Y., Dong, Z., Lancashire, L.J., Bessarabova, M., *et al.* (2014). An investigation of biomarkers derived from legacy microarray data for their utility in the RNA-seq era. *Genome Biol* *15*, 523.
- Subramanian, A., Tamayo, P., Mootha, V.K., Mukherjee, S., Ebert, B.L., Gillette, M.A., Paulovich, A., Pomeroy, S.L., Golub, T.R., Lander, E.S., *et al.* (2005). Gene set enrichment analysis: A knowledge-based approach for interpreting genome-wide expression profiles. *102*, 15545-15550.
- Swift, C.C., Eklund, M.J., Kravaka, J.M., and Alazraki, A.L. (2018). Updates in Diagnosis, Management, and Treatment of Neuroblastoma. *38*, 566-580.
- Timmermann, B., Kortmann, R.-D., Kühl, J., Rutkowski, S., Meisner, C., Pietsch, T., Deinlein, F., Urban, C., Warmuth-Metz, M., and Bamberg, M.J.J.o.c.o. (2006). Role of radiotherapy in supratentorial primitive neuroectodermal tumor in young children: results of the German HIT-SKK87 and HIT-SKK92 trials. *24*, 1554-1560.
- Tolbert, V.P., and Matthay, K.K. (2018). Neuroblastoma: clinical and biological approach to risk stratification and treatment. *Cell and Tissue Research* *372*, 195-209.
- Ugidos, N., Mena, J., Baquero, S., Alloza, I., Azkargorta, M., Elortza, F., and Vandebroek, K. (2019). Interactome of the Autoimmune Risk Protein ANKRD55. *Frontiers in immunology* *10*, 2067.

- Valentijn, L.J., Koster, J., Haneveld, F., Aissa, R.A., van Sluis, P., Broekmans, M.E.C., Molenaar, J.J., van Nes, J., and Versteeg, R. (2012). Functional MYCN signature predicts outcome of neuroblastoma irrespective of MYCN amplification. *109*, 19190-19195.
- Valentijn, L.J., Koster, J., Zwijnenburg, D.A., Hasselt, N.E., van Sluis, P., Volckmann, R., van Noesel, M.M., George, R.E., Tytgat, G.A., and Molenaar, J.J.J.N.g. (2015a). TERT rearrangements are frequent in neuroblastoma and identify aggressive tumors. *47*, 1411-1414.
- Valentijn, L.J., Koster, J., Zwijnenburg, D.A., Hasselt, N.E., van Sluis, P., Volckmann, R., van Noesel, M.M., George, R.E., Tytgat, G.A.M., Molenaar, J.J., *et al.* (2015b). TERT rearrangements are frequent in neuroblastoma and identify aggressive tumors. *Nature Genetics* *47*, 1411-1414.
- Van der Maaten, L., and Hinton, G.J.J.o.m.l.r. (2008). Visualizing data using t-SNE. *9*.
- Vita, M., and Henriksson, M. (2006). The Myc oncoprotein as a therapeutic target for human cancer. *Seminars in Cancer Biology* *16*, 318-330.
- Vitte, J., Gao, F., Coppola, G., Judkins, A.R., and Giovannini, M. (2017). Timing of Smarcb1 and Nf2 inactivation determines schwannoma versus rhabdoid tumor development. *Nat Commun* *8*, 300.
- Vogel, H., and Fuller, G.N. (2003). Primitive neuroectodermal tumors, embryonal tumors, and other small cell and poorly differentiated malignant neoplasms of the central and peripheral nervous systems. *Annals of Diagnostic Pathology* *7*, 387-398.
- von Hoff, K., Haberler, C., Robinson, G., Sumerauer, D., Cho, J., Mynarek, M., Hwang, E., Jacobs, S., de Rojas, T., Perek, M., *et al.* (2018). EMBR-15. DIAGNOSTIC RE-EVALUATION AND POOLED CLINICAL DATA ANALYSIS OF PATIENTS WITH PREVIOUS DIAGNOSIS OF CNS-PNET. *Neuro-oncology* *20*, i72-i72.
- von Hoff, K., Haberler, C., Schmitt-Hoffner, F., Schepke, E., de Rojas, T., Jacobs, S., Zapotocky, M., Sumerauer, D., Perek-Polnik, M., Dufour, C., *et al.* (2021). Therapeutic implications of improved molecular diagnostics for rare CNS-embryonal tumor entities: results of an international, retrospective study. *Neuro Oncol.*
- von Hoff, K., Hinkes, B., Gerber, N.U., Deinlein, F., Mittler, U., Urban, C., Benesch, M., Warmuth-Metz, M., Soerensen, N., and Zwiener, I.J.E.j.o.c. (2009). Long-term outcome and clinical prognostic factors in children with medulloblastoma treated in the prospective randomised multicentre trial HIT '91. *45*, 1209-1217.
- Wang, B., Gogia, B., Fuller, G.N., and Ketonen, L.M. (2018). Embryonal Tumor with Multilayered Rosettes, C19MC-Altered: Clinical, Pathological, and Neuroimaging Findings. *28*, 483-489.
- Wang, L.L., Teshiba, R., Ikegaki, N., Tang, X.X., Naranjo, A., London, W.B., Hogarty, M.D., Gastier-Foster, J.M., Look, A.T., Park, J.R., *et al.* (2015). Augmented expression of MYC and/or MYCN protein defines highly aggressive MYC-driven neuroblastoma: a Children's Oncology Group study. *British Journal of Cancer* *113*, 57-63.

- Wang, X., He, B., Gao, Y., and Li, Y. (2016). FOXR2 contributes to cell proliferation and malignancy in human hepatocellular carcinoma. *Tumour Biol* 37, 10459-10467.
- Ward, E., DeSantis, C., Robbins, A., Kohler, B., and Jemal, A. (2014). Childhood and adolescent cancer statistics, 2014. *64*, 83-103.
- Wee, S., Wiederschain, D., Maira, S.M., Loo, A., Miller, C., deBeaumont, R., Stegmeier, F., Yao, Y.M., and Lengauer, C. (2008). PTEN-deficient cancers depend on PIK3CB. *Proceedings of the National Academy of Sciences of the United States of America* 105, 13057-13062.
- Welcker, M., Orian, A., Grim, J.A., Eisenman, R.N., and Clurman, B.E. (2004). A Nucleolar Isoform of the Fbw7 Ubiquitin Ligase Regulates c-Myc and Cell Size. *Current Biology* 14, 1852-1857.
- Westermann, F., Muth, D., Benner, A., Bauer, T., Henrich, K.-O., Oberthuer, A., Brors, B., Beissbarth, T., Vandesompele, J., and Pattyn, F.J.G.b. (2008). Distinct transcriptional MYCN/c-MYC activities are associated with spontaneous regression or malignant progression in neuroblastomas. *9*, R150.
- WHO (accessed 04.11.2021). https://www.who.int/health-topics/cancer#tab=tab_1 (World Health Organization).
- Wiederschain, D., Wee, S., Chen, L., Loo, A., Yang, G., Huang, A., Chen, Y., Caponigro, G., Yao, Y.M., Lengauer, C., *et al.* (2009). Single-vector inducible lentiviral RNAi system for oncology target validation. *Cell cycle (Georgetown, Tex)* 8, 498-504.
- Wu, G., Broniscer, A., McEachron, T.A., Lu, C., Paugh, B.S., Becksfort, J., Qu, C., Ding, L., Huether, R., Parker, M., *et al.* (2012). Somatic histone H3 alterations in pediatric diffuse intrinsic pontine gliomas and non-brainstem glioblastomas. *Nat Genet* 44, 251-253.
- www.molecularneuropathology.org Heidelberg brain tumor classifier v11b4.
- Xu, W., Chang, J., Liu, G., Du, X., and Li, X. (2017). Knockdown of FOXR2 suppresses the tumorigenesis, growth and metastasis of prostate cancer. *Biomed Pharmacother* 87, 471-475.
- Xu, W., Hou, J., Chang, J., Li, S., Liu, G., and Cao, S.J.Z.y.x.z.z. (2019). The mechanism of HOTAIR regulating the proliferation and apoptosis of prostate cancer cells by targeting down-regulation of miR-152 to improve the expression of FOXR2. *99*, 1887-1892.
- Zeineldin, M., Federico, S., Chen, X., Fan, Y., Xu, B., Stewart, E., Zhou, X., Jeon, J., Griffiths, L., and Nguyen, R.J.N.C. (2020). MYCN amplification and ATRX mutations are incompatible in neuroblastoma. *11*, 1-20.
- Zhang, J.T., Weng, Z.H., Tsang, K.S., Tsang, L.L., Chan, H.C., and Jiang, X.H.J.P.o. (2016). MycN is critical for the maintenance of human embryonic stem cell-derived neural crest stem cells. *11*.
- Zhang, W., Yu, Y., Hertwig, F., Thierry-Mieg, J., Zhang, W., Thierry-Mieg, D., Wang, J., Furlanello, C., Devanarayan, V., Cheng, J., *et al.* (2015). Comparison of RNA-seq and microarray-based models for clinical endpoint prediction. *Genome Biol* 16, 133-133.

References

Zimmerman, M.W., Liu, Y., He, S., Durbin, A.D., Abraham, B.J., Easton, J., Shao, Y., Xu, B., Zhu, S., Zhang, X., *et al.* (2018). MYC Drives a Subset of High-Risk Pediatric Neuroblastomas and Is Activated through Mechanisms Including Enhancer Hijacking and Focal Enhancer Amplification. *Cancer Discov* 8, 320-335.

7 Supplementary data

Suppl. table 1: *FOXR2* signature based on the top100 differentially expressed genes of the *FOXR2* and OTHER group in the RNA-seq dataset. Table from (Schmitt-Hoffner et al., 2021).

Top 100 Differentially expressed genes of the *FOXR2* and the OTHER group

#Program: R2: Genomics analysis and visualization platform

#Website: <http://r2.amc.nl>

#Developer: Jan Koster (jankoster@amc.uva.nl)

#Pretty_dataset: Tumor Neuroblastoma - SEQC - 498 - RPM - seqcnb1

#Test: anova, Top100

#H:probeset	hugo	corrected-pvalue
NM_198451	FOXR2	2.66E-169
XR_109760	XAGE-4	3.76E-71
NM_145312	ZNF485	3.77E-56
NM_001384	DPH2	4.10E-49
NM_024658	IPO4	6.59E-49
NM_182679	GPATCH4	5.99E-42
NM_005674	ZNF239	1.06E-40
NM_006784	WDR3	1.28E-39
NM_005452	WDR46	9.20E-39
NM_015169	RRS1	1.19E-38
NM_016101	NIP7	4.50E-38
NM_133179	XAGE3	6.18E-37
NM_019014	POLR1B	1.23E-34
NR_033250	LOC388499	7.06E-32
NM_021830	C10ORF2	8.80E-32

Supplementary data

NM_004085	TIMM8A	2.01E-32
NM_018130	SHQ1	2.32E-31
NM_001722	POLR3D	8.33E-30
NM_006649	UTP14A	4.90E-29
NM_006824	EBNA1BP2	7.18E-28
NM_007260	LYPLA2	1.76E-27
NM_152305	POGLUT1	2.38E-27
NM_004234	ZNF235	7.62E-27
NM_004728	DDX21	8.49E-27
NM_001089591	UQCRHL	8.96E-27
NM_182490	ZNF227	1.83E-26
NM_016391	NOP16	5.26E-26
XR_133276	LOC100653149	9.60E-26
NM_022366	TFB2M	1.69E-25
NM_015179	RRP12	5.23E-25
NM_017647	FTSJ3	1.76E-24
NM_004461	FARSA	2.02E-25
NM_017916	PIH1D1	9.85E-25
NM_006004	UQCRH	1.01E-23
XR_109511	LOC728485	2.36E-23
NR_023382	ZNF815P	4.23E-23
XR_110308	LOC400879	6.26E-23
NM_030980	ISG20L2	2.15E-22
NM_001141969	DAXX	2.69E-23
NM_032509	MAK16	2.71E-22
NM_019037	EXOSC4	2.74E-21
NM_003904	ZNF259	1.17E-20
NM_001018068	SERBP1	3.95E-20

NM_003145	SSR2	5.90E-20
NM_020158	EXOSC5	2.47E-19
NM_032194	RPF2	2.52E-19
NM_003425	ZNF45	3.32E-19
NM_032907	UBL7	3.44E-19
NM_022490	POLR1E	5.78E-19
NM_018997	MRPS21	9.67E-19
NM_001080501	TMEM223	1.04E-18
XR_110283	LOC100506303	1.06E-18
NM_014976	PDCD11	1.10E-18
NM_012341	GTPBP4	1.00E-17
NM_006110	CD2BP2	1.14E-17
NR_027642	DCAF13P3	1.97E-17
NM_024640	YRDC	2.35E-17
NM_007362	NCBP2	4.00E-17
NM_006360	EIF3M	4.25E-17
NM_001002000	GMPR2	4.31E-17
NM_206898	MRAP	4.58E-17
NM_001031827	BOLA2	7.50E-17
NM_001039182	BOLA2B	7.54E-17
NM_015420	DCAF13	1.45E-16
NM_001145374	ALKBH2	1.47E-16
NM_014825	URB1	1.49E-16
NM_022341	PDF	1.69E-16
NM_032390	MKI67IP	2.65E-16
NM_030782	CLPTM1L	3.75E-16
NM_015935	METTL13	7.72E-17
NM_001293	CLNS1A	8.16E-16

Supplementary data

NM_006232	POLR2H	1.37E-15
NM_006098	GNB2L1	2.39E-16
NM_018983	GAR1	2.49E-15
NM_022917	NOL6	2.79E-15
NM_018115	SDAD1	4.51E-15
NM_003757	EIF3I	7.30E-15
NM_004044	ATIC	1.30E-14
NM_013285	GNL2	1.45E-14
NM_144631	ZNF513	2.10E-17
NR_027696	TAPT1-AS1	2.77E-14
NM_020410	ATP13A1	3.32E-14
NM_024775	GEMIN6	4.01E-14
NM_033416	IMP4	5.29E-14
XR_132758	LOC440157	6.51E-14
XR_110291	FLJ39632	9.40E-14
NR_034163	ZNF890P	1.32E-13
NR_024388	LOC152217	3.71E-13
NM_001037813	ZNF284	1.46E-12
NM_001033930	UBA52	1.67E-12
NM_016561	BFAR	1.96E-12
NM_001185181	PFDN6	2.19E-12
NM_002887	RARS	2.47E-12
NM_145232	CTU1	4.61E-12
NM_015659	RSL1D1	5.06E-12
NM_013237	PRELID1	6.14E-12
NM_001009	RPS5	7.23E-12
NM_181786	HKR1	9.92E-12
NM_015442	CNOT10	1.00E-11

NR_003024

EIF3IP1

1.23E-11

8 Acknowledgements

During my 3 years at the KiTZ and the DKFZ many people supported me and eventually made it possible to conduct my PhD successfully.

First of all I want to thank Marcel and Stefan who gave me the opportunity to do my PhD in the department of Pediatric Neurooncology. Marcel, thanks for the excellent guidance and support, which enabled and significantly boosted my scientific and also personal development. You created a great group environment with lots of group outings, a comfortable atmosphere and a very efficient working style, which also allowed for relaxing holidays every now and then ;). Stefan, thank you very much for the support and encouragement during my PhD. As my supervisor and member of my TAC committee, you always supported me and never lost track of the overall picture. In addition, you provided optimal conditions for me to successfully conduct my PhD in the highly collaborative and interdisciplinary department of Pediatric Neurooncology. Furthermore, I would like to thank Prof. Gert Fricker, who supported me already since my Master thesis in his group at Heidelberg University until now in my PhD where he is part of my TAC committee. Your scientific as well as strategic input and support has helped me a lot to reach my goals. Not to forget your input on sailing of course! I would also like to thank Prof. Trumpp, for being my first examiner, member of my TAC committee and for his excellent support during my PhD. You provided excellent feedback during the TAC committees and really pushed the project forward bringing in new ideas. Further thanks goes to Dr. Moritz Mall for being part of my oral defense committee.

I am very thankful for the fruitful collaborations with Katja von Hoff and Andrey Korshunov, which resulted in two important publications. Additionally I want to thank Sjoerd von Rijn for all the valuable previous work he did before I joined the lab, which was very important to publish our manuscript in JCO so efficiently and fast. Many other people were also involved and made this publication possible: Great thank goes to Frank Westermann, Kai-Oliver Henrich, Umut Toprak, of course Stefan Pfister and Marcel Kool, and everyone else who contributed. I am also very thankful for working together with Monika Mauermann, who supported me by conducting experiments incredibly fast and with outstanding precision. Equally skillful is her baking, which surely made not only me but the whole lab happy! Many thanks also to Norman Mack, Benjamin Schwalm, Andrea Wittmann and Laura Sieber for an excellent assistance in the lab. Moreover, I'd like to thank many other collaborators, primarily Johannes Gojo, Damian Stichel, Martin Sill, David Jones, Natalie Jäger and Felix Sahn.

I am especially grateful to my amazing lab members of the Kool group: Marcel, Sonja, Jens, Norman, Benni, Anne, Aylin, Aniello, Jurrian, Annett, Moni, Enrique, Anke, Shanzheng, Joudi, Pascal, Sander and Johannes who made my time at the DKFZ and beyond so much fun and who helped me in any possible way.

Furthermore, I'm grateful for all the friends I got to know during my PhD. Jasper and Apurva - loved and still loving our DKFZ Coffee Social Club and numerous meetings, which always cheered me up, even in challenging times. Sonja, Jens, Norman, Annett, Benni and Alex - thanks to you I enjoyed PhD life also outside DKFZ so much. We did amazing trips together, managed to stay connected even in times of Corona, discussed the weirdest topics and it is always a lot of fun to spend time with you. Looking very much forward to all the trips we still have in the pipeline!

Special thanks goes to my friends from Rettigheim/Mühlhausen, Heidelberg and Konstanz for all these awesome tips, vacations and meetings, which I enjoy so much and which are a great break and inspiration. Especially you, Saijoscha, had a substantial impact on my academic career and I'm deeply grateful I can call you my friend. Also, I would like to specifically mention Marian, Rok and Nicole for all their support, e.g. by proofreading this dissertation or boosting my motivation, the great time we spent during the last years and for being great friends.

For their unconditional support in any aspect of my life, a heartfelt thank you goes to my family. Without my parents, Anette and Andreas, who encourage me to follow my interests and who really are the harmonic, supportive and loving foundation, which my development is based on, I could not have accomplished this. Big thanks also goes to my (maybe not anymore) little brother Daniel. Furthermore, I will always be thankful for the close connection to my grandparents Erika and Bernhard, who supported me my whole life and encouraged me to pursue my goals.

Finally, I am deeply thankful to Olga. Thank you for being this loving and wonderful partner that you are. Thank you for all your support over so many years, for always backing me up in challenging times, for distracting me from work whenever needed and for all the wonderful moments we spend together.